Aprovechamiento y revalorización de un residuo proteico del maíz como estabilizante de productos alimentarios

Tesis doctoral

Jenifer Santos García

Directores de tesis

Prof. Dr. María del Carmen Alfaro Rodríguez

Prof. Dr. Luis Alfonso Trujillo Cayado

Departamento de Ingeniería Química

Escuela Politécnica Superior

Universidad de Sevilla, 2021

A mis Luises

Índice

Resumen

El objetivo principal de esta tesis fue el desarrollo y la caracterización de emulsiones de grado alimentario usando como estabilizante un residuo proteico de la industria del etanol y del maíz, la zeína. Aunque originalmente, esta proteína fue considerada un residuo, hoy en día se considera que posee un gran potencial para la ingeniería de tejidos, la administración de fármacos y su uso en productos alimentarios. Sin embargo, su uso como único estabilizante en emulsiones muestra estabilidades muy limitadas. Por ello, se ha empezado a usar su uso combinado con polisacáridos. En esta tesis, se han desarrollado sistemas basados en emulsiones formulados con diferentes complejos zeína-polisacaridos : zeína-goma xantana, zeína-goma guar y zeína-goma diutan. De este modo, se ha conseguido aumentar la estabilidad de estos sistemas alimentarios reduciendo sus mecanismos de desestabilización. Por otro lado, estas emulsiones serán formuladas con aceites ricos en ácidos grasos ω-3, como el aceite de girasol alto oleico. De este modo, estos sistemas están especialmente diseñados para celiacos, veganos, vegetarianos y mujeres embarazadas que necesitan altas dosis de estos ácidos grados y con ello se contribuye a cubrir las necesidades de estos nichos de mercado.

Esta tesis consta de cuatro capítulos. El primero es una introducción teórica donde se desarrollan conceptos tan importantes como emulsiones, procesado de emulsiones y mecanismos de desestabilización de emulsiones. Además, se presentan los compuestos usados en este proyecto y sus principales características.

El segundo capítulo se centra en el desarrollo de emulsiones Pickering usando un método de emulsificación simple como es un homogeneizador rotor-estator. Primero, se estudian las emulsiones basadas solo en zeína donde se optimiza la formulación usando la metodología de las superficies de respuesta.

Después, se evalúa la incorporación de la goma Xantana de alto rendimiento como estabilizante y espesante. Este estudio muestra que la incorporación de dicha goma además de conseguir unas emulsiones con propiedades viscoelásticas ya que forma un recubrimiento en las gotas (comprobado por FESEM), mejora en gran medida su estabilidad física reduciendo el fenómeno de cremado que presentaba la emulsión formulada solo con zeína.

En el tercer capítulo, se optimizan los parámetros de procesado usando un ultrasonido de alta intensidad para obtener emulsiones con zeína y aceite de girasol alto oleico. Después, se evalúa la formación de un complejo zeína-goma guar y zeína-goma diutan estudiando las propiedades reológicas, estabilidad física y microestructura de estas emulsiones. Un incremento en la potencia del ultrasonido, el tiempo de procesado y ciclos provocó una disminución del tamaño de gota en ausencia de recoalescencia. Además, la emulsión optimizada fue el punto de partida para formar los dos coacervatos: zeina con goma guar, y zeína con goma diutan a diferentes concentraciones. Los complejos de zeína y goma guar no formaron un gel reológico, como consecuencia, estas emulsiones sufrieron proceso de desestabilización con el tiempo de almacenamiento. Por el contrario, las emulsiones formuladas con goma diutan presentaron una red 3D, observada por FESEM y demostrada por las medidas reológicas. Este capítulo resalta la importancia de la elección del polisácarido usado en las emulsiones alimentarias formuladas con zeína.

En el último capítulo, el objetivo fue evaluar el proceso de homogenización basado en el uso del microfluidizer. Se estudió la influencia de la presión de homogenización y del número de pasadas en el tamaño de gota usando la metodología de las superficies de respuesta. Posteriormente, se investigó la concentración de la goma diutan en estas emulsiones preparadas con microfluidizer ya que anteriormente fue la goma que mejores resultados mostró. Teniendo en cuenta el análisis de las superficies de respuesta, la

emulsión procesada a 20000 psi y cuatro ciclos mostró el diámetro de Sauter mas pequeño (emulsión optimizada). Además, la emulsión con 0.4% p/p de goma diutan presentó propiedades reológicas de gel y una alta estabilidad física. Por lo tanto, se consiguió una emulsión estable con el tiempo con tamaño de gota submicrónico con la formación del complejo zeína- goma diutan.

Finalmente, se presentan las conclusiones más importantes de esta tesis.

Capítulo 1.
Introducción

1.1. Emulsiones

Una emulsión simple es un sistema termodinámicamente inestable formado por una dispersión de una fase inmiscible en forma de gotas (fase dispersa) en otra fase (fase continua). Estas dos fases suelen ser una orgánica y otra acuosa (Morrison & Ross, 2002). Una fina capa de un componente activo superficialmente, llamados emulsificantes, rodean y protegen las gotas de la fase dispersa. Las emulsiones se clasifican de acuerdo a la distribución de la fase oleosa y la fase acuosa (McClements, 2004). Las emulsiones aceite en agua (O/W) (figura 1.1.) son aquellas que su fase dispersa son las gotas de aceite mientras que la fase acuosa es la fase continua. Por otro lado, un sistema que contiene gotas de fase acuosa dispersas en un medio continuo oleoso son llamadas emulsiones agua en aceite (W/O). Además de las emulsiones simples, también existen las emulsiones múltiples como por ejemplo las emulsiones de agua/aceite/agua (W/O/W) y las de aceite/agua/aceite (O/W/O).

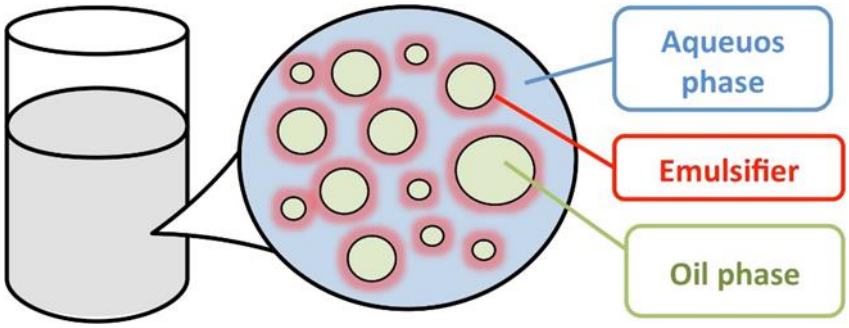

Figura 1.1. Dibujo esquematizado de una emulsión donde se muestran sus partes básicas.

La tecnología de emulsiones se ha usado durante muchos años para crear un amplio abanico de productos comerciales como mayonesas, cremas de ensalada, postres, formulaciones para el lavado, productos farmacéuticos, cosméticos, etc. La mencionada importancia de este tipo de sistemas en la industria justifica la gran cantidad de investigación básica que se realiza para

entender el origen de la inestabilidad de las emulsiones y métodos para prevenirla.

Casi todos los productos basados en emulsiones están formados por una variedad de ingredientes como aceites, emulsificantes, modificadores reológicos, conservantes, agentes antimicrobianos, antioxidantes, sales y agua (Rayner, 2015).

1.1.1. Emulsiones Pickering

El uso de partículas sólidas como estabilizante en emulsiones data de hace un siglo. Ramsen y Pickering fueron los autores de los primeros estudios sobre estos sistemas, a las que llamaron emulsiones Pickering. Los cambios actuales y las tendencias de investigación emergentes usando biopolímeros renovables, sostenibles, "clean-label", y amigables con el medio ambiente han provocado que están partículas se consideren materiales de uso alimentario (Rayner et al., 2014).

Nuevas oportunidades para la estabilización de emulsiones alimentarias usando partículas sólidas están desarrollándose cada vez más. La mayor ventaja de usar estas partículas es su estabilización a largo plazo frente a la coalescencia, sin presentar cambios estructurales durante el almacenamiento. Esto es debido a la efectiva barrera estérica que forman al adsorberse. (Dickinson, 2013; Semenova, 2017). Además, estas emulsiones también han representado una novedad para el transporte de sustancias bioactivas (Li et al., 2020; Mao et al., 2019). Sin embargo, una humectabilidad dual entre las partículas y el aceite y el agua es un factor crítico para obtener emulsiones con alta estabilidad. Por lo tanto, no todos los biopolímeros son adecuados para ser estabilizadores Pickering debido a su limitada humectabilidad y propiedades interfaciales.

Las emulsiones Pickering destinadas al sector alimentario suelen estar basadas en proteínas, polisacáridos o complejos proteína-polisacáridos.

1.2. Formulación de emulsiones alimentarias

1.2.1. Aceites alimentarios

La naturaleza del aceite tiene una gran influencia en la formación y estabilidad de las emulsiones (McClements, 2015). Las diferentes características moleculares de los aceites provocan diferencias en las propiedades como densidad, polaridad, viscosidad y solubilidad en agua. Muchas de estas propiedades tienen una gran influencia en la formación, estabilidad y propiedades de las emulsiones (Piorkowski & McClements, 2014). Por ejemplo, la viscosidad de la fase dispersa influye en la eficiencia de la formación de gotas durante el procesado, ya que cuanto más cercano a la unidad sea la relación entre viscosidad fase dispersa/viscosidad fase continua, más pequeñas serán las gotas producidas (Walstra,1993). La densidad del aceite también determina la velocidad de separaciones gravitacionales en las emulsiones (cremado o sedimentación). Cuanto mayor sea la diferencia de densidades entre en aceite y la fase acuosa, mayor será esta velocidad (McClements, 2015). Además, la concentración de las gotas de aceite en las emulsiones aceite/agua influye en su estabilidad física y sus propiedades reológicas (McClements & Rao, 2011).

Por otro lado, cada vez la sociedad es más consciente sobre como la alimentación repercute a su salud. Por esta razón, se ha producido un incremento en el consumo de alimentos bajos en grasas (Vazquez et al., 2005). El aceite de girasol alto oleico es muy importante para incorporarlo en la dieta de una persona ya que contiene altos porcentajes de acidos grasos monosaturados (MUFA) como el ácido oleico (al menos un 82%). Estos compuestos, al contrario que los ácidos saturados, tienen beneficios e influyen

positivamente en funciones digestivas (Aranceta et al., 2005). El aceite de girasol contiene gran cantidad de ácidos ω-6, un ácido graso poliinsaturado que es considera un ácido graso esencial. Además, posee beneficios para la presión sanguínea y el sistema inmune. Como solo son producidos por las plantas y el fitoplacton, estos ácidos deben ser incorporados en la dieta. Sin embargo, son muy sensibles a la oxidación y el calor. Por lo tanto, se necesita la formación de una barrera física para proteger la fase lipídica. Hasta hoy, se ha investigado diversas proteínas animales para encapsular estos aceites ricos en ácidos grasos poliinsaturados.

1.2.2. Emulsificantes.

Un emulsificante es un compuesto activo superficialmente que se adsorbe en la superficie de las gotas de una emulsión para formar una capa protectora que previene la agregación de gotas y la fusión de éstas. Son ejemplos de emulsificantes ciertas proteínas, polisacáridos, fosfolípidos, tensioactivos y algunas partículas sólidas (Stauffer, 1999; Whitehurst, 2008). Un emulsificante también reduce la tensión interfacial y, por tanto, facilita la formación de gotas durante la homogenización (Walstra, 2002). El tipo de emulsificante usado para estabilizar la emulsión es uno de los factores mas importantes que determina la estabilidad física de la emulsión.

La idoneidad de un emulsificante para un determinado uso se determina por diferentes factores como son la concentración óptima, su capacidad para formar gotas pequeñas durante la homogenización, y su capacidad para prevenir la agregación (McClements, 2015). Estos factores dependen de la naturaleza del emulsificante, pero también influyen las características de la emulsión como el pH, fuerza iónica, el tipo de aceite, y su historia termo-mecánica. Por esta razón, normalmente es complicado predecir el comportamiento de un emulsificante conociendo solo su estructura química (McClements, 2015).

1.2.2.1. Tensioactivos

Un tensioactivo es un tipo de emulsificante que se caracteriza por adsorberse en la interfase de manera reversible. Para caracterizarlos se utiliza un parámetro conocido como el número HLB. Este concepto fue introducido como una escala empírica para describir el balance del tamaño o fuerza de los grupos hidrófilos y lipófilos de una molécula de tensioactivo. Esta escala puede tener valores entre 0 y 20 para tensioactivos no ionicos. Para valores de HLB bajos (<9) se considera un tensioactivo lipófilo (soluble en aceite) mientras que para valores de HLB > 11 se consideran tensioactivos hidrófilos (solubles en agua). Normalmente, los tensioactivos que forman emulsiones agua en aceite tienen valores de HLB entre 3-8 y los que son adecuados para emulsiones aceite en agua presentan valores sobre 8-18.

1.2.2.2. Proteínas.

Cada vez atrae más atención el uso de proteínas en la estabilización de emulsiones debido a la importancia de usar componentes naturales en productos alimentarios. Las proteínas son amigables con el medio ambiente además de ser moléculas anfifílicas con buenas propiedades emulsificantes (Encina et al., 2016) Las proteínas pueden evitar la floculación de las gotas de las emulsiones porque tiene una fuerte tendencia a adsorberse en las interfaces hidrofóbicas-hidrofílicas y luego desplegarse parcialmente formando una fina capa (2-6 nm) que genera una estabilización estérica y electroestática (Dickinson et al., 2010). Las fuerzas de Van der Waals de atracción entre las partículas coloidales superan a la repulsión electroestática, al mismo tiempo que la carga de la proteína pueda ser la principal razón de perder la estabilidad coloidal. En el punto isoeléctrico (pI), las cargas negativas y positivas están igualadas, reduciendo las fuerzas de repulsión electroestática

y causando agregación y precipitación (Vaclavik et al.,2014). Por otro lado, algunos estudios sobre proteínas demuestran la influencia del pH, fuerza iónica, concentración y tratamiento térmico en el pI (Pelegrine & Gasparetto, 2005).

La zeína, una proteína rica en prolina, se extrae del maíz y es un subproducto de la industria del etanol y alimentaria. Aunque originalmente, esta proteína fue considerada un residuo, hoy en día se considera que posee un gran potencial para la ingeniería de tejidos y la administración de fármacos (Reddy & Yang, 2011). Otras características que la hacen muy interesante para su uso es que es biodegradable, amigable con el medioambiente y ha sido reconocida como segura para aplicaciones alimentarias por la Administración de Drogas y Alimentos (Estados Unidos) (Weissmueller et al., 2016). Además, cabe mencionar que la tasa de alergia es mucho menor comparada con otras proteínas más consumidas como la proteína del huevo o la leche (Rona el al., 2007). Este tipo de proteína vegetal es adecuada para la estabilización de emulsiones ya que es insoluble en agua y en los aceites comúnmente usados. Por otro lado, las partículas de zeína han probado su eficacia como estabilizante de emulsiones Pickering (Rutkevičius et al., 2018.). A bajos pH, la zeína forma geles en emulsiones debido a la agregación de partículas. Sin embargo, a altos pHs (pH > pI), las partículas de zeína no muestran agregación (De Folter et al., 2012).

Tradicionalmente, las proteínas y los polisacáridos han coexistido en productos alimentarios debido a su efecto sinérgico en las propiedades reológicas y su estabilidad física (van de Velde et al., 2015). El éxito de esta interacción viene condicionado por el pH, la concentración de ambas y la agregación de la proteína. Hay multitud de estudios sobre la formación de interacciones proteína-polisacárido para mejorar la estabilidad física en emulsiones , como proteína de la leche-goma arábiga, proteína del guisante-

goma arábiga (Liu et al., 2010), proteína de patata-goma guar (Santos et al., 2015), quitosano-alginato (Li et al., 2005).

1.2.3. Polisacáridos

Dos polisacáridos muy usados en la industria alimentaria son la goma xantana y la goma guar. La goma xantana es una macromolécula de origen biológico producida por *Xanthomonas campestris*. Presenta muy buena estabilidad frente a cambios de pH, sal y temperatura. Normalmente, se añade a la fase continua para mejorar la estabilidad de emulsiones aceite en agua formando una red tridimensional tipo gel en la fase acuosa. Esto provoca un retraso en el posible proceso de desestabilización por cremado que pudieran sufrir dichas emulsiones. Recientemente, se ha estudiado un nuevo tipo de goma xantana. Esta nueva versión es llamada goma xantana de alto rendimiento y posee viscosidades mayores y menores valores del módulo viscoso que las disoluciones de goma xantana estándares a la misma concentración (Carmona et al,. 2015) Esto podría ser una ventaja para la formación de complejos con proteínas.

Por otro lado, la goma guar es un polisacárido no iónico ampliamente conocido que se obtiene de las semillas de *Cyamopsis tetragonolobus* o *Cyamopsis psoraloides* de la familia de las leguminosas. Esta goma es muy utilizada también en productos alimentarios (Heyman et al., 2014; Santos et al., 2015). Su estructura está formada por cadenas lineales de D-manosa y D-galactosa (Peso molecular: 2.2 kDa).

El uso de nuevas macromoléculas como estabilizantes es necesario para satisfacer las necesidades de un mercado en expansión que busca fuentes eficientes en la industria. Los polisacáridos secretados por microrganismos son considerados fuentes renovables y son usados en muchos campos diferentes debido a sus propiedades como estabilizantes, emulsificantes y espesantes

(Hamcerencu et al.,2009; Xu et al., 2019). Estos polisacáridos microbianos poseen multitud de grupos oxígeno y hidroxilos además de grupos carboxilatos que conllevan que se produzcan fuerzas dipolares, ión-dipolo y puentes de hidrógeno consigo mismo o con otros compuestos en disolución (Brewer et al., 1973). La goma diutan, que es secretada por el microorganismo *Sphingomonas sp*., es un polisacárido microbiano considerado biodegrable y biocompatible. Su estructura consiste en una combinación de unidades de β-D-glucosa, β-D-ácido gluconico y α-L-ramnosa (Peso molecular: 2.88 - 5.18 kDa). Este espesante novedoso ha sido recientemente usado para evitar la desestabilización de nanoemulsiones formuladas con aceite de limón (Santos et al., 2019). Sin embargo, su uso en combinación con proteínas no ha sido estudiado hasta la fecha.

1.2.3.1. Interacción proteína-polisacárido

Las combinaciones de proteína-polisacárido permiten diseñar un conjugado anfifilico que puede anclarse a la interfase aceite-agua mediante las regiones hidrofóbicas de la proteína formando una capa viscoelástica y con la región que no se adsorbe del polisacárido que provocaría estabilización esterica. Hay dos tipos diferentes de interacciones proteína-polisacárido: covalentes o no covalentes. La unión covalente se obtiene mediante una reacción tipo llamada Maillard que se da en aquellos complejos con alta estabilidad térmica. Las condiciones (pH y temperatura) pueden determinarse para obtener la deseada reacción. Las fuerzas para las uniones no covalentes son electroestáticas, hidrofóbicas, enlaces de hidrógeno y fuerzas de Van der Waals. Estas uniones no covalentes pueden generar coacervatos que son muy útiles para cambiar texturas en productos alimentarios o para encapsular compuestos activos.

1.3. Preparación de emulsiones

La formación de una emulsión es normalmente la combinación de dos procesos que compiten entre ellos: la ruptura de la interfase de las gotas y la unión de estas (coalescencia).

Los métodos para preparar emulsiones pueden ser divididos en dos categorías diferentes: procesos de baja o de alta energía. Los métodos de alta energía utilizan equipos mecánicos (homogeneizadores) que generan fuerzas disruptivas intensas capaces de romper y entremezclar la fase continua y la fase dispersa. Ejemplos de estos equipos son los mezcladores de alta cizalla, homogeneizadores de alta presión, microfluidizers, y ultrasonidos (Leong et al, 2009; Wooster et al, 2008; Gutiérrez et al, 2008). Las características que tendrán las gotas creadas usando procesos de alta energía dependerán del equipo usados, las condiciones de preparación y la formulación usada (McClements, 2012).

Los métodos de baja energía son aquellos que usan la formación espontanea de gotas en sistemas tensioactivo-aceite-agua cuando se alteran la disolución o las condiciones medioambientales, por ejemplo, una inversión de fases o métodos de emulsificación espontaneas (Anton et al., 2008).

1.3.1. Principios de la formación de emulsiones usando métodos de alta energía

La formación de una emulsión se puede dividir en dos etapas: primero, la creación de las gotas, segundo, la reducción del tamaño de las gotas existentes. Estas etapas se llaman primera y segunda homogeneización, respectivamente. La preparación de una emulsión puede llevarse a cabo en una sola fase o en dos, dependiendo de la naturaleza del disolvente y fase acuosa, la aplicación de la emulsión y el método de preparación de la misma. Normalmente, se usa un tipo de homogeneizador en la primera

homogeneización y otro tipo diferente en la segunda homogeneización (figura 1.2).

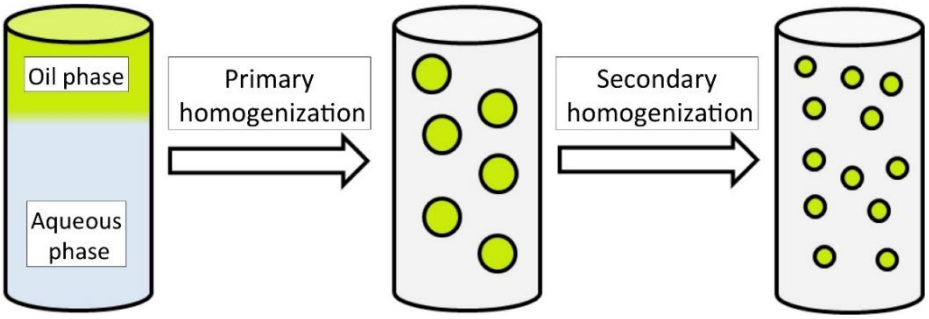

Figura 1.2. Esquema del proceso de emulsificación dividido en dos etapas: homogenización primaria y homogenización secundaria.

Los procesos físicos que ocurren durante la homogeneización se pueden explicar teniendo en cuenta los cuatro ingredientes principales de ésta: la fase dispersa (el aceite en una emulsión aceite en agua), la fase continua (el agua en una emulsión aceite en agua), un tensioactivo o proteína y la energía suministrada. Las tecnologías de emulsificación estudian como la energía suministrada es capaz de crear y estabilizar nuevas áreas interfaciales. Cuando el aceite y el agua se mezclan en un recipiente tienden a adoptar el estado termodinámicamente más estable, minimizando el contacto entre los dos líquidos inmiscibles. Esta es la razón por la que las gotas de las emulsiones tienden a ser esféricas. Los tensioactivos se adsorben en la superficie de las gotas durante la homogeneización formando una capa de protección que previene que las gotas vuelvan a fusionarse.

1.3.2. Equipos de homogeneización

- Rotores-estator.

Los equipos llamados rotores-estator son los más usados para preparar emulsiones y están caracterizados por un rotor de alta velocidad muy cerca de

un elemento fijo llamado estator. La complejidad de estos sistemas varía desde agitadores simples hasta rotores-estator con dos partes móviles. Uno de los principales beneficios de estos equipos es el hecho de que pueden trabajar en continuo, semicontinuo o discontinuo (Rayner, 2015).

El modo discontinuo ofrece la ventaja de que se pueden realizar procesos en paralelo. De este modo, los compuestos pueden ser mezclados, pasteurizados, homogeneizados y enfriados en un mismo vaso. Esto se usa especialmente para productos tipos mayonesa o salsas de la industria alimentaria. Sin embargo, este tipo de equipos en discontinuo presenta la desventaja de que el volumen total del producto puede no ser procesado de la misma manera. Esto puede provocar distribuciones anchas de tamaño de gota. Por lo tanto, las emulsiones con tamaño de gota submicrónico suelen ser preparadas en procesos continuos.

Por otro lado, en los molinos coloidales o equipos basados en discos dentados, las gotas se crean en el hueco entre la parte fija y la parte que se mueve. En los molinos coloidales, las gotas se crean y rompen en el hueco cónico, el cual puede ser liso o serrado con varios diseños. En este caso, el esfuerzo que causa la perturbación viene determinado por el ancho del hueco (normalmente 100-300 micras), el radio del rotor, la velocidad de rotación (5-40 m/s) y la velocidad del líquido a través del hueco (4-20000 l/h) (Karbstein & Schubert, 1995). Estos equipos son los más adecuados para la producción de productos de viscosidad alta o intermedia y que pueden llegar a rangos de 1 a 5 micras de tamaño de gota (McClements, 2015). Los equipos basados en dientes dentados son muy similares a los molinos coloidales, excepto que el flujo no está acotado.

- Equipos de ultrasonidos

Estos equipos están basados en la creación de ondas de alta intensidad para generar gradientes de cizalla y presión intensos en el líquido y así crear gotas principalmente por cavitación y flujo turbulento (McClements, 2015). Hay dos métodos normalmente usados en la industria para producir ondas de ultrasonidos. Uno de ellos es el uso de transductores piezoeléctricos para baños (sistemas discontinuos) pequeños (desde unos pocos centímetros cúbicos a unos cientos de ellos). Por otro lado, existen los basados en generadores "jet" que se usan a grandes escalas donde un chorro de pre-emulsión es obligado a incidir en una paleta afilada. El flujo del "jet" causa que la paleta vibre muy rápidamente, generando un campo de ultrasonidos que rompe las gotas que están inmediatamente cerca. Estos equipos pueden producir volúmenes grandes de producto con velocidades de flujo entre 1 a 500000 l/h. Los factores que influyen en la creación de gotas, son la intensidad, duración y frecuencia de las ondas de ultrasonido en relación con el volumen de la emulsión (McClements, 2015).

- Homogeneizadores de válvula a alta presión

Estos homogeneizadores se usan para reducir el tamaño de gota de gotas pre-existentes o para romper partículas como células o macromoléculas. La aplicación fundamental es la reducción del tamaño de las gotas de emulsiones. Se muestra un esquema de este equipo en la figura 1.3. Los fluidos entran por la válvula desde abajo a través de un tubo de alimentación. El "forcer" (parte alta de la figura) es la parte que fuerza al flujo a pasar por un hueco estrecho creado entre el "forcer" y el asiento (parte inmóvil). A menudo, el asiento está inclinado, dándole altura a la región estrecha del hueco/canal en la parte de arriba, referido aquí como la cámara de entrada. Descendiendo por el hueco, el fluido se expande, referido aquí como la cámara de salida. Anillos de impacto específicos se montan a veces en la válvula para modificar la geometría de la cámara de salida. La altura del canal, h, puede variar bajando

o subiendo la posición del forcer. Las fuerzas de fricción se incrementan cuando decrece la altura del canal, y de este modo se requiere mayor presión para una altura pequeña del canal/hueco. En la práctica, la presión de homogeneización se ajusta por la fuerza que aplica el forcer, el cual fija la altura del canal. Las presiones de homogeneización suelen estar en un rango entre 5-40 MPa para aplicaciones en la industria alimentaria, como productos de uso diario como la leche, y por encima de 100 MPa para aplicaciones especiales como la rotura celular (Middelberg, 1995) o de macromoléculas (Floury et al., 2002).

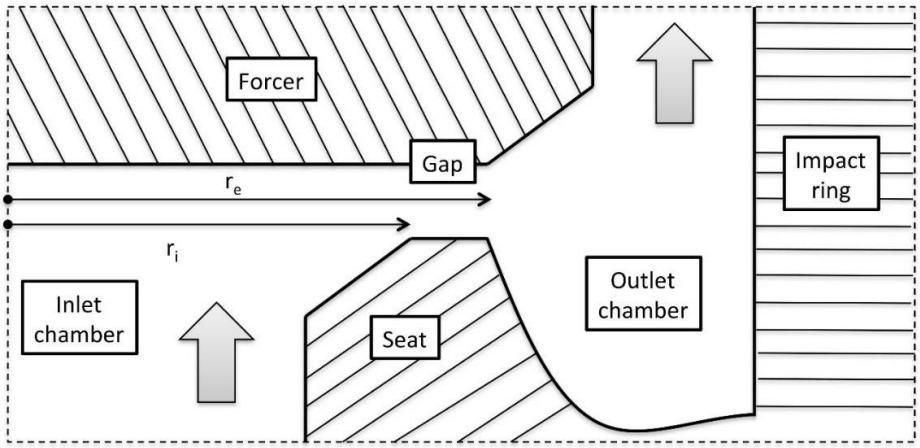

Figura 1.3. Esquema de un homogeneizador a presión.

- Microfluidización

Los microfluidizers convencionales se pueden considerar como una homogeneización secundaria basada en microcanales ya que la alimentación al reservorio de entrada es una emulsión con tamaño de gota relativamente grande y premezclada. (McClements, 2015; Galooyak & Dabir, 2015).

La ruptura de las gotas ocurre en el microfluidizer debido al impacto de dos jets que inciden en la cámara de interacción llegando a presiones similares a aquellas obtenidas en un homogeneizador de valvula a presión. En este

proceso, la alta cizalla crea una alta turbulencia. Como consecuencia, esto fuerza al flujo de emulsión a pasar a través de los microcanales que están perfectamente definidos. Como resultado, se obtienen emulsiones con tamaño de gota extraordinariamente pequeños. De hecho, al comparar las distribuciones de tamaño de gota obtenidas con microfluidizer y homogeneizadores de alta presión, se observa que se obtienen distribuciones más estrechas al usar el quipo basados en microcanales (Strawbridge et al, 1995; Perrier-Cornet et al, 2005). Ademas, generalmente los tamaños de gota disminuyen con la presión usada (Qian & McClements, 2011). Sin embargo, esto no es siempre así. Puede darse el caso que a presiones altas se produzcan fenómenos de recoalescencia, debido a un sobreprocesado (Jafari et al., 2008). En estos casos, no será favorable el uso de presiones altas o incluso en casos muy específicos el uso de microfluidizer.

Las cámaras de interacción se pueden dividir en tipo Z y en tipo Y. Las tipo Y son las más usadas en la preparación de emulsiones aceite en agua. En esta tesis doctoral se ha empleado una cámara F12Y. En ella, la preemulsión se separa en dos canales e impacta en la zona de alto impacto que mide 75 micras. Adicionalmente, también se ha usado, dispuesta en serie, la cámara H30Z que posee un diámetro de 200 micras. Además de sus diferentes geometrías y tamaño de microcanales, estas cámaras difieren en las velocidades de cizalla que son capaces de alcanzar: $8 \cdot 10^6$ s^{-1} en el caso de la F12Y y $2 \cdot 10^6$ s^{-1} en el caso de la H30Z.

Recientemente se han publicado estudios que muestran las ventajas de usar estas cámaras en serie para la preparación de nanoemulsiones (Trujillo-Cayado et al., 2018).

1.4. Propiedades de las emulsiones

1.4.1. Propiedades interfaciales.

Los tensioactivos y proteínas son capaces de reducir la tensión interfacial, γ, entre el aceite y el agua, lo cual puede traducirse en la creación de gotas más pequeñas. La cantidad de tensioactivo o proteína que se requiere para producir el tamaño de gota mínimo dependerá de su actividad (a) en el seno del sistema. Esta relación viene determinada por la ecuación de adsorción de Gibbs:

$-d\gamma = RT \cdot \Gamma \cdot d\ ln\ a$ (Ecuación 1.1)

Donde R es la constante de los gases ideales, T en la temperatura en grados Kelvin, y Γ es el número de moles adsorbidos por unidad de área en la interfase. Γ aumenta con la concentración de tensioactivos hasta que llega a un valor constante (la adsorción se satura). El valor de γ obtenido depende de la naturaleza del aceite y del tensioactivo (Tadros, 2009). Por ejemplo, pequeñas moléculas de tensioactivos no iónicos reducen la tensión interfacial en un mayor grado que los tensioactivos poliméricos como el polivinil alcohol.

1.4.2. Distribución del tamaño de gota. (DTG)

Una de las propiedades importantes en las emulsiones es su distribución del tamaño de gota, la cual define la concentración de gotas en los diferentes tamaños de gotas (McClements, 2015). La concentración de gotas se presenta normalmente como porcentaje en volumen o porcentaje en número de gotas en función del tamaño. Las gotas más grandes que están presentes en la emulsión no se observan en la DTG cuando se representa en porcentaje en número, incluso si el porcentaje de estás sea un 25% en volumen.

Las DTG de las emulsiones pueden ser definidas como monomodales, biomodales o multimodales dependiendo de si hay uno, dos o varios picos en la DTG. En algunas ocasiones es más conveniente representar esta información como una medida de la tendencia central y de la anchura del pico. Para ello, se suelen utilizar la media, la mediana o la moda del tamaño de gota.

Para dar un valor de la anchura de pico o anchura de la distribución se suele usar la desviación estándar o el parámetro llamado span (Walstra, 2002).

$$Span = \frac{D(v,0.9)-D(v,0.1)}{D(v,0.5)} (Ecuación\ 1.2)$$

donde D(v, 0.9), y D(v, 0.1) son los diámetros de gota por debajo de los cuales se encuentran el 90% y el 10%, respectivamente, del volumen de las partículas y D(v, 0.5), el 50%, o mediana de la distribución.

Los diámetros medios más usados suelen ser el diámetro de Sauter o también llamado diámetro medio de superficie ($D_{3,2}$) o el diámetro volumétrico ($D_{4,3}$).

$$D_{3,2} = \frac{\sum n_i d_i^3}{\sum n_i d_i^2} \ (Ecuación\ 1.3)$$

$$D_{4,3} = \frac{\sum n_i d_i^4}{\sum n_i d_i^3} \ (Ecuación\ 1.4)$$

donde d_i es el diámetro de la partícula y n_i el porcentaje de partículas que presenta este diámetro.

Normalmente, el diámetro volumétrico es más sensible que el diámetro de Sauter a la presencia de gotas grandes. Diferencias llamativas entre ambos diámetros suelen indicar que la DTG es ancha o multimodal.

1.4.3. Reología de emulsiones

La reología es la ciencia que estudia la deformación y como fluyen los materiales. Todas las formas del comportamiento frente al flujo están entre dos comportamientos extremos: el flujo de líquidos ideales y la deformación de los sólidos elásticos ideales. Los líquidos ideales siguen la ley de Newton donde el esfuerzo es proporcional a la velocidad de cizalla. Por el contrario, el comportamiento sólido se basa en la ley de Hooke donde el esfuerzo es proporcional a la deformación. El comportamiento real de los materiales se

basa en la combinación de ambos comportamientos (el viscoso y el elástico). Debido a ello, se llaman materiales viscoelásticos (Macosko, 1994).

Las propiedades reológicas determinan en gran medida la posible aplicación técnica de los sistemas basados en emulsiones. Además, también es necesario conocer estas propiedades para asegurar la eficiencia, consumo energético, velocidades de bombeo para el mezclado, el flujo en tuberías del producto y el empaquetado, entre otros. Por otro lado, la apreciación del consumidor sobre la emulsión comercial es muy importante como la cremosidad, el cuerpo y consistencia, pudiendo así modificar las preferencias de éste. Estas propiedades están íntimamente relacionadas con la reología (Barnes, 1994).

Los parámetros principales que influyen en la reología de una emulsión son:

i. La reología de la fase continua
ii. Naturaleza de las gotas, distribución de tamaños, viscosidad interna, concentración
iii. Naturaleza de las interacciones gota-gota

La viscosidad de un sistema disperso de gotas viene descrita por la ecuación de Krieger-Dougherty modificada, conocida como ecuación de Quemada:

$$\eta = \eta_c \left(\frac{\Phi}{\Phi_m}\right)^{-2} \quad (Ecuación\ 1.5)$$

Donde η es la viscosidad de la emulsión (normalmente a una velocidad de cizalla específica); ηc es la viscosidad de la fase continua, Φ es el volumen de fase dispersa y Φm es el volumen máximo de fase dispersa cuando la viscosidad diverge. Esto muestra que:

i. La sensibilidad de la viscosidad de la fase continua es multiplicativa, no aditiva y que, por ejemplo, la temperatura tiene la misma tendencia

ii. La sensibilidad del volumen de fase dispersa comienza a ser muy importante cuando es mayor de 0.3 y
iii. Que para volúmenes mayores la viscosidad es fuertemente influida por Φ

A menudo se habla de que a menores tamaños de gota, existe un aumento de la viscosidad. Normalmente este hecho se hace más acusado cuando el tamaño de gota es menor de 1 micra ya que son más importantes las interacciones gota-gota. Sin embargo, emulsiones con tamaños de gota mayores muestran similares tendencias. Esto puede ser debido a primero a que la deformabilidad de las gotas disminuye con el tamaño de gota y segundo, que al incrementar la anchura de la distribución de gota, la fracción máxima de empaquetado aumenta; lo cual significa un descenso en la viscosidad.

La reología de las emulsiones es desde un punto de vista aplicado una herramienta muy importante para detectar fenómenos de desestabilización. Por ejemplo, medir la viscosidad a velocidades de cizalla bajas puede predecir el cremado. Además, esta medida con el tiempo de envejecimiento, puede detectar aumentos del tamaño de gota (Tadros, 2010).

1.4.4. Estabilidad física

Las emulsiones son sistemas termodinámicamente inestables. Esta inestabilidad es causada por diferentes mecanismos de desestabilización que conlleva la pérdida del estado disperso. Los mecanismos de desestabilización que pueden sufrir las emulsiones son: cremado, sedimentación, floculación. Coalescencia, maduración de Ostwald e inversión de fase.

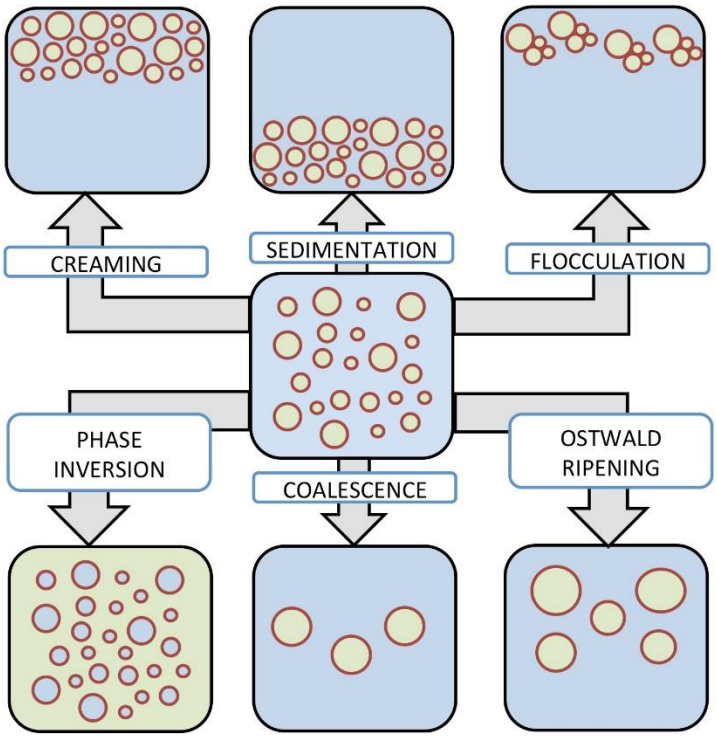

Figura 1.4. Mecanismos de desestabilización en emulsiones.

1.4.4.1. Cremado/sedimentación

Este proceso de desestabilización es el resultado de las fuerzas externas, concretamente de la fuerza de la gravedad o fuerza centrífuga. Cuando estas fuerzas son mayores que el movimiento Browniano, existe un gradiente de concentración que hace que las gotas con mayor tamaño se desplacen hacia la zona alta del bote donde se encuentre la emulsión mientras que las gotas más pequeñas se mueven hacia abajo. Esto ocurre cuando la densidad de la fase dispersa es menor que la de la fase continua. Este mecanismo conlleva un cambio en la concentración de aceite en emulsiones aceite en agua dependiendo de la altura. Este cambio puede provocar otros fenómenos de desestabilización como la floculación o la coalescencia.

En principio, la estabilidad a largo plazo de las emulsiones debido a las separaciones gravitacionales se puede predecir con la ley de Stokes o sus modificaciones (McClements, 2015). Para ello, se necesita información sobre la densidad de las fases continua y dispersa, el tamaño de gota y las propiedades reológicas de la fase continua. Esta ecuación predice la velocidad a la cual ocurre la separación gravitacional en emulsiones (ecuación 1.5).

$$\nu_{Stokes} = -\frac{2\,g\,r^2(\delta_2-\delta_1)}{9\eta_1} \quad (Ecuación\ 1.6)$$

Donde ν_{Stokes} es la velocidad de cremado, r es el radio de la gota, g es la aceleración de la gravedad, δ es la densidad, η es la viscosidad y los subíndices 1 y 2 se refieren a la fase continua y dispersa, respectivamente. El signo de la velocidad determina si la gota se mueve hacia arriba (+) o hacia abajo (-); es decir, si la gota crema o sedimenta, respectivamente. Si las gotas se mueven hacia arriba, abajo del bote aparece una capa clarificada y arriba una capa enriquecida en gotas llamada capa de cremado. Esta última aparece al encontrarse muy juntas todas las gotas concentradas. La concentración de gotas en la capa intermedia suele ser similar a la emulsión original, y se llama capa de emulsión. En una emulsión monodispersa, la capa clarificada suele ser transparente porque no contiene gotas y la capa cremada suele ser ópticamente opaca.

Se usa el índice de cremado (CI) como un parámetro para caracterizar y cuantificar el cremado que ocurre en una emulsión (McClements, 2007):

$$CI = \frac{H_S}{H_E} \cdot 100\ (Ecuación\ 1.7)$$

Siendo HE la altura total de la emulsión y HS la altura de la capa cremada (figura 1.5).

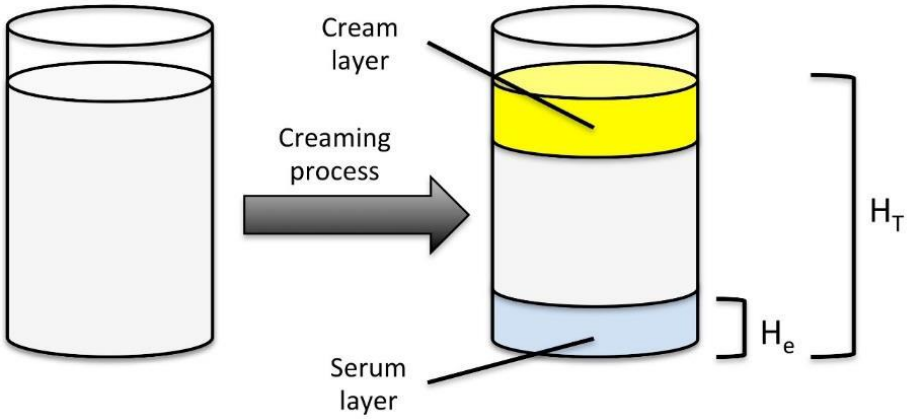

Figura 1.5. Esquema del proceso de cremado en emulsiones.

1.4.4.2. Floculación

La floculación es un proceso por el cual dos o más gotas se asocian unas con otras, pero manteniendo cada una su integridad individual. Esto ocurre cuando las fuerzas de atracción entre las gotas dominan a las fuerzas de repulsión de largo alcance, pero no a las de corto alcance. Por lo tanto, las gotas permanecen muy cerca unas de otras (floculan) pero no se fusionan (coalescencia). Normalmente, la floculación no es buena para la estabilidad de las emulsiones, aunque en algunos casos puede ser deseable. En emulsiones relativamente diluidas (como refrescos, leches de formula y bebidas nutricionales), la floculación conlleva un incremento en el tamaño de gota que acelera la separación gravitacional, lo cual reduce la vida media de las emulsiones (Chanamai et al, 2000). Por otro lado, la floculación también causa un incremento en la viscosidad de la emulsión (un “espesamiento”), e incluso puede provocar la formación de un gel en una emulsión lo suficientemente concentrada (Demetriades & McClements, 1999; Quemada & Berli, 2002).

En algunos productos, una floculación controlada puede ser una ventaja ya que conlleva la generación de una textura deseable (Parker et al, 1995).

La tendencia a la floculación de una emulsión depende principalmente del balance entre fuerzas atractivas y repulsivas. Las principales fuerzas atractivas en emulsiones son las fuerzas de Van der Waals, las fuerzas hidrofóbicas y de vaciamiento ("depletion forces"), mientras que las de repulsión son fuerzas electroestáticas y estéricas. La velocidad a la que ocurre la floculación se puede caracterizar en términos de la frecuencia de colisión gota-gota y la eficiencia de colisión. La frecuencia de colisión (fc) es el número de gotas que colisionan por unidad de volumen y por unidad de tiempo. Dependiente principalmente del mecanismo predominante del movimiento de gotas: movimiento Browniano o fuerzas mecánicas. La frecuencia de colisión aumenta al incrementar la concentración de las gotas, al disminuir el tamaño de gota y al disminuir la viscosidad de la fase continua (McClements, 2015).

1.4.4.3. Coalescencia.

La coalescencia es el proceso por el cual dos o más gotas de líquido se fusionan para formar una sola. La coalescencia puede provocar que las gotas de una emulsión cremen o sedimenten más rápido debido al aumento de tamaño. En emulsiones aceite en agua, la coalescencia suele conllevar la formación de una capa de aceite en la parte alta de la emulsión. Esto es conocido como "oiling-off". En las emulsiones agua en aceite, este mecanismo de desestabilización conlleva la acumulación de agua en el fondo de la emulsión.

Cuando la coalescencia es el principal mecanismo de desestabilización, su evolución con el tiempo puede seguir diferentes comportamientos: desde un perfecto crecimiento homogéneo (distribución monomodal cuyo tamaño medio se incrementa con el tiempo) hasta un crecimiento fuertemente heterogéneo (distribuciones plurimodales con la posibilidad de una separación temprana). Excepto en casos particulares, por regla general la coalescencia suele ser heterogénea (Deminiere, 1999a; Deminiere, 1999b; Schmitt, 2004).

La coalescencia tiende a ocurrir después de que las gotas hayan estado en contacto por periodos extensos (por ejemplo, en una capa cremada, en flóculos o en emulsiones concentradas) (van Aken & van Vliet, 2002).

1.4.4.4. Maduración de Ostwald.

La maduración de Ostwald es el proceso por el cual las gotas con tamaño mayor crecen a expensas de las gotas pequeñas debido al transporte de masa de la fase dispersa de una gota a otra a través de la fase continua (Kabalnov, 2001; Kabalnov & Weers, 1996).

La coalescencia suele estar relacionada con distribuciones bimodales (coalescencia heterogénea) mientras que la maduración de Ostwald con distribuciones monomodales que perduran con el tiempo (Kabalnov, 2001). Además, el cubo del tamaño medio aumenta linealmente con el tiempo en el caso de la maduración de Ostwald siguiendo la conocida teoría de Lifshitz-Slyozov-Wagner (LSW). Este modelo se basa en que la difusión del aceite a través de la fase continua determina la velocidad del proceso (Ardell, 1972; Solans, 2005). Esta teoría predice que, a tiempos suficientemente largos, existe una velocidad de maduración de Ostwald contante que viene determinada por el crecimiento en el cubo del radio de gota medio basado en número ($\bar{r}$).

$$\omega_T = \frac{d\bar{r}^3}{dt} = \frac{8\gamma c_w^{eq} D_w V_m}{9kT} \quad (Ecuación\ 1.8)$$

Donde, γ es la tensión interfacial entre el aceite y el agua en la superficie de la gota, V_m es el volumen molecular del aceite, $c_w{}^{eq}$ es la solubilidad del aceite en el agua, D_w es la difusividad del aceite, k es la constante de Boltzmann y T es la temperatura en grado Kelvin.

1.4.4.5. Inversión de fases.

Este mecanismo de desestabilización es definido como aquel que existe un intercambio entre la fase dispersa y la fase continua. Por ejemplo, una emulsión aceite en agua se convierte en una emulsión agua en aceite con el tiempo o por un cambio en determinadas condiciones.

Las teorías más tradicionales apuntan a que este mecanismo está basado en parámetros de empaquetamiento. Cuando la concentración de fase dispersa excede el empaquetamiento máximo (0.64 en empaquetamiento desordenado y 0.74 para empaquetamiento hexagonal), ocurre la inversión de fases. Sin embargo, estas teorías tienen fallos ya que en muchas emulsiones se da la inversión de fases por debajo del empaquetamiento máximo por un cambio de las características del tensioactivo al variar alguna condición. Por ejemplo, muchas emulsiones invierten de fase a una temperatura crítica que depende del número HLB del tensioactivo y de la presencia de electrolitos (Tadros, 2013).

Referencias

Anton, N., Benoit, J. P., & Saulnier, P. (2008). Design and production of nanoparticles formulated from nano-emulsion templates—a review. Journal of Controlled Release, 128(3), 185-199.

Aranceta-Bartrina, J., Serra-Majem, L., Foz-Sala, M., Moreno-Esteban, B., & SEEDO, G. C. (2005). Prevalencia de obesidad en España. Medicina clínica, 125(12), 460-466.

Ardell, A. J. (1972). The effect of volume fraction on particle coarsening: theoretical considerations. Acta metallurgica, 20(1), 61-71.

Barnes, H. A. (1994). Rheology of emulsions—a review. Colloids and Surfaces A: Physicochemical and Engineering Aspects, 91, 89-95. Bigorra, J. (2010).

Innovative solvents based on renewable raw materials. In Proceedings of 40th Annual Meeting of CED. Barcelona, Spain.

Brewer, C. F., Sternlicht, H., Marcus, D. M., & Grollman, A. P. (1973). Interactions of saccharides with concanavalin A. Mechanism of binding of α- and β-methyl D-glucopyranoside to concanavalin A as determined by carbon-13 nuclear magnetic resonance. Biochemistry, 12(22), 4448-4457.

Carmona, J. A., Lucas, A., Ramírez, P., Calero, N., & Muñoz, J. (2015). Nonlinear and linear viscoelastic properties of a novel type of xanthan gum with industrial applications. Rheologica Acta, 54(11), 993-1001.

Chanamai, R., & McClements, D. J. (2000). Creaming stability of flocculated monodisperse oil-in-water emulsions. Journal of Colloid and Interface Science, 225(1), 214-218.

de Folter, J. W., van Ruijven, M. W., & Velikov, K. P. (2012). Oil-in-water Pickering emulsions stabilized by colloidal particles from the water-insoluble protein zein. Soft Matter, 8(25), 6807-6815.

Demetriades, K., & McClements, D. J. (1999). Ultrasonic attenuation spectroscopy study of flocculation in protein stabilized emulsions. Colloids and Surfaces A: Physicochemical and Engineering Aspects, 150(1), 45-54.

Deminiere, B., Colin, A., Leal-Calderon, F., Muzy, J. F., & Bibette, J. (1999a). Cell growth in a 3D cellular system undergoing coalescence. Physical review letters, 82(1), 229.

Deminiere, B., Stora, T., Colin, A., Leal-Calderon, F., & Bibette, J. (1999b). Surfactant phase transition inducing coalescence in dense emulsions. Langmuir, 15(7), 2246-2249.

Dickinson, E. (2010). Flocculation of protein-stabilized oil-in-water emulsions. Colloids and Surfaces B: Biointerfaces, 81(1), 130-140.

Dickinson, E. (2013). Stabilising emulsion-based colloidal structures with mixed food ingredients. Journal of the Science of Food and Agriculture, 93(4), 710-721.

Encina, C., Vergara, C., Giménez, B., Oyarzún-Ampuero, F., & Robert, P. (2016). Conventional spray-drying and future trends for the microencapsulation of fish oil. Trends in Food Science & Technology, 56, 46-60.

Floury, J., Desrumaux, A., Axelos, M. A., & Legrand, J. (2002). Degradation of methylcellulose during ultra-high pressure homogenisation. Food Hydrocolloids, 16(1), 47-53.

Galooyak, S. S., & Dabir, B. (2015). Three-factor response surface optimization of nano-emulsion formation using a microfluidizer. Journal of food science and technology, 52(5), 2558-2571.

Gutiérrez, J. M., González, C., Maestro, A., Sole, I., Pey, C. M., & Nolla, J. (2008). Nano-emulsions: New applications and optimization of their preparation. Current Opinion in Colloid & Interface Science, 13(4), 245-251.

Hamcerencu, M., Desbrieres, J., Popa, M., & Riess, G. (2009). Stimuli-sensitive xanthan derivatives/N-isopropylacrylamide hydrogels: influence of cross-linking agent on interpenetrating polymer network properties. Biomacromolecules, 10(7), 1911-1922.

Heyman, B., De Vos, W. H., Depypere, F., Van der Meeren, P., & Dewettinck, K. (2014). Guar and xanthan gum differentially affect shear induced breakdown of native waxy maize starch. Food Hydrocolloids, 35, 546-556.

Jafari, S. M., Assadpoor, E., He, Y., & Bhandari, B. (2008). Re-coalescence of emulsion droplets during high-energy emulsification. Food hydrocolloids, 22(7), 1191-1202.

Kabalnov, A. (2001). Ostwald ripening and related phenomena. Journal of Dispersion Science and Technology, 22(1), 1-12.

Kabalnov, A., & Weers, J. (1996). Kinetics of mass transfer in micellar systems: surfactant adsorption, solubilization kinetics, and ripening. Langmuir, 12(14), 3442-3448.

Karbstein, H., & Schubert, H. (1995). Developments in the continuous mechanical production of oil-in-water macro-emulsions. Chemical Engineering and Processing: Process Intensification, 34(3), 205-211.

Leong, T. S. H., Wooster, T. J., Kentish, S. E., & Ashokkumar, M. (2009). Minimising oil droplet size using ultrasonic emulsification. Ultrasonics Sonochemistry, 16(6), 721-727.

Li, S., Zhang, B., Li, C., Fu, X., & Huang, Q. (2020). Pickering emulsion gel stabilized by octenylsuccinate quinoa starch granule as lutein carrier: Role of the gel network. Food chemistry, 305, 125476.

Li, Z., Ramay, H. R., Hauch, K. D., Xiao, D., & Zhang, M. (2005). Chitosan–alginate hybrid scaffolds for bone tissue engineering. Biomaterials, 26(18), 3919-3928.

Liu, S., Elmer, C., Low, N. H., & Nickerson, M. T. (2010). Effect of pH on the functional behaviour of pea protein isolate–gum Arabic complexes. Food Research International, 43(2), 489-495.

Macosko, C. W., & Rheology, P. (1994). Measurements and Applications. VCH, New York.

Mao, L., Lu, Y., Cui, M., Miao, S., & Gao, Y. (2020). Design of gel structures in water and oil phases for improved delivery of bioactive food ingredients. Critical reviews in food science and nutrition, 60(10), 1651-1666.

McClements, D. J. (2004). Protein-stabilized emulsions. Current opinion in colloid & interface science, 9(5), 305-313.

McClements, D. J. (2007). Critical review of techniques and methodologies for characterization of emulsion stability. Critical Reviews in Food Science and Nutrition, 47(7), 611-649.

McClements, D. J. (2012). Advances in fabrication of emulsions with enhanced functionality using structural design principles. Current Opinion in Colloid & Interface Science, 17(5), 235-245.

McClements, D. J. (2015). Food emulsions: principles, practices, and techniques. CRC press.

McClements, D. J., & Rao, J. (2011). Food-grade nanoemulsions: formulation, fabrication, properties, performance, biological fate, and potential toxicity. Critical reviews in food science and nutrition, 51(4), 285-330.

Middelberg, A. P. (1995). Process-scale disruption of microorganisms. Biotechnology advances, 13(3), 491-551.

Morrison, I. D., & Ross, S. (2002). Colloidal dispersions: suspensions, emulsions, and foams. Wiley-Interscience.

Parker, A., Gunning, P. A., Ng, K., & Robins, M. M. (1995). How does xanthan stabilise salad dressing?. Food Hydrocolloids, 9(4), 333-342.

Pelegrine, D. H. G., & Gasparetto, C. A. (2005). Whey proteins solubility as function of temperature and pH. LWT-Food Science and Technology, 38(1), 77-80.

Perrier-Cornet, J. M., Marie, P., & Gervais, P. (2005). Comparison of emulsification efficiency of protein-stabilized oil-in-water emulsions using jet,

high pressure and colloid mill homogenization. Journal of Food Engineering, 66(2), 211-217.

Piorkowski, D. T., & McClements, D. J. (2014). Beverage emulsions: Recent developments in formulation, production, and applications. Food Hydrocolloids, 42, 5-41.

Qian, C., & McClements, D. J. (2011). Formation of nanoemulsions stabilized by model food-grade emulsifiers using high-pressure homogenization: factors affecting particle size. Food Hydrocolloids, 25(5), 1000-1008.

Quemada, D., & Berli, C. (2002). Energy of interaction in colloids and its implications in rheological modeling. Advances in colloid and interface science, 98(1), 51-85.

Rayner, M., & Dejmek, P. (Eds.). (2015). Engineering Aspects of Food Emulsification and Homogenization. CRC Press.

Rayner, M., Marku, D., Eriksson, M., Sjöö, M., Dejmek, P., & Wahlgren, M. (2014). Biomass-based particles for the formulation of Pickering type emulsions in food and topical applications. Colloids and Surfaces A: Physicochemical and Engineering Aspects, 458, 48-62.

Reddy, N., & Yang, Y. (2011). Potential of plant proteins for medical applications. Trends in biotechnology, 29(10), 490-498.

Rona, R. J., Keil, T., Summers, C., Gislason, D., Zuidmeer, L., Sodergren, E., ... & Madsen, C. (2007). The prevalence of food allergy: a meta-analysis. Journal of Allergy and Clinical Immunology, 120(3), 638-646.

Rutkevičius, M., Allred, S., Velev, O. D., & Velikov, K. P. (2018). Stabilization of oil continuous emulsions with colloidal particles from water-insoluble plant proteins. Food Hydrocolloids, 82, 89-95.

Santos, J., Calero, N., Guerrero, A., & Muñoz, J. (2015). Relationship of rheological and microstructural properties with physical stability of potato protein-based emulsions stabilized by guar gum. Food hydrocolloids, 44, 109-114.

Santos, J., Jiménez, M., Calero, N., Undabeytia, T., & Muñoz, J. (2019). A comparison of microfluidization and sonication to obtain lemongrass submicron emulsions. Effect of diutan gum concentration as stabilizer. Lwt, 114, 108424.

Semenova, M. (2017). Protein–polysaccharide associative interactions in the design of tailor-made colloidal particles. Current Opinion in Colloid & Interface Science, 28, 15-21.

Solans, C., Izquierdo, P., Nolla, J., Azemar, N., & Garcia-Celma, M. J. (2005). Nano-emulsions. Current opinion in colloid & interface science, 10(3), 102-110.

Stauffer, C. E.(1999). Emulsifiers.

Strawbridge, K. B., Ray, E., Hallett, F. R., Tosh, S. M., & Dalgleish, D. G. (1995). Measurement of particle size distributions in milk homogenized by a microfluidizer: estimation of populations of particles with radii less than 100 nm. Journal of Colloid and Interface Science, 171(2), 392-398.

Tadros, T. F. (2009). Emulsion science and technology: a general introduction. Emulsion science and technology, 1-56.

Tadros, T. F. (2010). Rheology of dispersions: Principles and applications.

Tadros, T. F. (Ed.). (2013). Emulsion formation and stability. John Wiley & Sons.

Trujillo-Cayado, L. A., Santos, J., Ramírez, P., Alfaro, M. C., & Muñoz, J. (2018). Strategy for the development and characterization of environmental friendly

emulsions by microfluidization technique. Journal of Cleaner Production, 178, 723-730.

Vaclavik, V. A., & Christian, E. W. (2014). Proteins in food: an introduction. In Essentials of Food Science (pp. 117-131). Springer, New York, NY.

Van Aken, G. A., & van Vliet, T. (2002). Flow-induced coalescence in protein-stabilized highly concentrated emulsions: Role of shear-resisting connections between the droplets. Langmuir, 18(20), 7364-7370.

van de Velde, F., de Hoog, E. H., Oosterveld, A., & Tromp, R. H. (2015). Protein-polysaccharide interactions to alter texture. Annual review of food science and technology, 6, 371-388.

Vázquez, C. E., Cos, A. I., & Lopez Nomdedeu, C. E. (2005). Alimentacion Y Nutricion: Manual Teorico-Práctico./Ed. Clotilde Vázquez; Ana I. De Cos Y Consuelo Lopez Nomdedeu (No. Tx353. A44 2005.).

Walstra, P. (1993). Principles of emulsion formation. Chemical Engineering Science, 48(2), 333-349.

Walstra, P. (2002). Physical chemistry of foods. CRC Press.

Weissmueller, N. T., Lu, H. D., Hurley, A., & Prud'homme, R. K. (2016). Nanocarriers from GRAS zein proteins to encapsulate hydrophobic actives. Biomacromolecules, 17(11), 3828-3837.

Whitehurst, R. J. (Ed.). (2008). Emulsifiers in food technology. John Wiley & Sons.

Wooster, T. J., Golding, M., & Sanguansri, P. (2008). Impact of oil type on nanoemulsion formation and Ostwald ripening stability. Langmuir, 24(22), 12758-12765.

Xu, L., Qiu, Z., Gong, H., Zhu, C., Li, Z., Li, Y., & Dong, M. (2019). Rheological behaviors of microbial polysaccharides with different substituents in aqueous solutions: Effects of concentration, temperature, inorganic salt and surfactant. Carbohydrate polymers, 219, 162-171.

Chapter 2.

Development of food-grade Pickering emulsions stabilized by a biological macromolecule (xanthan gum) and zein

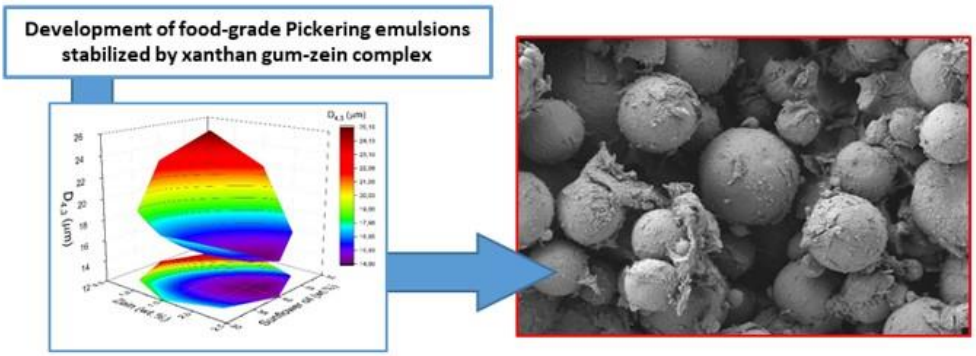

Abstract

In this work, food-grade sunflower oil/W Pickering emulsions stabilized by xanthan gum-zein complex were developed. For this purpose, laser diffraction, rheological, multiple light scattering, confocal laser scanning microscopy (CLSM) and field emission scanning electron microscopy (FESEM) measurements were carried out. A response surface methodology was used to determine the optimized zein and oil concentration of the emulsion by using $D_{4,3}$ and Turbiscan stability index (TSI) as objective functions to minimize. Subsequently, the optimized formulation with minimum $D_{4,3}$ was selected and the biological macromolecule, advanced performance xanthan gum (APXG), was added. CLSM results of emulsions without gum showed the location of zein in the oil-water interface protecting droplets against coalescence as Pickering stabiliser. They also demonstrated that zein did not present important aggregation at the working pH. The addition of APXG changed the flow behaviour from Newtonian to shear thinning which fitted to the Cross model. This fact provoked the occurrence of viscoelastic properties and an increase in stability. FESEM results suggested the formation of a zein-gum complex, which forms a layer covering the droplets, protecting them against oxidation and physical destabilization. Therefore, this research supports the role of zein-APXG complex as a stabiliser of future emulsions.

Keywords: zein; protein; advanced performance xanthan gum; rheology; protein-polysaccharide complex.

2.1. Introduction

The use of proteins in the stabilization of emulsions is attracting more and more attention due to the importance of using natural compounds. Proteins are environmentally friendly and amphiphilic molecules with good emulsifying properties (Encina, Vergara, Giménez, Oyarzún-Ampuero, & Robert, 2016).

Furthermore, proteins can stabilize emulsions due to the creation of a physical barrier and the occurrence of repulsive interactions between droplets (Wilde, Mackie, Husband, Gunning, & Morris, 2004). Zein, a proline-rich protein, is extracted from corn and is a sub-product of the food and ethanol industry. Although originally zein was considered a residue, nowadays it has shown its great potential for tissue engineering and drug delivery (Reddy & Yang, 2011). In addition, it is a biodegradable eco-friendly non-toxic polymer, and has been recognised as safe for food applications (GRAS) (Weissmueller, Lu, Hurley, & Prud'homme, 2016). This type of water insoluble plant protein is suitable for emulsion stabilization because they are insoluble both in water and in commonly used oils. In addition, zein particles have proved their efficiency at stabilizing Pickering emulsions (Rutkevičius, Allred, Velev, & Velikov, 2018). These emulsions can be influenced by zein concentration, pH and ionic strength. At low pH, zein can form gels in emulsions due to the aggregation of particles. However, at higher pH (pH> pI), zein particles do not show aggregation (De Folter, Van Ruijven, & Velikov, 2012).

Traditionally, proteins and polysaccharides have coexisted in food products due to their synergic effect on rheological properties and physical stability (van de Velde, de Hoog, Oosterveld, & Tromp, 2015). The success of this interaction is governed by pH, concentration and aggregation of the protein. Xanthan gum (XG) is a biological macromolecule produced by *Xanthomonas campestris*. It presents good stability in terms of temperature, pH, salts, and enzyme degradation. It is usually added to the aqueous phase to improve the stability of food (O/W) emulsions since it forms a three-dimensional gel-like network in the aqueous phase. This provokes a delay in the creaming process. Recently, a new type of xanthan gum has been evaluated in order to stabilize food emulsions (J. Santos, Calero, Muñoz, & Cidade, 2018). Advanced performance xanthan gum (APXG) solutions possess higher viscosities and lower viscous moduli than standard xanthan gum solutions at the same

concentration (Carmona, Lucas, Ramírez, Calero, & Muñoz, 2015). This could be an advantage for the formation of complexes with proteins. Thus far, no studies on the stability of emulsions with APXG-zein complex have been reported. In the present study, we examined the preparation of stable O/W emulsions using APXG-zein complexes.

Sunflower oil contains a large amount of ω-6 acid, a polyunsaturated fatty acid (PUFA), which is known as an essential fatty acid. These acids are essential for human growth. In addition, they have benefits on blood pressure regulation, the immune system and inflammation responses. As they are only produced by plants and phytoplankton, they should be incorporated into the diet (Rustan & Drevon, 2005). On the other hand, they are very sensitive to oxidation and heat. Hence, the formation of a physical barrier is necessary in order to protect the lipid phase (Berton-Carabin, Ropers, & Genot, 2014). To date, a limited diversity of proteins has been investigated for the encapsulation of PUFAs-rich oils and most of the research has focused on animal proteins such as caseins, whey protein isolates (WPI) and gelatine (Chen & Subirade, 2009; Gharsallaoui, Roudaut, Chambin, Voilley, & Saurel, 2007).

The main goal of this study is to develop stable emulsions formulated with zein protein-xanthan gum complex and sunflower oil. Sunflower oil was used as a model for this study since its fatty acid composition contains a large amount of PUFAs. These emulsions, which possess health benefits, can be considered as matrices to encapsulate different active ingredients with applications for food industry. The effect of zein protein and sunflower oil concentration on droplet size distribution and physical stability were analysed using surface response methodology. Furthermore, the formation of xanthan gum-zein complex and the influence of advanced performance xanthan gum

concentration on rheological properties and physical stability of these food emulsions were evaluated.

2.2. Materials and Methods

2.2.1. Materials

Zein protein, nile red and nile blue were purchased from Sigma Aldrich. KELTROL® Advanced Performance "Food Grade" xanthan gum, donated by CP Kelco, was used to prepare gum solutions. The solutions studied were prepared with deionized water. All materials were used as received. All emulsions were prepared at room temperature and samples kept at room temperature.

2.2.2. Preparation of food emulsions

In the first part of this research, the influence of the homogenization rate on droplet sizes of emulsions formulated with 2 wt.% of zein and 40 wt.% of sunflower oil was studied. The continuous phases were prepared by adding the zein protein to deionized water at room temperature. Then, the pH of the suspension was adjusted to 11.5 by adding a small amount of NaOH 1M. Emulsions (50 g) were developed using an Ultraturrax T25 (IKA®-Werke GmbH & Co. KG, Germany) for 300 s at 13500, 17500, 21500 and 23000 rpm. The optimal emulsification method was used for the development of an optimal formulation of emulsions, depending on the concentrations of zein (1.5-2.5 wt.%) and sunflower oil (30-50 wt.%). Both independent variables were studied at five different levels (-1.414, -1, 0, +1 and +1.414) and the central point of the design (0,0) was carried out in triplicate to determine the reproducibility of the emulsification process (see Table 1). In order to optimize the emulsion formulation, volumetric mean droplet diameter ($D_{4,3}$) and Turbiscan Stability Index (TSI) were used as dependent variables.

The emulsion with optimized values of zein concentration and sunflower oil concentration was used as a starting point for the addition of a biopolymer, Advanced Performance Xanthan Gum (APXG) to the formulation. Three samples were prepared using different APXG concentrations (0.1, 0.2 and 0.3 wt.%). Advanced Performance Xanthan Gum stock solution was prepared by dissolving 1 wt.% powder in deionized water. The APXG solution was stirred using a Ikavisc MR-D1 (IKA®-Werke GmbH & Co. KG, Germany) for at least 8 h at 700 rpm at room temperature. The system was left to stand for 48 hours at 7°C for complete hydration of the polymer. The final emulsions were prepared by slowly dispersing the APXG solution in the optimal emulsion at room temperature using a Ikavisc MR-D1 at 300 rpm for 5 minutes.

2.2.3. Laser diffraction measurements

Droplet size distributions (DSD) were characterized by using a Malvern Mastersizer 2000 (Malvern, UK) that is based on laser diffraction technology. In addition, $D_{4,3}$ was used in order to quantify and compare the mean diameters of the emulsions developed. This parameter was calculated using the following equation:

$$D_{4,3} = \sum_{i=1}^{N} n_i d_i^4 / \sum_{i=1}^{N} n_i d_i^3 \qquad \text{Eq. (2.1)}$$

Span parameter values were analysed in order to quantify the polidispersity of the DSDs.

$$span = \frac{D_{90} - D_{10}}{D_{50}} \qquad \text{Eq. (2.2)}$$

All laser diffraction measurements were performed at least by triplicate.

2.2.4. Rheological study

Flow curves and Small Amplitude Oscillatory Shear tests (SAOS) were performed using a controlled-stress rheometer Haake MARS II (Thermo Fisher

Scientific, USA). These measurements were conducted using a serrated plate-plate geometry (60 mm of diameter) as measuring geometry. Stress sweeps at 0.1, 1 and 3 Hz were executed in order to obtain the Linear Viscoelastic Range. Frequency sweeps were carried out from 20 to 0.05 rad/s at a stress in the LVR. Furthermore, flow behaviour was analysed by means of a stress-based multistep protocol (3 min/point). All rheological measurements were carried out at 20°C. All rheological measurements were performed at least by duplicate.

2.2.5. Physical stability

Turbiscan Lab Expert (Formulaction, France) was used in order to detect and quantify destabilization mechanisms by means of backscattering (BS) measurements. The influence of aging time on BS is related to the kinetics of different destabilization processes (J. Santos et al., 2018; Jenifer Santos, Alfaro, Trujillo-cayado, Calero, & Muñoz, 2019; Luis A. Trujillo-Cayado, Santos, Ramírez, Alfaro, & Muñoz, 2018). These measurements were determined at 25°C. In addition, the Turbiscan Stability Index (TSI) was used, which is a parameter that allows different destabilization mechanisms to be compared (Llinares, Ramírez, Carmona, Carrillo, & Munñoz, 2018; J. Santos, Jimenez, Calero, Alfaro, & Muñoz, 2019).

$$TSI = \sum_j \left| scan_{ref}\left(h_j\right) - scan_i\left(h_j\right) \right| \qquad \text{Eq. (2.3)}$$

where $scan_{ref}$ and $scan_i$ are the initial backscattering value and the backscattering-value at a specific time, respectively, and h_j is a specific height in the measuring cell. All multiple light scattering measurements were performed by duplicate.

2.2.6. Confocal Laser Scanning Microscopy

The microstructure of a selected emulsion was observed by using a confocal laser-scanning microscope (Zeiss LSM 7 DUO; Carl Zeiss, Germany). Concerning sample preparation, 1 mL of emulsion was placed in an eppendorf and subsequently Nile red solution (1 mM in Dimethylsulfoxide) was added and mixed thoroughly. That solution is selective to lipids. Then, a solution of Fast Green (1 mg/mL) was also added to the sample mixture and mixed. This solution is selective to proteins. This protocol was firstly used by Calero et al (Calero, Muñoz, Cox, Heuer, & Guerrero, 2013). Finally, the mixture was placed on a microscope slide, which was covered with a cover slip and observed under the microscope. The samples were excited at 488 nm and 633 nm.

2.2.7. Field Emission Scanning Electron Microscopy (FESEM).

Samples for FESEM were prepared using a chemical fixation with glutaraldehyde (4 wt.%, cacodylate 0.1M) and osmium tetroxide (1 wt.%, cacodylate 0.1M). The samples were dehydrated using ethanol and acetone. This protocol is based on the study of B. Douglas (Bray, 2000). Subsequently, samples were placed in a critical point dryer (CPD; Leica EM CPD 300) and passed through an automatic programme of slow speed procedure. CPD conditions: cooling temperature, 15°C; heating temperature, 40°C, CO_2 influx speed, slow; gas out speed, 90% slow. Process time: 2 h 30 min.

2.3. Results and discussion

2.3.1. Optimization of the formulation

Figure 2.1A shows droplet size distributions (DSD) for emulsions containing 2 wt.% of zein protein and 40 wt.% of sunflower oil as a function of homogenization rate in Ultraturrax T25. There is a decrease in droplet size with homogenization rate from 13500 rpm to 21500 rpm. Subsequently, a tendency of DSD to level off is observed. This fact is also clearly illustrated in volumetric diameter (see Figure 2.1B). It seems that there are no benefits in

homogenization rates higher than 21500 rpm. Hence, this homogenization rate was chosen for further study. In addition, recoalescence due to over-processing did not take place, which suggests the effectiveness of the protein protecting the oil-water interface.

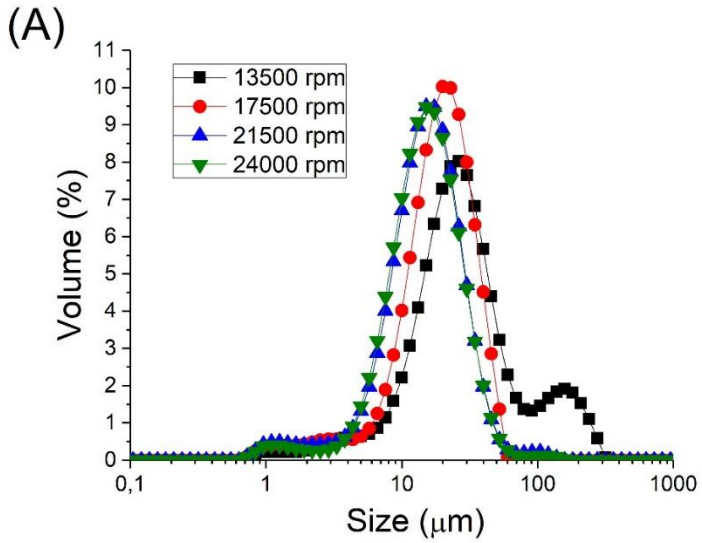

Figure 2.1A. Droplet size distribution for emulsions formulated with 2 wt.% zein and 40 wt.% sunflower oil prepared in UltraTurrax T25 as a function of homogenization rate.

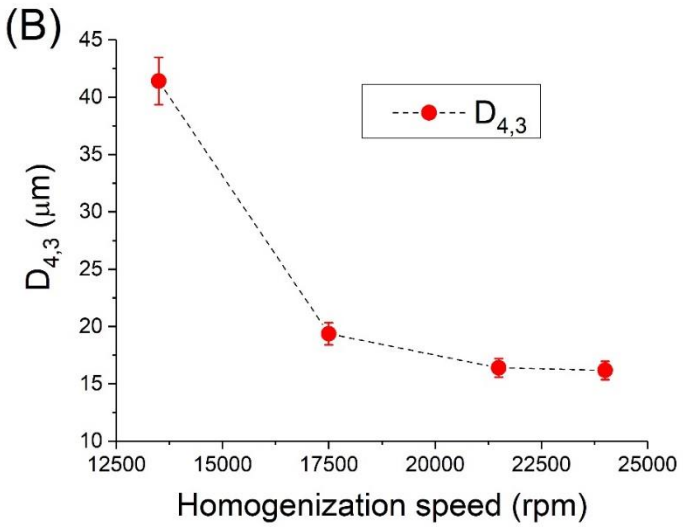

Figure 2.1B. Volumetric mean diameter ($D_{4,3}$) for emulsions formulated with 2 wt.% zein and 40 wt.% sunflower oil prepared in UltraTurrax T25 as a function of homogenization rate.

Table 2.1 shows volumetric mean diameters for all emulsions studied in the experimental design. Emulsions 9, 10 and 11 are replicates for the same formulation. Hence, this standard deviation of volumetric diameter (±0.4 μm) is a measure of the reproducibility of the emulsification method. In order to deeply analyse the tendencies of diameters, figure 2A and 2B are shown.

Table 2.1. Experimental design used for the study of emulsions, volumetric mean diameter ($D_{4,3}$), span and Turbiscan Stability Index (TSI) values obtained for each sample. X_1 corresponds to zein concentration and X_2 corresponds to sunflower oil concentration. Standard deviation of the mean (3 replicates) for $D_{4,3}$< 4%. Standard deviation of the mean (3 replicates) for span< 6%. Standard deviation of the mean (2 replicates) for TSI< 5%.

Sample	X_1	X_2	Zein (wt.%)	Oil (wt.%)	$D_{4,3}$ (μm)	Span	TSI
1	1	1	2.21	47.09	16.2	1.43	1.10
2	-1	1	0.791	47.09	20.4	1.98	2.06
3	1	-1	2.21	32.91	16.8	1.54	4.36
4	-1	-1	0.791	32.91	17.7	1.69	4.28
5	1.414	0	2.5	40	15.7	1.51	1.70
6	-1.414	0	0.5	40	23.6	1.93	2.81
7	0	1.414	1.5	50	22.2	2.11	1.12
8	0	-1.414	1.5	30	18.9	1.66	4.26
9	0	0	1.5	40	16.4	1.59	1.68
10	0	0	1.5	40	15.9	1.46	1.75
11	0	0	1.5	40	15.7	1.61	1.51

Figure 2.2A shows droplet size distributions for emulsions formulated with 40 wt.% sunflower oil as a function of zein concentration. Firstly, it is important to note that the DSDs obtained are bimodal with a very similar shape. The first peak is centred at 1-2 μm and the second and the most intense is centred at above 10 μm. In addition, there is a decrease in droplet size from 0.5 wt.% to

1.5 wt.% zein, which suggests 0.5 wt.% is not enough to cover the interfaces formed. In addition, there are no changes in DSDs from 1.5 wt.% zein to 2.5 wt.% zein emulsions. This result indicates that there is enough zein protein to protect the interface and to avoid recoalescence.

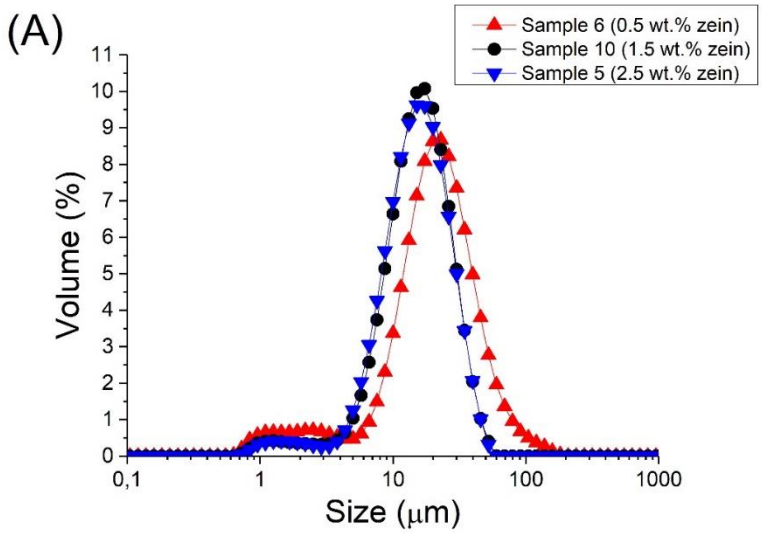

Figure 2.2A. Droplet size distributions for emulsions as a function of (A) zein concentration and (B) sunflower oil concentration.

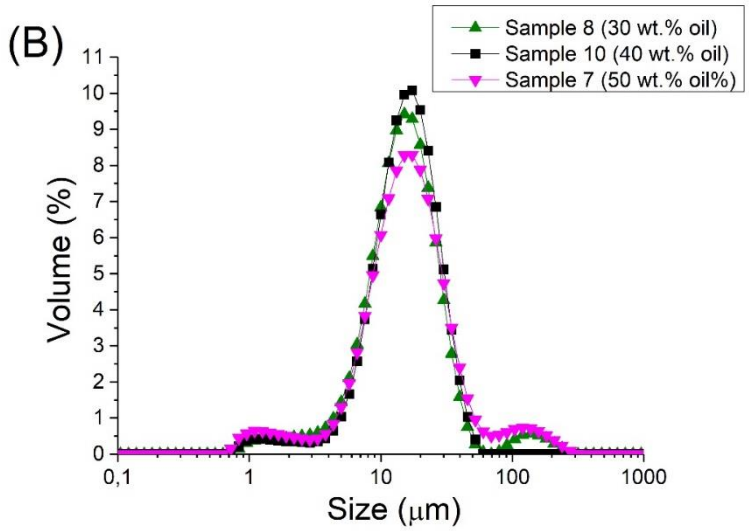

Figure 2.2B. Droplet size distributions for emulsions as a function of (A) zein concentration and (B) sunflower oil concentration.

The influence of sunflower oil concentration on DSDs for emulsions formulated with 1.5 wt.% zein is illustrated in figure 2.2B. All emulsions present a very broad distribution with a high polydispersity (see span values in table 2.1). Furthermore, it seems that there are no changes in DSD from 30 to 40 wt.% emulsions but a slight increase in droplet size is observed above 40 wt.% emulsion.

Figure 2.3 illustrates the three-dimensional response surface curve of volumetric mean diameter for the studied variables (zein concentration and sunflower oil concentration). This graph provides a visual interpretation of the interaction between zein and sunflower oil concentration. The volumetric mean diameter ($D_{4.3}$) fitted the following quadratic model equation (R^2=0.96):

$$D_{4,3} = 16{,}00 - 2{,}53 \cdot X_1 + 1{,}34 \cdot X_2 - 1{,}82 \cdot X_1 \cdot X_2 + 1{,}47 \cdot {X_1}^2 + 1{,}95 \cdot {X_2}^2 \quad \text{Eq. (2.4)}$$

where X_1 and X_2 are the codified values for zein concentration and sunflower oil concentration respectively.

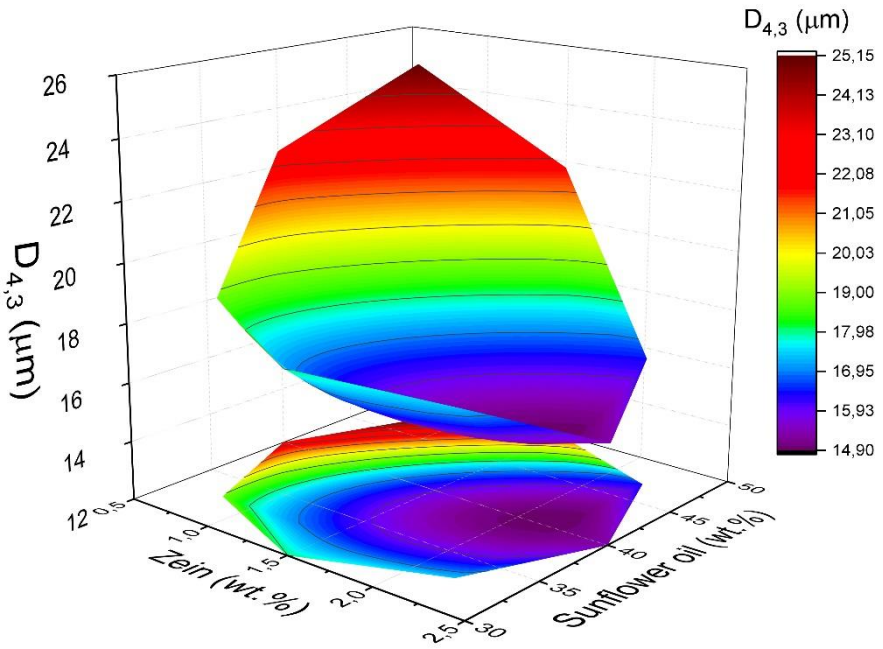

Figure 2.3. Response surface 3D plots of volumetric mean diameter as a function of zein concentration and sunflower oil concentration.

This model points out that both factors affect volumetric mean diameter. However, the most significant factor that influenced $D_{4.3}$ was zein concentration, as supported by the mean squares value (MSE=31.71), in comparison with sunflower oil concentration (MSE=17.98). There is a strong interaction between both variables, which suggests a negative synergic effect. This fact is supported by their mean squares value (MSE=13.34). Taking into account the surface response analysis, the minimum for $D_{4.3}$ was obtained using the values of X_1 = 0.92 and X_2 =0 .13 (wt.% zein = 2.15 and wt.% sunflower oil = 40.92 respectively). This point has been predicted since it is not an experimental one. Although results shown in Figure 2.2A and table 2.1 indicate that it is not necessary to increase the protein concentration above 1.5 wt.% to reduce droplet size at 40 wt.% sunflower oil concentration, there is a minimum of $D_{4,3}$ at 2.15 wt.% zein concentration as previously commented. In

spite of the fact that some studies claim that higher oil concentration provokes lower mean diameters in rotor stator devices (J Santos, Calero, & Munoz, 2016; Vankova et al., 2007), results bring to light the occurrence of an optimum. This could be due to the emulsification method not being able to produce finer droplets with such high oil concentration. Finally, it was not possible to obtain a statically significant equation to model the effect of the zein and oil concentrations on span using this experimental design approach.

Figure 2.4A shows the variation of delta-backscattering (ΔBS= backscattering at t aging time (BS_t)- backscattering at t=0 (BS_0)) with aging time as a function of the measuring cell height for emulsion 1, by way of example. There is a clear drop in the BS in the low zone of the measuring cell. This fact is an evidence of a creaming process (Mengual, Meunier, Cayré, Puech, & Snabre, 1999). Hence, the droplets of the emulsion migrate to the upper part of the measuring cell, leading to creaming. This destabilization process may be provoked by the high polydispersity of DSD and the high volumetric mean diameter values obtained. These factors facilitate the migration of the droplets to the upper part of the measuring cell. Furthermore, low values of viscosity of the continuous phase can speed the creaming. On the other hand, variation of BS in the middle part of the measuring cell was not observed. This points out the lack of coalescence and flocculation with aging time, highlighting the role of zein protein protecting the interface. Some authors have indicated the absence of coalescence at pH values higher than pI of zein (pI=6.2) (De Folter et al., 2012; Shukla & Cheryan, 2001). All the emulsions studied followed the same tendency with different values of BS. In order to analyse the differences between samples, Turbiscan Stability Index (TSI) values were calculated for all the emulsions (table 1). TSI values obtained were fitted to the following quadratic model (R^2= 0.97):

$$TSI = 1{,}64 - 0{,}37 \cdot X_1 - 1.18 \cdot X_2 + 0{,}39 \cdot {X_1}^2 + 0{,}61 \cdot {X_2}^2 \qquad \text{Eq. (2.5)}$$

where X_1 and X_2 are the codified values for zein concentration and sunflower oil concentration respectively.

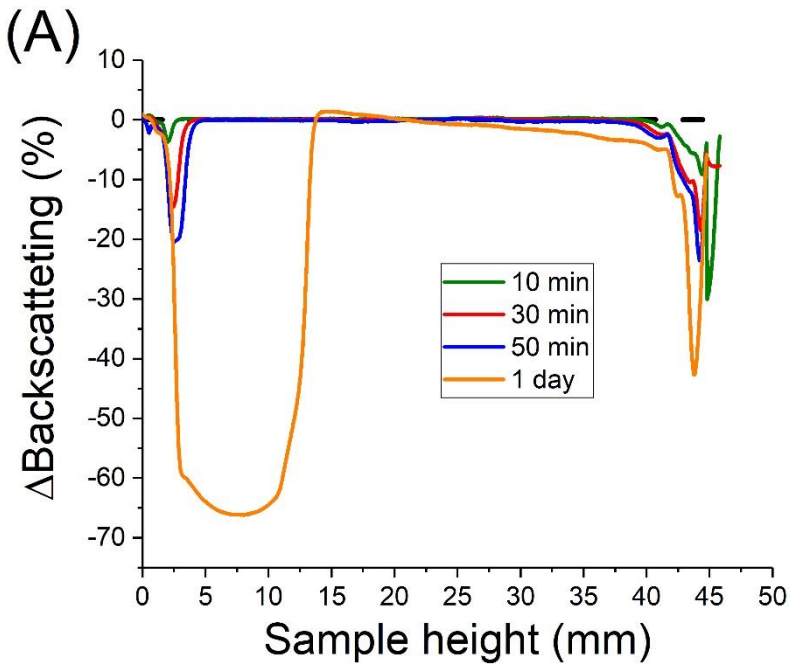

Figure 2.4A. Variation of ΔBS with the height of the measuring cell as a function of aging time for the sample 1 (2.21 wt.% zein and 47.09 wt.% sunflower oil).

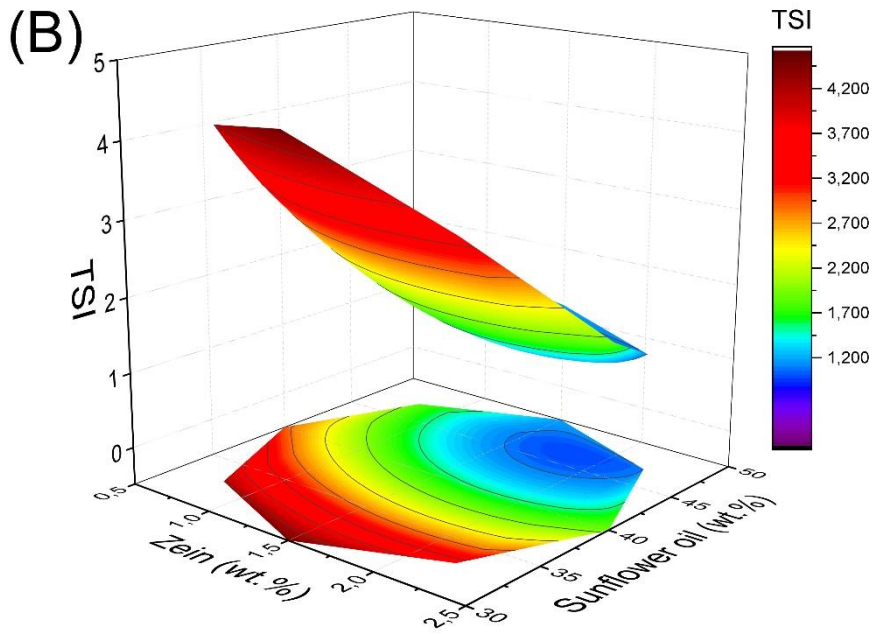

Figure 2.4B. Response surface 3D plots of Turbiscan Stability Index as a function of zein concentration and sunflower oil concentration.

Figure 2.4B illustrates the three-dimensional response surface of TSI values as a function of zein concentration and sunflower oil concentration. The minimum of TSI value is obtained for 1.85 wt.% zein concentration and 47 wt.% sunflower oil concentration (Y_1= 0.5; Y_2= 1). This minimum is not the same as that obtained for $D_{4.3}$. This fact brings to light that the stability of these systems is explained not only by volumetric diameter, but probably also by the viscosity of the emulsion and continuous phase.

As advanced performance Xanthan gum (APXG) is going to be incorporated into the continuous phase to reduce the creaming process, emulsion formulated with 2.15 wt.% zein and 40.92 wt.% sunflower oil (minimum $D_{4.3}$) was chosen as a starting point. In order to check the adequacy of the model, verification experiments were carried out at the predicted optimal conditions. The mean $D_{4,3}$ of the optimum emulsion (wt.% zein = 2.15 and wt.% sunflower

oil = 40.92 respectively) from triplicate trials was 15.5 ± 0.5 μm, which was close to the predicted value (14.9 ± 1.2 μm). In addition, TSI value for the optimum sample was 1.63 ± 0.08, while the predicted TSI value was 1.47 ± 0.35. Thus, the models from equations 4 and 5 were proved to be adequate. For this reason, these conditions were fixed for the following tests.

2.3.2. Incorporation of the biological macromolecule (APXG) to reduce creaming

As mentioned above, advanced performance Xanthan gum (APXG), a biological macromolecule produced by *Xanthomonas campestris,* was incorporated in different concentrations to the optimized emulsion in order to form a gel-like structure and reduce the creaming destabilization process. Flow curves are shown in figure 2.5 as a function of APXG concentration. In contrast with emulsion with no gum, which presented Newtonian behaviour with a viscosity value of 2.83 mPa·s, all the emulsions formulated with APXG showed shear thinning behaviour. In addition, viscosity presented a tendency to reach a plateau at very low shear rates (zero-shear viscosity). This change in flow behaviour is related to the increase of emulsion structuration due to the incorporation of the gum, as previously reported with other gums (Santos, Jiménez, Calero, Undabeytia, & Muñoz, 2019; L A Trujillo-Cayado, Alfaro, Muñoz, Raymundo, & Sousa, 2016). Shear thinning flow curves were fitted to the Cross model (R^2> 0.99) (Macosko & Larson, 1994). Fitting parameters are shown in table 2.2.

$$\eta = \frac{\eta_0}{1+\left(\frac{\dot{\gamma}}{\dot{\gamma}_c}\right)^{1-n}} \qquad \text{Eq. (2.6)}$$

Where $\dot{\gamma}_c$ is the critical shear rate for the onset of the shear-thinning fall, η_0 stands for the zero-shear viscosity and n is the well-known “flow index”.

There is an increase in zero-shear viscosity with APXG concentration, as expected. The higher the APXG concentration, the higher the structuration grade, and the higher the viscosity. Furthermore, the flow index decreases with gum concentration. This fact indicates a higher shear thinning behaviour.

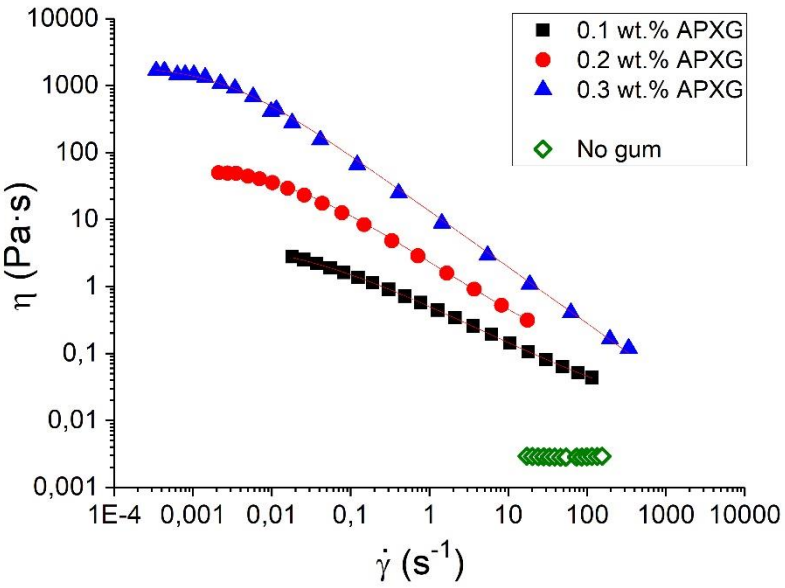

Figure 2.5. Flow curves of emulsions containing different advanced performance xanthan gum concentrations. Continuous lines correspond to the Cross model fitting equation.

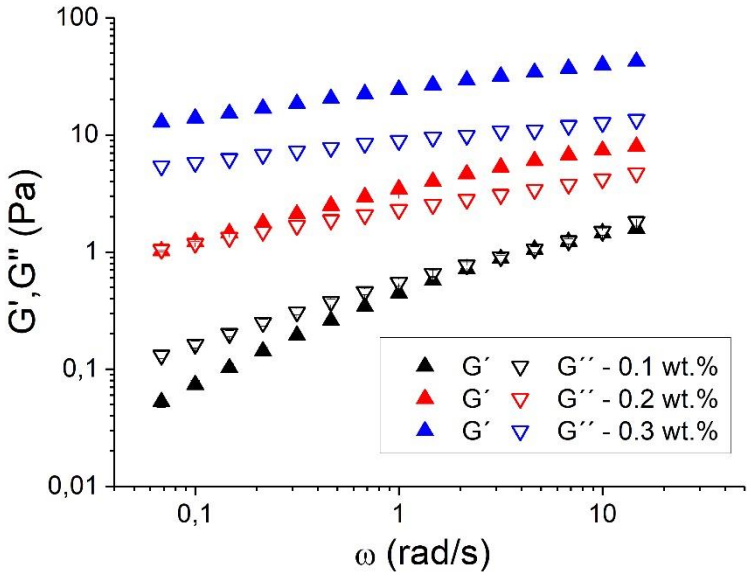

Figure 2.6. Mechanical spectra of emulsions containing different advanced performance xanthan gum concentrations.

Figure 2.6 shows mechanical spectra for zein emulsions as a function of APXG concentration. An increase in viscoelastic functions with APXG concentration was observed. 0.1 wt.% APXG emulsion presents the viscous modulus (G'') higher than the elastic one (G') with a tendency to cross at high frequencies. This predominant liquid behaviour may not be enough to inhibit the creaming process. In addition, 0.2 wt.% APXG emulsion exhibits G' higher than G'' at higher frequency values and G' lower than G'' at lower frequency values, with the occurrence of a crossover point. This crossover point is inversely related to the relaxation time. Shorter relaxation times (0.1 wt.% APXG emulsion) could lead to relatively fast rearrangements. This fact correlates well with the instability of emulsions against creaming (Santos, Trujillo, Calero, Alfaro, & Munoz, 2013). Interestingly, 0.3 wt.% APXG emulsion showed a weak gel behaviour with G' higher than G'' in all the frequency range studied. This gum concentration was enough to form a gel structure.

In order to get a deeper insight into the role of the zein in these emulsions, figure 2.7 shows the microstructure observed by using a confocal laser scanning microscope (CLSM) for emulsion without APXG, by way of example. Two fluorophores were chosen, namely nile red and fast green, which are selective for oils and the protein, respectively (de Boer, Imhof, & Velikov, 2019; Santos, Trujillo-Cayado, Calero, & Muñoz, 2014). Oil droplets (coloured in red) of 5-30 µm were observed. This supports the high polydispersity obtained by laser diffraction measurements. In addition, zein (coloured in green) is situated not only in the continuous phase but also in the interface of droplets, protecting them as Pickering stabiliser. However, zein particles did not present important aggregation, in contrast with other studies at lower pH pH (De Folter et al., 2012). It is clear that zein protein does not have a tendency to aggregate at this pH. This is the reason why this emulsion presents Newtonian flow behaviour (figure 2.5). Furthermore, it is important to note that zein protein is not visible in optical microscopy at this pH.

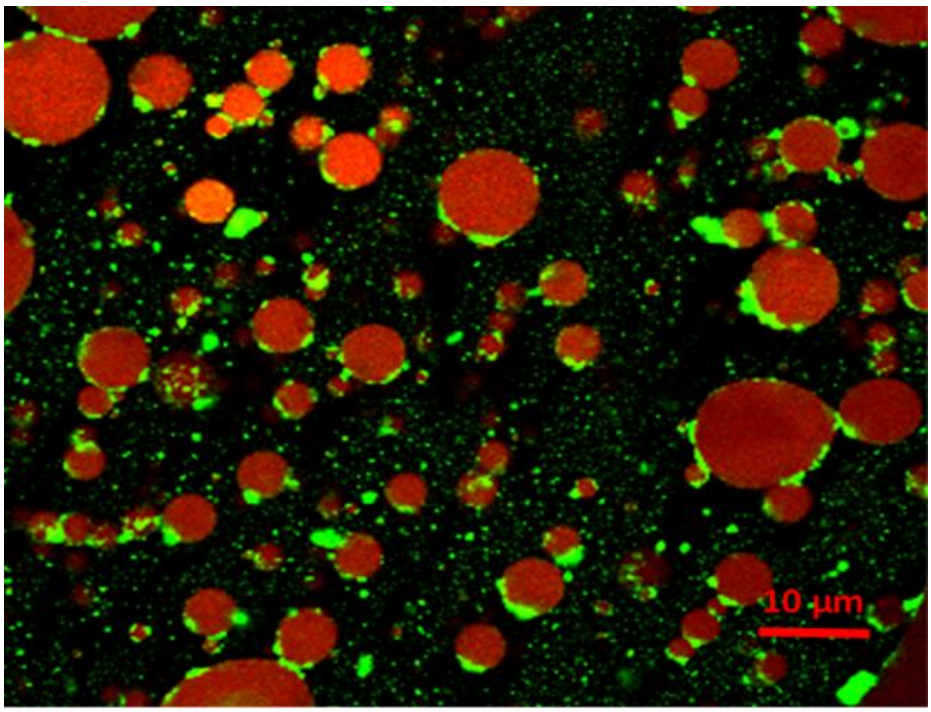

Figure 2.7. Microphotograph of emulsion formulated with zein, observed by Confocal Laser Scanning Microscope.

Figure 2.8A illustrates ΔBS variation with the height of the measuring cell for emulsions formulated with different APXG concentrations. It is important to note that the BS variation plotted for the emulsion with no gum is at 1 day of aging time while the other BS variations for emulsions containing different gum concentrations are at 22 days of aging time. The emulsion without gum presented a big drop of BS in the low zone of the measuring cell at just one day of aging time. This fact indicates a very strong creaming process. On the contrary, emulsions formulated with APXG showed a slight decrease in BS in the middle zone of the measuring cell. This suggests the inhibition of the creaming process but the occurrence of a slight coalescence/flocculation destabilization mechanism. In addition, this mechanism is less and less marked with the increasing APXG concentration.

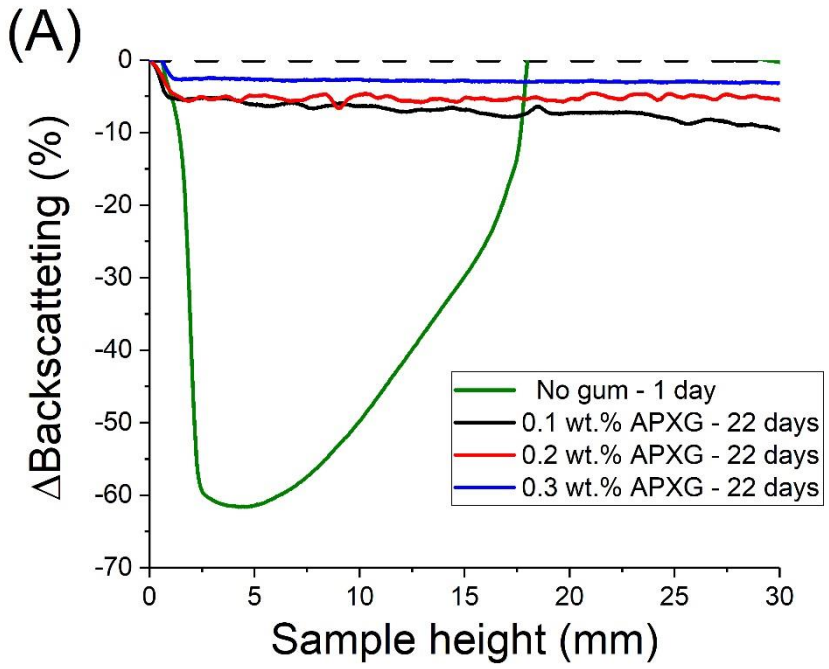

Figure 2.8A. Variation of ΔBS with the height of the measuring cell as a function of APXG concentration.

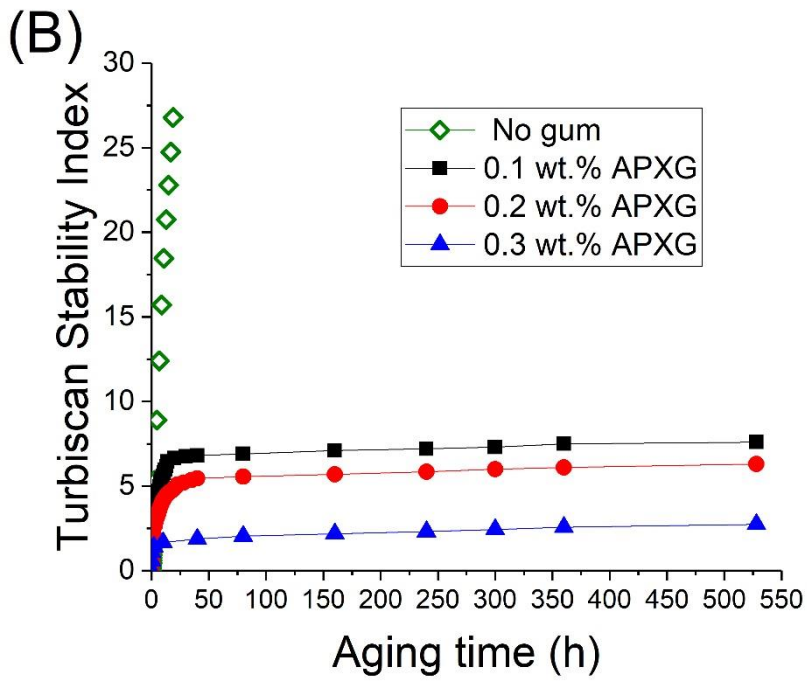

Figure 2.8B. Turbiscan Stability Index as a function of emulsion aging time and Advanced Performance Xanthan Gum concentration.

Turbiscan Stability Index (TSI) values are shown in figure 2.8B. This parameter, which is inversely related to physical stability, greatly increased in the first 24 hours for the emulsion with no gum. By contrast, emulsions containing gum presented an increase in TSI in the first 50 hours with a tendency to level off. TSI values allow different destabilization mechanism to be compared, for instance, creaming and coalescence/flocculation. Hence, the emulsion formulated with 0.3 wt.% APXG showed the best physical stability, indicated by the lowest TSI value.

Figure 2.9A shows the microstructure of emulsion formulated with zein and with no gum observed by FESEM. Interestingly, aggregated droplets with some zein particles can be observed. These zein particles are deposited on the

droplet surface and some are in the continuous phase forming layers. On the other hand, figure 2.9B presents the microstructure formed by an emulsion containing zein and 0.3wt.% of APXG. The surface of the droplets seems to be different compared to figure 2.9A. This fact suggests the formation of a zein-gum complex, which would increase the viscoelastic properties and the stability of the emulsion. An isolated droplet formulated with zein-APXG complex is observed in figure 2.9C. It shows a strong coating with not only one layer covering the surface. This coating is probably responsible for the increase in physical stability of emulsions formulated with zein and APXG.

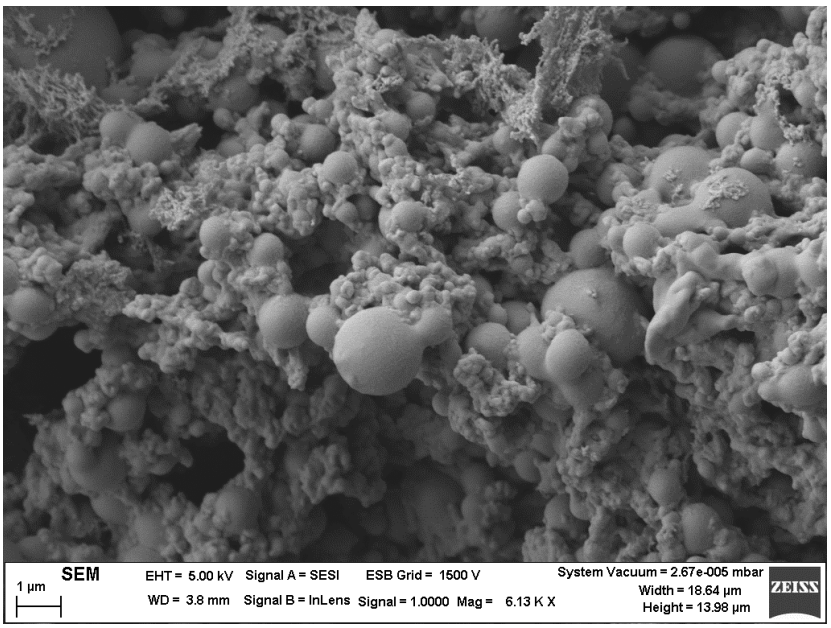

Figure 2.9A. Microstructure of emulsion formulated with zein and without APXG, observed by FESEM.

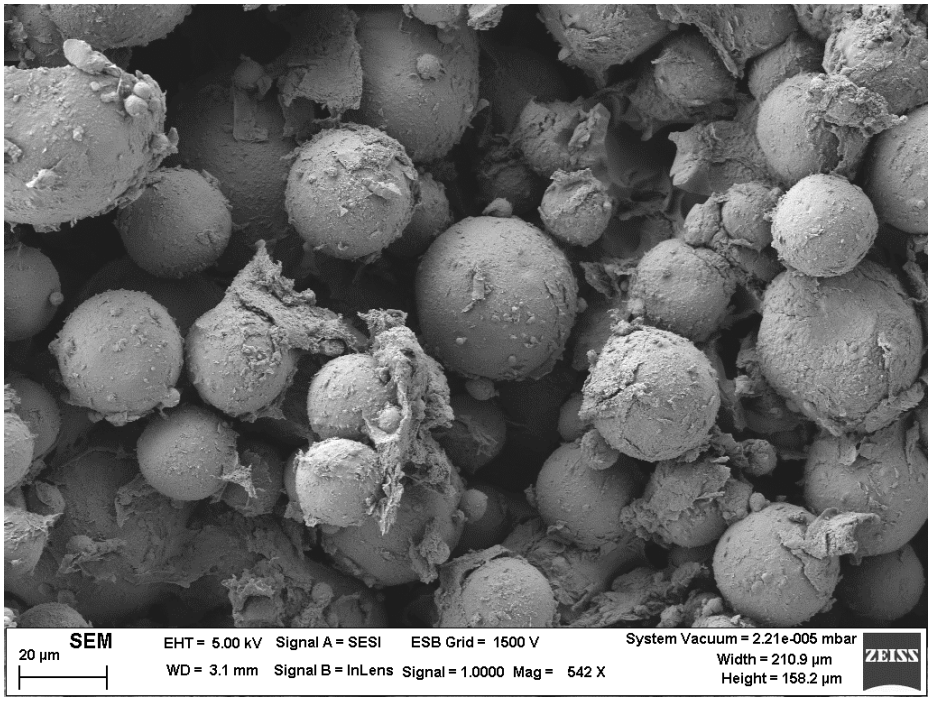

Figure 2.9B. Microstructure of emulsion formulated with zein and 0.3 wt.% APXG, observed by FESEM.

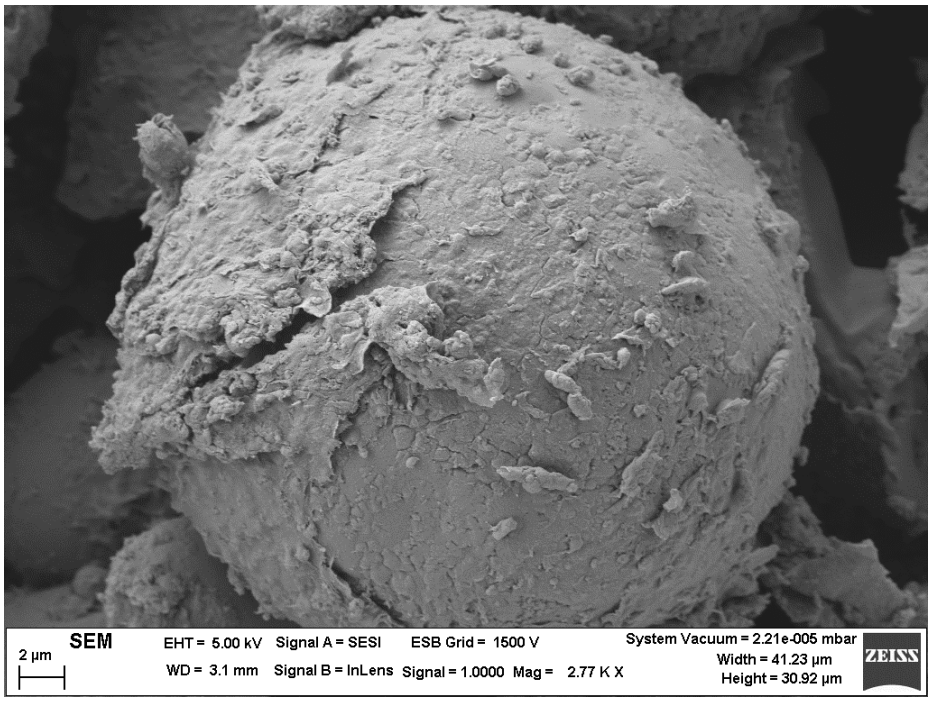

Figure 2.9C. Microstructure of a droplet of emulsion formulated with zein and 0.3 wt.% APXG, observed by FESEM.

Conclusions

At first sight, zein protein seems to effectively protect the oil-water interface since emulsions formulated with zein and sunflower oil did not present recoalescence due to over-processing, even at high homogenization rates. Subsequently, the optimum of mean diameter and TSI was evaluated by using surface response methodology. Interestingly, the optimum values for TSI and mean diameter are not the same. Results showed an optimized formulation with minimum volumetric mean diameter that contained 2.15 wt.% of zein and 40.92 wt.% of sunflower oil. Hence, the viscosity could be a key-factor concerning the stability of these emulsions since they underwent creaming with aging time. Confocal laser scanning microscopy results proved the location of zein in the oil-water interface, preventing a coalescence process.

In order to increase the viscosity of the continuous phase and inhibit or reduce creaming, the biological macromolecule called Advance Performance Xanthan Gum was incorporated. This addition provoked the occurrence of viscoelastic properties and a clear increase in zero-shear viscosity. In addition, the physical stability of these emulsions was enhanced thanks to the formation of a protein-polysaccharide complex. This complex forms a layer covering the droplets that can protect sunflower oil against possible oxidation and against physical destabilization processes.

Results obtained suggest that mixtures of zein and advanced performance xanthan gum present great emulsifying and stabilizing properties for the preparation of high stability emulsions with adjustable viscosity and viscoelasticity for the food industry.

References

Berton-Carabin, C. C., Ropers, M., & Genot, C. (2014). Lipid oxidation in oil-in-water emulsions: Involvement of the interfacial layer. *Comprehensive Reviews in Food Science and Food Safety*, *13*(5), 945–977.

Bray, D. (2000). Critical point drying of biological specimens for scanning electron microscopy. In *Supercritical Fluid Methods and Protocols* (pp. 235–243). Springer.

Calero, N., Muñoz, J., Cox, P. W., Heuer, A., & Guerrero, A. (2013). Influence of chitosan concentration on the stability, microstructure and rheological properties of O/W emulsions formulated with high-oleic sunflower oil and potato protein. *Food Hydrocolloids*, *30*(1), 152–162.

Carmona, J. A., Lucas, A., Ramírez, P., Calero, N., & Muñoz, J. (2015). Nonlinear and linear viscoelastic properties of a novel type of xanthan gum with industrial applications. *Rheologica Acta*, *54*(11–12), 993–1001.

Chen, L., & Subirade, M. (2009). Elaboration and characterization of soy/zein protein microspheres for controlled nutraceutical delivery. *Biomacromolecules*, *10*(12), 3327–3334.

de Boer, F. Y., Imhof, A., & Velikov, K. P. (2019). Color-tunable particles through affinity interactions between water-insoluble protein and soluble dyes. *Colloids and Surfaces A: Physicochemical and Engineering Aspects*, *562*, 154–160.

De Folter, J. W. J., Van Ruijven, M. W. M., & Velikov, K. P. (2012). Oil-in-water Pickering emulsions stabilized by colloidal particles from the water-insoluble protein zein. *Soft Matter*, *8*(25), 6807–6815. https://doi.org/10.1039/c2sm07417f

Encina, C., Vergara, C., Giménez, B., Oyarzún-Ampuero, F., & Robert, P. (2016). Conventional spray-drying and future trends for the microencapsulation of fish oil. *Trends in Food Science & Technology*, *56*, 46–60.

Gharsallaoui, A., Roudaut, G., Chambin, O., Voilley, A., & Saurel, R. (2007). Applications of spray-drying in microencapsulation of food ingredients: An overview. *Food Research International*, *40*(9), 1107–1121.

Llinares, R., Ramírez, P., Carmona, J., Carrillo, F., & Munñoz, J. (2018). Formulation and optimization of emulsions based on bitter fennel essential oil and EO/BO block copolymer surfactant. *Colloids and Surfaces A: Physicochemical and Engineering Aspects*, *536*(September

2016), 142–147. https://doi.org/10.1016/j.colsurfa.2017.07.027

Macosko, C. W., & Larson, R. G. (1994). *Rheology: principles, measurements, and applications*.

Mengual, O., Meunier, G., Cayré, I., Puech, K., & Snabre, P. (1999). TURBISCAN MA 2000: multiple light scattering measurement for concentrated emulsion and suspension instability analysis. *Talanta*, *50*(2), 445–456.

Reddy, N., & Yang, Y. (2011). Potential of plant proteins for medical applications. *Trends in Biotechnology*, *29*(10), 490–498.

Rustan, A. C., & Drevon, C. A. (2005). *Fatty Acids: Structures and Properties. London: Encyclopedia of Life Sciences*. Nature Publishing, http://www. els. net.

Rutkevičius, M., Allred, S., Velev, O. D., & Velikov, K. P. (2018). Stabilization of oil continuous emulsions with colloidal particles from water-insoluble plant proteins. *Food Hydrocolloids*, *82*, 89–95. https://doi.org/10.1016/j.foodhyd.2018.04.004

Santos, J., Calero, N., Muñoz, J., & Cidade, M. T. (2018). Development of food emulsions containing an advanced performance xanthan gum by microfluidization technique. *Food Science and Technology International*, *24*(5), 373–381. https://doi.org/10.1177/1082013218756140

Santos, J., Jimenez, M., Calero, N., Alfaro, M. C., & Muñoz, J. (2019). Influence of a shear post-treatment on rheological properties, microstructure and physical stability of emulgels formed by rosemary essential oil and a fumed silica. *Journal of Food Engineering*, *241*(August 2018), 136–148. https://doi.org/10.1016/j.jfoodeng.2018.08.013

Santos, J, Calero, N., & Munoz, J. (2016). Optimization of a green emulsion stability by tuning homogenization rate. *RSC Advances*, *62*(6), 57563–57568.

Santos, Jenifer, Alfaro, M. C., Trujillo-cayado, L. A., Calero, N., & Muñoz, J. (2019). LWT - Food Science and Technology Encapsulation of β - carotene in emulgels-based delivery systems formulated with sweet fennel oil. *LWT - Food Science and Technology*, *100*(October 2018), 189–195. https://doi.org/10.1016/j.lwt.2018.10.057

Santos, Jenifer, Jiménez, M., Calero, N., Undabeytia, T., & Muñoz, J. (2019). A comparison of microfluidization and sonication to obtain lemongrass submicron emulsions. Effect of diutan gum concentration as stabilizer. *Lwt*, *114*(February), 108424. https://doi.org/10.1016/j.lwt.2019.108424

Santos, Jenifer, Trujillo-Cayado, L. A., Calero, N., & Muñoz, J. (2014). Physical characterization of eco-friendly O/W emulsions developed through a strategy based on product engineering principles. *AIChE Journal*, *60*(7), 2644–2653.

Santos, Jenifer, Trujillo, L. A., Calero, N., Alfaro, M. C., & Munoz, J. (2013). Physical Characterization of a Commercial Suspoemulsion as a Reference for the Development of Suspoemulsions. *Chemical Engineering & Technology*, *36*(11), 1883–1890.

Shukla, R., & Cheryan, M. (2001). Zein: the industrial protein from corn. *Industrial Crops and Products*, *13*(3), 171–192.

Trujillo-Cayado, L A, Alfaro, M. C., Muñoz, J., Raymundo, A., & Sousa, I. (2016). Development and rheological properties of ecological emulsions formulated with a biosolvent and two microbial polysaccharides. *Colloids and Surfaces B: Biointerfaces*, *141*, 53–58.

Trujillo-Cayado, Luis A., Santos, J., Ramírez, P., Alfaro, M. C., & Muñoz, J. (2018). Strategy for the development and characterization of environmental friendly emulsions by microfluidization technique. *Journal of Cleaner Production*, *178*, 723–730. https://doi.org/10.1016/j.jclepro.2018.01.028

van de Velde, F., de Hoog, E. H. A., Oosterveld, A., & Tromp, R. H. (2015). Protein-polysaccharide interactions to alter texture. *Annual Review of Food Science and Technology*, *6*, 371–388.

Vankova, N., Tcholakova, S., Denkov, N. D., Ivanov, I. B., Vulchev, V. D., & Danner, T. (2007). Emulsification in turbulent flow: 1. Mean and maximum drop diameters in inertial and viscous regimes. *Journal of Colloid and Interface Science*, *312*(2), 363–380.

Weissmueller, N. T., Lu, H. D., Hurley, A., & Prud'homme, R. K. (2016). Nanocarriers from GRAS zein proteins to encapsulate hydrophobic actives. *Biomacromolecules*, *17*(11), 3828–3837.

Wilde, P., Mackie, A., Husband, F., Gunning, P., & Morris, V. (2004). Proteins and emulsifiers at liquid interfaces. *Advances in Colloid and Interface Science*, *108*, 63–71.

Chapter 3.

Optimization of sonication parameters to obtain food emulsions stabilized by zein. Formation of zein-diutan gum/zein-guar gum complexes.

Abstract

Zein as a sole material is not suitable for technological applications since it is not flexible. The possible solution for extend the applications of zein was the formation of zein-polysaccharide complexes. At the first step, sonication parameters were optimized to obtain finer emulsions formulated with zein, rosemary essential oil as food preservative and sunflower oil, by means of surface response methodology. Subsequently, the formation of guar or diutan-zein complexes on rheological properties for these food emulsions were evaluated. An increase in sonication power, sonication time and cycles provoked a decrease in mean droplet size and a lack of recoalescence. The optimized emulsion was the starting point to form two different complexes: zein with diutan gum and zein with guar gum at different concentrations. Rheological properties as well as the microstructure observed by FESEM were analysed. Interestingly, zein-guar gum complexes did not form a rheological gel, as a consequence, emulsions containing them seems to suffer destabilization process with aging time. In contrast, emulsions formulated with zein-diutan gum presented a 3D-network, observed by FESEM technique and proved by rheological measurements. While emulsions containing zein-guar gum complexes did not form networks to stabilise oil droplets, zein-diutan gum complexes did. This work brings to light the importance of the election of polysaccharide used in food emulsions formulated with zein.

Keywords: zein protein; diutan gum; guar gum; surface response methodology; sonication.

3.1. INTRODUCTION

Maize is commonly used in many fields, since it is easy processed, ready digested, and cheaper than other cereals. A by-product from the maize industry, zein, is considered a promising biopolymer of the 21st century (Luo & Wang, 2014) . Zein is biodegradable, non-toxic and eco-friendly, which are very interesting characteristics. Furthermore, it has been approved for oral

use by the FDA (Food and Drug Administration, USA). In contrast to other proteins, such as egg or milk protein, allergy to zein protein is uncommon (Moneret-Vautrin, Kanny, & Beaudouin, 1998). Although initially it was a waste product, recently modified zein nanoparticles have proved their potential as delivery systems (Karthikeyan, Guhathakarta, Rajaram, & Korrapati, 2012; J. Li et al., 2018; X. Liu, Sun, Wang, Zhang, & Wang, 2005). Zein nanoparticles possess a unique amphiphilic character, high antioxidant properties and come from renewable resources (Weissmueller, Lu, Hurley, & Prud'homme, 2016). However, zein as a sole material is not suitable for technological applications since it is not flexible. The possible solution for extend the applications of zein nanoparticles was the formation of zein-polysaccharide complexes. In addition, other technical disadvantage of zein is its low solubility in water due to its high content of hydrophobic amino acids. Recent studies have shown that structural modifications (e.g., change in particle size, charge, surface characteristics) of zein could increase its encapsulation efficiency. The ultrasound treatment of zein could potentially induce these modifications, that could be useful in the development of delivery systems with improved encapsulation efficiency and changes in binding affinity. In addition, some authors have suggested that an increase of the solubility of zein and encapsulation efficiency can be provoked by ultrasound treatment (Liang et al., 2018), which could influence on its stabilizing properties. On top of that, protein-stabilized Pickering emulsions typically present great stability against coalescence (Dai, Sun, Wei, Mao, & Gao, 2018; Wang et al., 2016). Nevertheless, some factors such as big droplets, great densities differences, or low aqueous phase viscosity could provoke creaming with aging time. This fact can limit their application to food products.

The formation of complex coacervates such as whey protein-gum Arabic, pea protein isolate-gum Arabic (S. Liu, Elmer, Low, & Nickerson, 2010), potato protein-guar gum (Jenifer Santos, Calero, Guerrero, & Muñoz, 2015), chitosan-

alginate (Z. Li, Ramay, Hauch, Xiao, & Zhang, 2005) in order to enhance emulsion stability has been reported. In emulsions stabilized by proteins, stability strongly depends on pH since protein charge goes from positive to negative with pH. At pH higher than pI (isoelectric point) of zein, zein nanoparticles are negatively charged. Recently, some studies have pointed out that negatively zein nanoparticles could stabilize emulsions in combination with an anionic polysaccharide (Davidov-Pardo, Joye, Espinal-Ruiz, & McClements, 2015; Luo, Teng, & Wang, 2012) . Furthermore, the use of novel biomacromolecules can help meet the needs of an expanding market that looks for efficient resources in the industry. Biological macromolecules secreted by microorganisms are renewable resources. They are used in many fields because of its enhanced properties for thickening, emulsifying and stabilizing (Hamcerencu, Desbrieres, Popa, & Riess, 2009; Xu et al., 2019). Microbial polysaccharides have plenty of oxygen and hydroxyl centres as well as ionic carboxylate centres which may lead to dipolar, ion-dipolar and hydrogen bonding interactions with each other or other materials in solution (Brewer, Sternlicht, Marcus, & Grollman, 1973) .

Diutan gum (DG), secreted by *Sphingomonas sp*., is an aqueous anionic biological macromolecule that is considered biodegradable and biocompatible. Its structure consists of a repeating unit with β-1,3-D-glucopyranosyl, β-1,4-D-glucuronopyranosyl, β-1,4-D-glucopyranosyl, and α-1,4-L-rhamnopyranosyl, and a two-saccharide L-rhamnopyranosyl side-chain attached to the (1→4) linked glucopyranosyl residue (Banerjee et al., 2009; Sonebi & McKendry, 2008) .Its molecular weight is 2.88 - 5.18 kDa. The rheological properties of this novel thickener have been recently evaluated (Carmen García, Trujillo, Carmona, Muñoz, & Carmen Alfaro, 2019) and used to avoid destabilization processes in lemongrass nanoemulsions (Jenifer Santos, Jiménez, Calero, Undabeytia, & Muñoz, 2019). However, this biological macromolecule has never been used in combination with a protein. On the

other hand, guar gum (GG) is a well-known non-ionic polysaccharide obtained from the seeds of *Cyamopsis tetragonolobus* or *Cyamopsis psoraloides* (leguminosae family), which is commonly used in food products (Heyman, De Vos, Van der Meeren, & Dewettinck, 2014; Mukherjee, Sarkar, & Moulik, 2010; Jenifer Santos et al., 2015). Its structure is formed by a chain of β-d-mannopyranosyl units joined by 1→4 linkages. Each second residue (a d-galactopyranosyl) has a side chain bound to the main chain by α (1→6) linkage (Belitz, Grosch, & Schienberle, 1999). Its molecular weight is 2.2 kDa. Guar gum is commonly used with other gums (Cao, Lv, Zhou, Chen, & Qian, 2021; Xia, Wei, Hu, & Peng, 2021) and with proteins (Duhan, Sahu, Mohapatra, & Naik, 2021; Shen & Li, 2021).

The main goal of this study is to compare the formation of two coacervates formed by zein and two different polysaccharides: diutan gum as a novel biological macromolecule and guar gum as a well-known compound used in food emulsions. Firstly, a systematic research about the ultrasonication method on the formation of food emulsions stabilised by zein nanoparticles was carried out. The effect of processing parameters on droplet size was analysed by surface response methodology. Subsequently, the formation of guar or diutan-zein complexes and the influence of their concentration on rheological properties of these food emulsions were evaluated. To our knowledge, there are no previous studies about the impact of diutan gum or guar gum on the physical stability of Pickering emulsions containing oil droplets coated by zein particles.

3.2. MATERIALS AND METHODS

3.2.1. Materials

Zein protein and rosemary essential oil were purchased from Sigma Aldrich. KELTROL® diutan gum, donated by CP Kelco, and guar gum (Sigma Aldrich) were used to prepare gum solutions. The solutions studied were prepared

with deionized water. Sunflower oil containing 400 g · kg^{-1} of oleic acid was obtained from the local supermarket. All materials were used as received.

3.2.2. Methods

3.2.2.1. Preparation of food emulsions stabilized by zein

The emulsions were formulated with 21 g · kg^{-1} of zein, 400 g · kg^{-1} of sunflower oil and 2 g · kg^{-1} of rosemary essential oil as natural food preservative (Gavahian, Chu, Lorenzo, Mousavi Khaneghah, & Barba, 2020). These concentrations have been selected taking into account the study reported by Santos et al (J. Santos, Alcaide-González, Trujillo-Cayado, Carrillo, & Alfaro-Rodríguez, 2020).In the first part of this research, the influence of ultrasonication power, time and cycles on droplet sizes was studied. The continuous phase was formed by adding zein protein to deionized water and subsequently, adjusting the pH to 11.5 using a NaOH solution. Firstly, a coarse emulsion (batches of 100 g) was prepared, at room temperature, using an IKA-Visc homogenizer for 300 s at 56 xg. Then, finer emulsions were homogenized using an ultrasonicator UP 400S (Hielscher-Ultrasound technology) at different processing parameters (table 1). This step was carried out using an ice batch.

The emulsion with optimized values of ultrasonication power, time and cycle was used as a starting point for the addition of the biopolymers (diutan gum, DG, or guar gum, GG) to form protein-polysaccharide complexes. These samples were prepared using different DG or GG amounts to obtain three final gum concentration (2, 3 and 4 g · kg^{-1}). Gums stock solutions were prepared by dissolving 10 g · kg^{-1} powder in deionized water. Gums solutions were stirred (IKAVISC MR-D1) for at least 8 h at 7 xg at room temperature. The system was left to stand for 48 hours at 7°C for complete hydration of the polymer. The final emulsions were prepared by dispersing the gum solution in

the optimal emulsion at room temperature using a Ikavisc MR-D1 at 1 xg for 5 minutes.

3.2.2.2. Experimental design and data analysis

The effect of ultrasonic power, ultrasonication time and ultrasonication cycle on the mean droplet diameter of emulsions, as a dependent variable, was studied. This was carried out by means of using central composite design and surface response methodology. Dependent variables were studied at five different levels (-1.68, -1, 0, +1 and +1.68) and the central point of the study was prepared in triplicate (see Table 1). Ultrasonication power ranged from 50 to 100% of the total power (400 W), ultrasonication time from 5 to 25 minutes and the cycles from 0.5 to 1. The cycle value equals the acoustic irradiation time in seconds, the difference to 1 second is the pause time. For example, a cycle of 0.6 means that the power discharge 0.6 seconds and pause 0.4 seconds. The energy density supplied by the ultrasonicator was calculated as follows:

$$E_V = \frac{W \cdot t \cdot c}{V} \qquad \text{Equation (3.1)}$$

Where E_v is the energy density, W is the ultrasonic power, t is the ultrasonic time, c is the cycles and V is the volume of the sample (50 ml).

Statistical analysis of the data was performed with Echip software (Experimentation by Design). For model construction, terms with $p > 0.05$ were removed and the analysis was recalculated without these terms. The suitability of the models was determined by using the coefficient of determination.

3.2.2.3. Droplet size analysis

Emulsion droplet size was characterized by optical microscopy (Olympus BX51 microscope) with a 50x objective. Samples were diluted 1:10 with deionised

water. The microphotographs obtained were analysed using ImageJ software to determinate the medium droplet size of the samples.

3.2.2.4. Rheological characterization

Rheological tests were carried out using a controlled-stress rheometer Anton Paar MCR 501 equipped with a sand-blasted plate (25 mm diameter). Stress sweeps at 0.1, 1 and 3 Hz were performed in order to obtain the Linear Viscoelastic Range (LVR) of the different samples. Frequency sweeps were carried out from 20 to 0.05 rad/s at a stress in the LVR. Furthermore, flow behavior was analyzed by means of a stress-based multistep protocol (3 min/point). All rheological measurements were carried out at 20°C. Flow curves were fitted to Cross model:

$$\eta = \eta_\infty + \frac{\eta_0 - \eta_\infty}{1 + (k\dot{\gamma})^{1-n}} \qquad \text{Equation (3.2)}$$

Where, η is the viscosity, $\dot{\gamma}$ is the shear rate, η_0 is the viscosity at very low shear rates, η_∞ is the viscosity at very high shear rates, k is the inverse of critical shear rate, and n is the flow index

3.2.2.5. Field Emission Scanning Electron Microscope

Emulsions for FESEM were fixed with glutaraldehyde (40 g · kg^{-1} cacodylate 0.1M) and osmium tetroxide (10 g · kg^{-1} , cacodylate 0.1M). These samples were dehydrated using ethanol and acetone, following the protocol reported by Santos et al 2020 (J. Santos et al., 2020). Finally, samples were dried by means of a critical point dryer (CPD; Leica EM CPD 300) following the conditions: cooling temperature, 15°C; heating temperature, 40°C, CO_2 influx speed, slow; gas out speed, 90% slow; for 2 hours and 30 min.

3.2.2.6. ANOVA tests

Results were expressed as means with standard deviations of three experimental runs. Tukey test was used as a post-hoc analysis to separate

means with significant differences ($p < 0.05$). For all statistical analyses the Excel software package was used (Microsoft). All statistical calculations were conducted at a significance level of $p = 0.05$.

3.3. RESULTS AND DISCUSSION

3.3.1. Influence of processing parameters on mean diameter using sonicator of emulsions formulated with zein and sunflower oil.

Figures 3.1A and 3.1B are the microphotographs of zein emulsions processed at 75% of power, 0.75 cycles (cycles of 75% time on/25% of time off) for A) 5 minutes and A) 25 minutes, by way of example. It is evident that there is a decrease in mean diameter with processing time. These microphotographs have been analysed using ImageJ software in order to determine the mean diameter of the droplet size distribution.

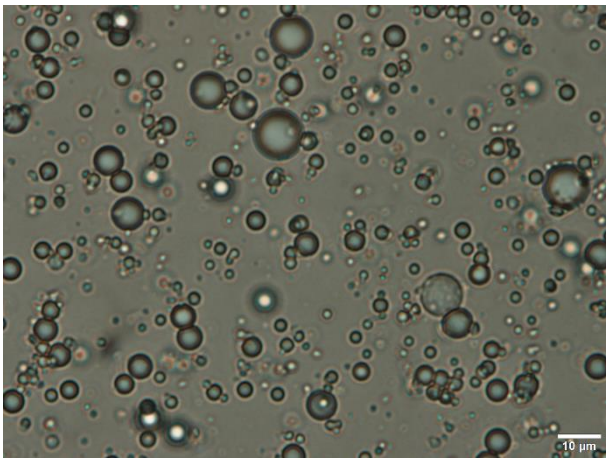

Figure 3.1A. Microphotograph of zein emulsion processed at 75% of power, 0.75 cycles for 5 minutes (sample 13)

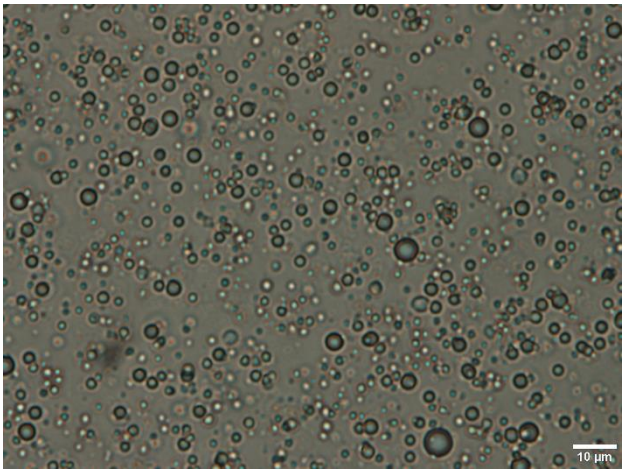

Figure 3.1B. Microphotograph of zein emulsion processed at 75% of Power, 0.75 cycles for 25 minutes (sample 14)

Table 3.1. Experimental design, processing parameters used for the development of emulsions, and mean diameter values for all emulsions studied. Y1 corresponds to power, Y2 to cycles and Y3 to homogenization time in sonicator.

	Y_1	Y_2	Y_3	Power (%)	Cycles	Time (min)	Energy density (MJ/m^3)	Mean diameter (µm)
1	-1	-1	-1	60	0.60	9	1.55	3.28
2	1	-1	-1	90	0.60	9	2.33	2.82
3	-1	1	-1	60	0.90	9	2.33	2.84
4	1	1	-1	90	0.90	9	3.49	2.05
5	-1	-1	1	60	0.60	21	3.62	2.52
6	1	-1	1	90	0.60	21	5.44	1.76
7	-1	1	1	60	0.90	21	5.44	2.09
8	1	1	1	90	0.90	21	8.16	1.54
9	-1.68	0	0	50	0.75	15	2.70	3.24
10	1.68	0	0	100	0.75	15	5.40	1.81
11	0	-1.68	0	75	0.50	15	2.70	3.40
12	0	1.68	0	75	1.00	15	5.40	1.43
13	0	0	-1.68	75	0.75	5	1.35	5.13
14	0	0	1.68	75	0.75	25	6.75	1.77
15	0	0	0	75	0.75	15	4.05	2.83
15	0	0	0	75	0.75	15	4.05	2.48

15	0	0	0	75	0.75	15	4.05	2.66

Table 3.1 presents the mean diameter values obtained from image analysis for all emulsions studied in the experimental design. Emulsions named as 15 are replicates obtained from the same processing. Therefore, the reproducibility of the sonication process can be measured by the standard deviation of mean diameter (±0.17 μm). In order to get a deeper insight into these results, figures 3.2A, 3.2B and 3.2C are illustrated. These figures present the influence of processing time, cycles and power on mean diameter of droplets, respectively. Interestingly, there is a decrease in droplet size with power, cycles and processing time. Hence, it seems that more energy provokes the reduction of droplet size for this formulation. In this sense, recoalescence is not taking part, since zein particles are able to stabilize the interface created.

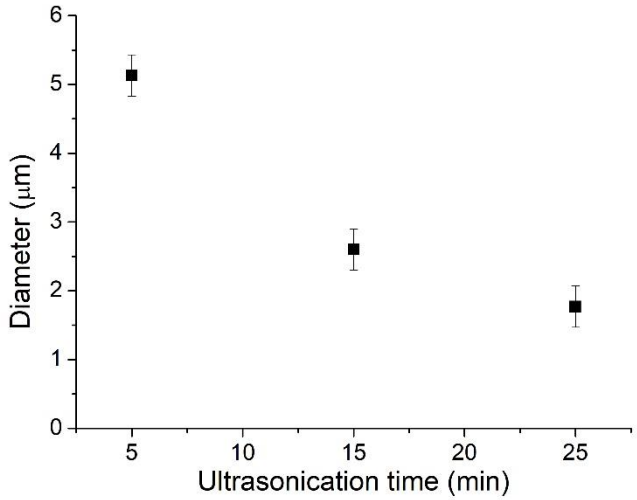

Figure 3.2A. Influence of processing time on mean diameter for emulsions 13, 14 and 15.

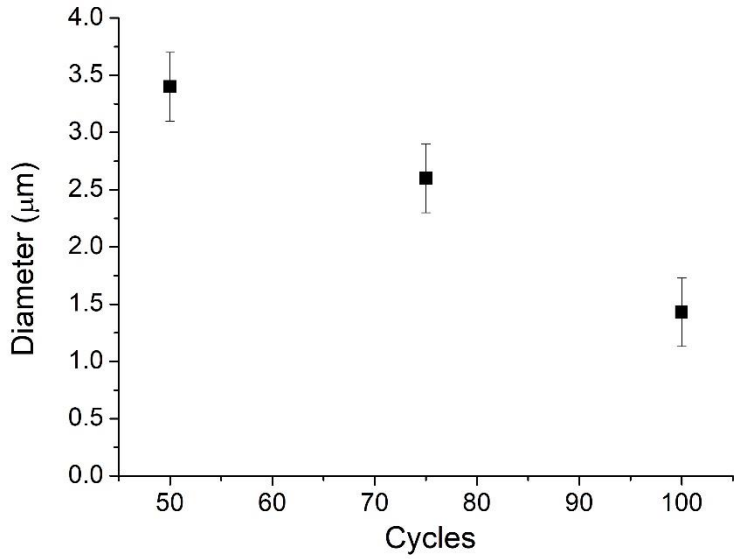

Figure 3.2B. Influence of cycles on mean diameter for emulsions 11,12 and 15.

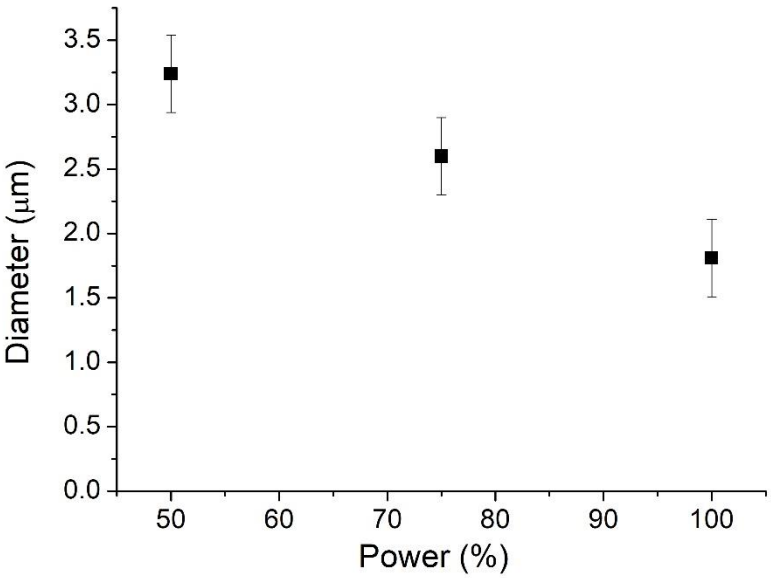

Figure 3.2C. Influence of ultrasonication power on mean diameter for emulsions 9,10 and 15.

Figure 3.3 shows the mean diameter obtained as a function of the energy density for each experiment. Energy density has been calculated using equation 3.2. This figure illustrates a big decrease in droplet diameter with energy density from 1.3 to 1.55 MJ/m^3. Then, the decrease is much slighter with a tendency to stabilise above 5.5 MJ/m^3. The latter has been also observed in other studies using ultrasounds (Kulkarni, 2017; Mahdi Jafari, He, & Bhandari, 2006).

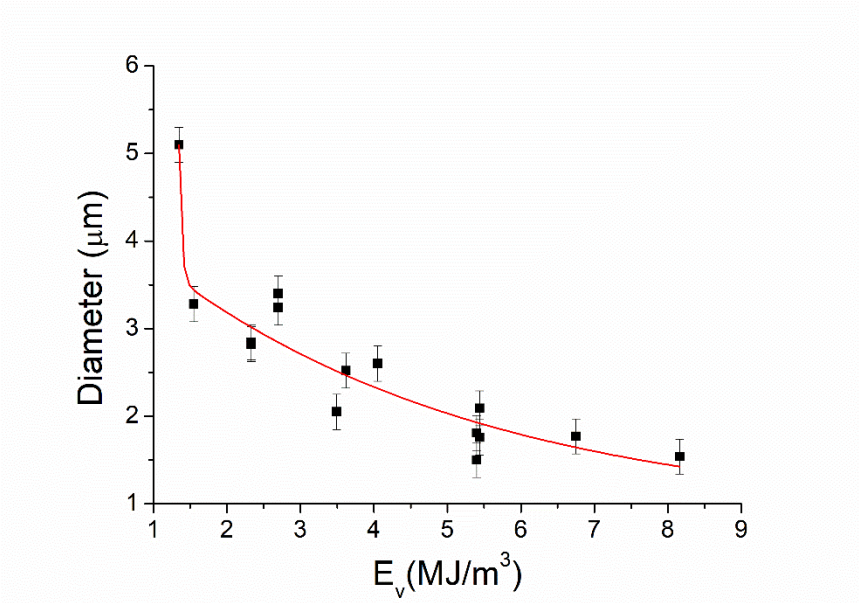

Figure 3.3. Influence of energy density on droplet size obtained in a sonicator using the processing parameters showed in experiments design (table 3.1).

Figure 3.4 illustrates the three-dimensional response surface curve of droplet mean diameter for A) ultrasonic power and cycles used, B) ultrasonic power and ultrasonic time and C) cycles and ultrasonic time. In addition, these figures are the representation of Equation (3), which relates the droplet mean diameter with the variables studied: power (P), cycles (C) and time (T).

$$D = 2.63 - 0.36P - 0.35C - 0.52T - 0.16C^2 \qquad \text{Equation (3.3)}$$

These figures prove the fact that an increase of time, cycles and power provokes a reduction of droplet mean diameter.

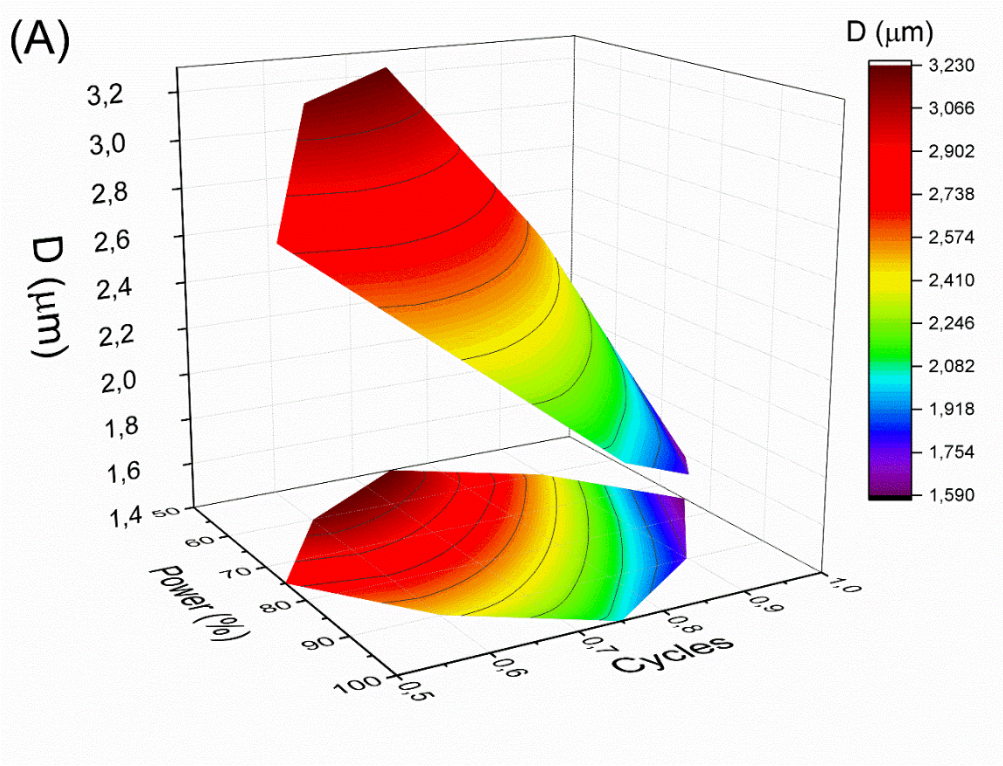

Figure 3.4A. Response surface 3D plots of mean diameter as a function of power and cycles used in sonicator.

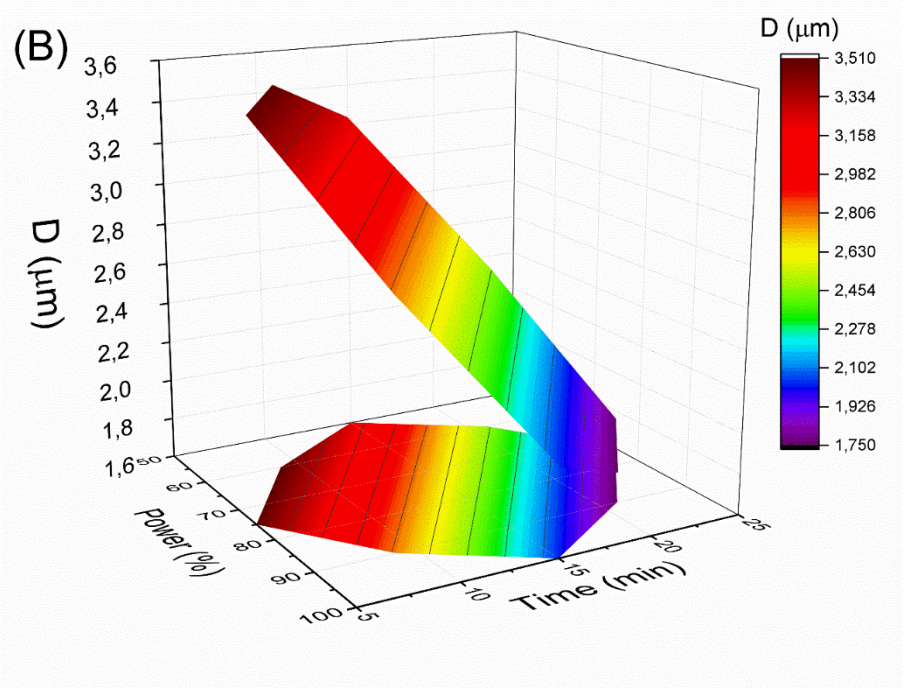

Figure 3.4B. Response surface 3D plots of mean diameter as a function of power and homogenization time in sonicator.

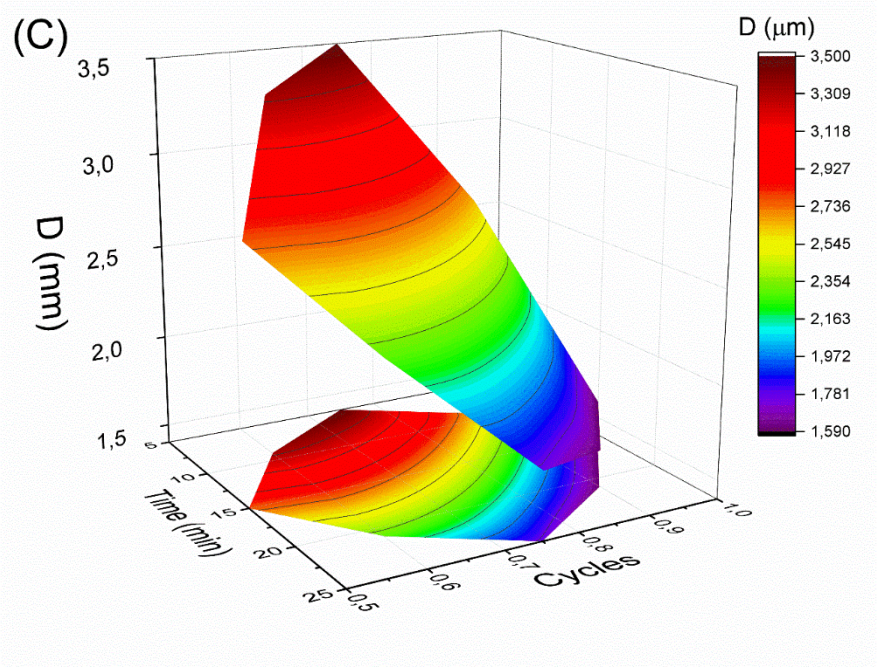

Figure 3.4C. Response surface 3D plots of mean diameter as a function of homogenization time and cycles used in sonicator.

3.3.2. Influence of guar gum concentration or diutan gum concentration on rheological properties, stability and microstructure of emulsions formulated with zein and sunflower oil

Once the processing parameters have been selected, two different thickeners have been incorporated to the continuous phase in order to enhance the physical stability. Figure 3.5 shows the flow behaviour for all emulsions developed: without gum, with guar gum and with diutan gum. Interestingly, all emulsions present shear-thinning behaviour, which fitted fairly well to Cross model (equation 3.2 and table 3.2; $R^2 > 0.98$). In all the cases, an increase in gum concentration provoked an increase in zero-shear viscosity. But the values for zero-shear viscosity for emulsions formulated with diutan gum were significantly higher than those obtained for emulsions with guar gum, which was demonstrated by Tukey test. In addition, this difference is also observed

for flow index values (n), which is one for Newtonian fluids and decreases with the shear-thinning character. Flow index values were lower for emulsions formulated with diutan gum than those obtained for emulsions with guar gum. These facts are evidences of a higher structuration grade provoked for the presence of diutan gum. Some authors suggest the ability of diutan gum to form a 3D network in aqueous continuous phases (Jenifer Santos et al., 2019; Xu et al., 2018). This could be why the rheological behaviour of emulsions containing DG is very different comparing to emulsions with GG. In addition, this could provoke an enhanced physical stability.

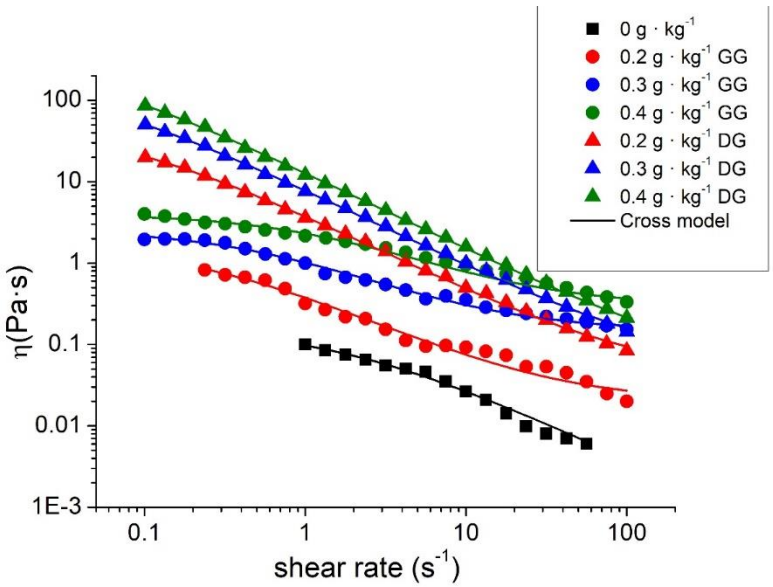

Figure 3.5. Flow behaviour of emulsions formulated with zein and sunflower oil as a function of guar gum concentration and diutan gum concentration.

Table 3.2. Fitting parameters to Cross model for emulsions developed as a function of guar gum and diutan gum concentrations. Different letters indicate significant differences between means for all parameters as calculated by Tukey tests for a significance level of p=0.05.

Emulsion samples	η_0 (Pa·s)	η_∞(Pa·s)	k (s)	n (-)
0 g · kg^{-1} gum	0.16 ± 0.01 ^{a}	0	0.60 ± 0.05 ^{a}	0.10 ± 0.01 ^{a}
2 g · kg^{-1} guar	1.64 ± 0.18 ^{b}	0.02	4.07 ± 0.83 ^{b}	0.10 ± 0.01 ^{a}

3 g · kg^{-1} guar	2.57 ± 0.16 ^{c}	0.14	1.93 ± 0.11 ^{c}	0.10 ± 0.01 ^{a}
4 g · kg^{-1} guar	4.02 ± 0.54 ^{d}	0.3	0.83 ± 0.15 ^{a}	0.10 ± 0.02 ^{a}
2 g · kg^{-1}diutan	47.77 ± 3.72 ^{e}	0.04	13.69 ± 1.01 ^{d}	0.05 ± <0.01 ^{b}
3 g · kg^{-1} diutan	171.93 ± 12.21 ^{f}	0.05	25.09 ± 1.41 ^{e}	0.05 ± <0.01 ^{b}
4 g · kg^{-1} diutan	345.88 ± 25.94 ^{g}	0.05	31.36 ± 1.66 ^{f}	0.05 ± <0.01 ^{b}

Figure 3.6 illustrates the mechanical spectra for emulsions developed using guar gum and diutan gum. Two different behaviours are presented: i) emulsions formulated with guar gum showed a cross-over point (ω^*) while ii) emulsions containing diutan gum showed elastic modulus (G') higher than the viscous modulus (G'') in all the frequency range studied. The former is typical of weakly structured materials, where G' is lower than G'' at low frequencies up to the cross-over point, and then G' is higher than G''. This crossover frequency determines the onset of the terminal relaxation zone. On the other hand, emulsions with G' values higher than G'' values in all frequency range studied are considered as gel-like materials. Gels are related to a network microstructure, which can confer a great physical stability. Furthermore, a strong slope of G', and a slight difference between G' and G'' is observed for diutan gum emulsions. It is a typical weak gel-like material. In addition, there is an increase in both viscoelastic functions (G' and G'') with gum concentration. Generally, higher G' values are related to a higher physical stability if depletion flocculation is not taking part.

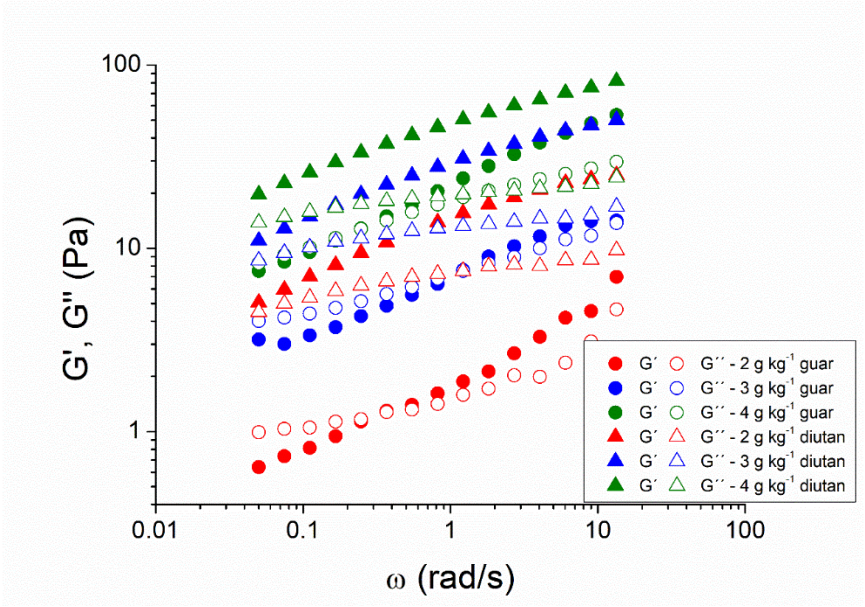

Figure 3.6. Mechanical spectra for emulsions developed as a function of guar gum and diutan gum concentration.

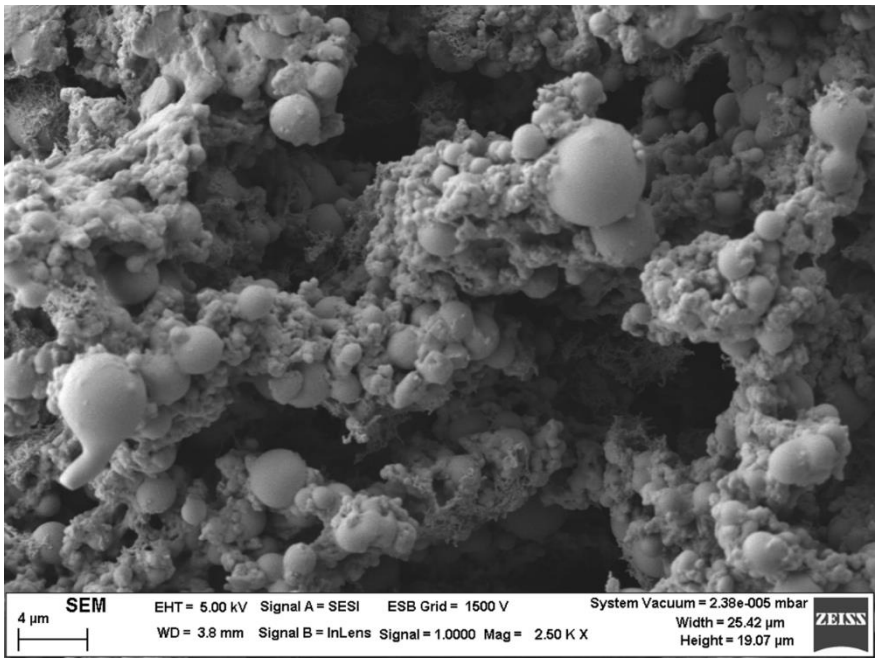

Figure 3.7A. Microstructure of emulsion formulated with zein but without gums observed by Field Emission Scanning Electron Microscope.

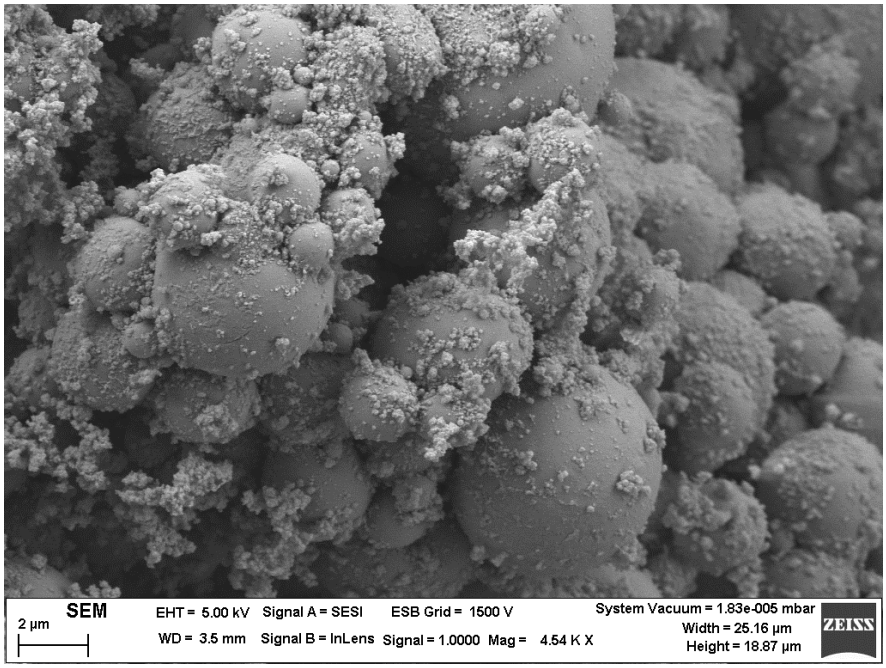

Figure 3.7B. Microstructure of emulsion formulated with zein and 0.3 g · kg^{-1} of Guar gum observed by Field Emission Scanning Electron Microscope.

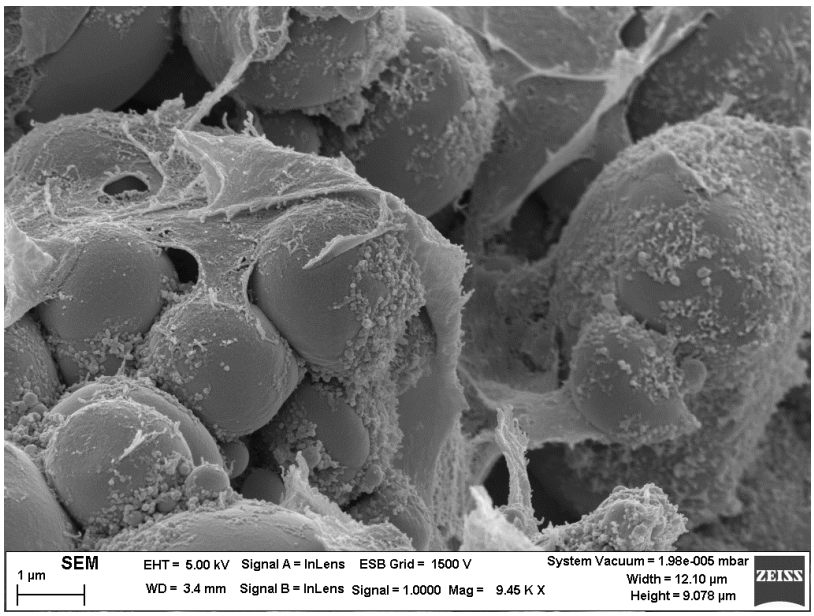

Figure 3.7C. Microstructure of emulsion formulated with zein and 0.3 g · kg^{-1} of Diutan gum observed by Field Emission Scanning Electron Microscope.

In order to get a deeper insight into the microstructure of the emulsions, Field Emission Scanning Electron Microscopy was conducted. Figure 3.7A shows the microstructure of emulsion formulated with zein but without gums. Droplets are flocculated and zein appears to be in the interface covering droplets. These facts were also reported by Santos et al., 2020 (J. Santos et al., 2020). The microstructure created by the emulsion containing 3 g · kg^{-1} guar gum and zein is observed in figure 3.7B. Flocculated droplets are also observed covered by small solid particles, which suggests zein protein is situated in the interface protecting droplets. This fact was also observed in resveratrol-loaded zein particles by Liang et al, 2018 (Liang et al., 2018). However, comparing to figure 3.7A, the solid particles seems to be finer. Guar gum cannot be clearly identified, which may be an indication of a weak structure. On the other hand, the microstructure observed in emulsions formulated with diutan gum is quite different (figure 3.7C). This was also indicated by rheological results. Interestingly, diutan gum seems to form a 3D-network covering droplets. It is like a thin layer that could protect the droplets against coalescence. This is similar to the microstructure formed by zein/pectin nanoparticles reported by Jiang, 2019 (Jiang, Li, Li, Sun-Waterhouse, & Huang, 2019). In addition, this microstructure could inhibit the movement of the droplets in emulsions, which is also suggested by rheological measurements. In this way, the use of diutan gum in emulsions can reduce creaming or flocculation.

To study the influence of storage time, frequency sweeps were carried out not only at 1 day of aging time but also at 7 days of aging time. By way of example, this influence is shown in figure 3.8A for emulsion containing 4 g kg^{-1} guar gum and in figure 3.8B for emulsion containing 4 g kg^{-1} diutan gum. On the one hand, emulsion containing GG presented an increase of viscoelastic moduli (G' and G'') with aging time. In addition, while this sample showed a cross-over point at one day of aging time, this did not occur at 7 days of aging time. This is a clear evidence of an increase of structuration grade. This fact suggests a

destabilization mechanism by creaming or flocculation. On the other hand, emulsion containing DG did not show any variance in viscoelastic properties with aging time, which points out a high physical stability.

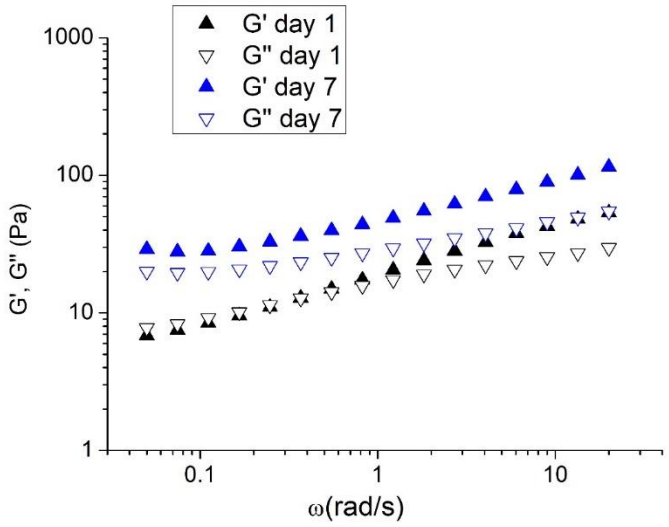

Figure 3.8A. Influence of storage time on viscoelastic properties for emulsion containing 0.4 g · kg^{-1} GG.

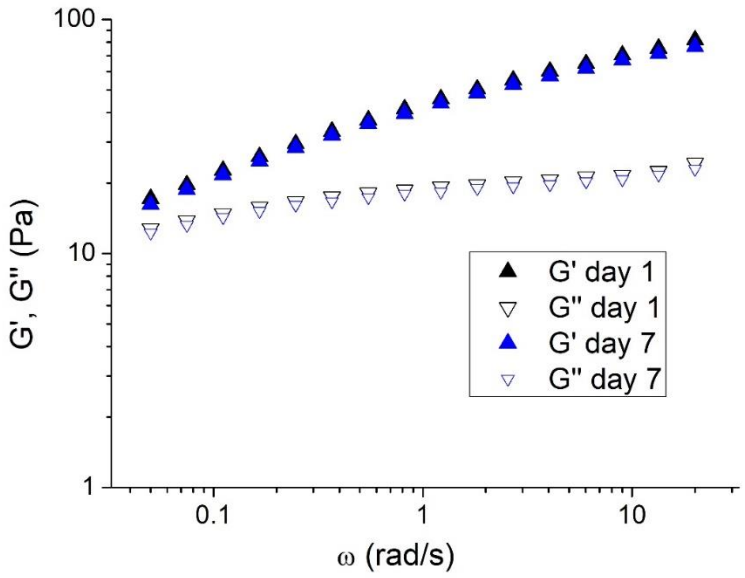

Figure 3.8B. Influence of storage time on viscoelastic properties for emulsion containing 0.4 g · kg^{-1} DG.

Figure 3.9 illustrates the elastic modulus at 0.1 rad/s (day 1 and day 7) for emulsions containing guar gum (GG) or diutan gum (DG). G' values at one day of aging time for guar gum emulsions are lower than their counterpart, suggesting a weaker microstructure again. But the most revealing point is the influence of aging time on G'. There is a big increase in G' for emulsions containing guar (specially for 4 g · kg^{-1}). This fact suggests the occurrence of a destabilization process like creaming or flocculation. However, G' at 1 day and 7 days of aging time did not present significant differences for emulsions containing diutan gum, revealing a greater physical stability. This is explained by the formation of a 3D-network of diutan that not only inhibits the movement of droplets but also protect these of collisions, as seen in figure 3.7C.

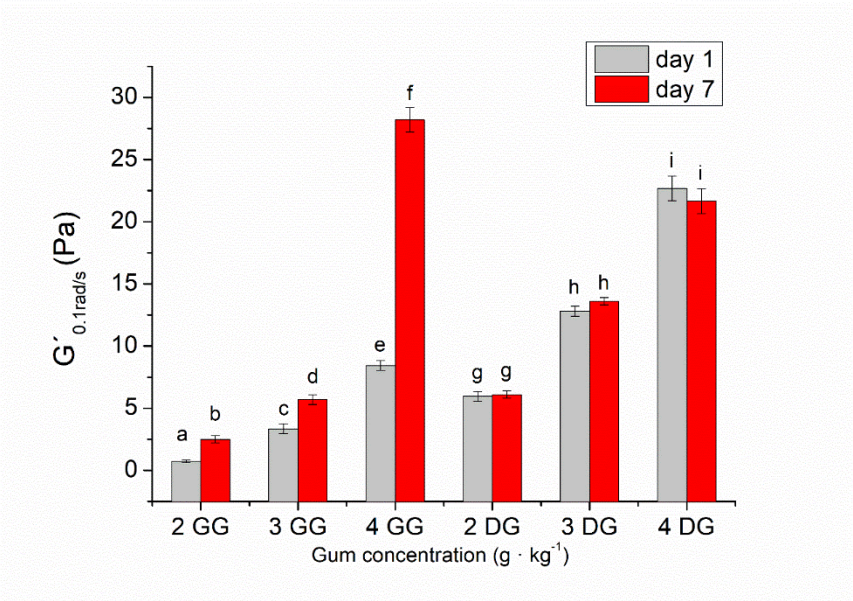

Figure 3.9. Elastic modulus at 0.1 rad/s for emulsions as a function of guar gum (GG) and diutan gum (DG) concentration at 1 and 7 days of aging time. Different letters indicate significant differences between means for all parameters as calculated by Tukey tests for a significance level of p=0.05.

CONCLUSIONS

Optimization of sonication parameters in order to minimise the mean droplet size of emulsions containing zein was carried out. It has been proved that an increase of energy input provokes a reduction of droplet size for these emulsions, with a trend to stabilise at high energies. In addition, the recoalescence was not observed regardless the processing parameters.

Once the sonication process was optimised, two different gums (diutan gum and guar gum) were tested to enhance the physical stability of emulsions formulated with zein. On the one hand, the presence of guar gum is not able to form a strong network and consequently, a rheological gel. On the other hand, emulsions formulated with zein-diutan gum presented G' values higher than G'' in all the frequency range studied, proving the stronger structure formed. In addition, this network formed is observed by FESEM technique.

These different microstructures provoked the differences reported in terms of physical stability. Emulsions containing zein-diutan gum complexes did not show variances in rheological properties with aging time. This work extends the knowledge about zein-gums complexes, bringing to light the importance of the correct election of the polysaccharide.

References

Banerjee, P., Mukherjee, I., Bhattacharya, S., Datta, S., Moulik, S. P., & Sarkar, D. (2009). Sorption of water vapor, hydration, and viscosity of carboxymethylhydroxypropyl guar, diutan, and xanthan gums, and their molecular association with and without salts (NaCl, CaCl2, HCOOK, CH3COONa,(NH4) 2SO4 and MgSO4) in aqueous solution. *Langmuir*, *25*(19), 11647–11656.

Belitz, H., Grosch, W., & Schienberle, P. (1999). Polysaccharides. *Food Chemistry*, 237–318.

Brewer, C. F., Sternlicht, H., Marcus, D. M., & Grollman, A. P. (1973). Interactions of saccharides with concanavalin A. Mechanism of binding of α- and β-methyl D-glucopyranoside to concanavalin A as determined by carbon-13 nuclear magnetic resonance. *Biochemistry*, *12*(22), 4448–4457.

Cao, D., Lv, Y., Zhou, Q., Chen, Y., & Qian, X. (2021). Guar gum/gellan gum interpenetrating-network self-healing hydrogels for human motion detection. *European Polymer Journal*, *151*, 110371.

Carmen García, M., Trujillo, L. A., Carmona, J. A., Muñoz, J., & Carmen Alfaro, M. (2019). Flow, dynamic viscoelastic and creep properties of a biological polymer produced by Sphingomonas sp. as affected by concentration. *International Journal of Biological Macromolecules*, *125*, 1242–1247. https://doi.org/10.1016/j.ijbiomac.2018.09.100

Dai, L., Sun, C., Wei, Y., Mao, L., & Gao, Y. (2018). Characterization of Pickering emulsion gels stabilized by zein/gum arabic complex colloidal nanoparticles. *Food Hydrocolloids*, *74*, 239–248.

Davidov-Pardo, G., Joye, I. J., Espinal-Ruiz, M., & McClements, D. J. (2015). Effect of maillard conjugates on the physical stability of zein nanoparticles prepared by liquid antisolvent coprecipitation. *Journal of Agricultural and Food Chemistry*, *63*(38), 8510–8518.

Duhan, N., Sahu, J. K., Mohapatra, A., & Naik, S. N. (2021). Microencapsulation of ghee flavorants with whey protein concentrate and

guar gum using spray drying. *Journal of Food Processing and Preservation*, e15537.

Gavahian, M., Chu, Y. H., Lorenzo, J. M., Mousavi Khaneghah, A., & Barba, F. J. (2020). Essential oils as natural preservatives for bakery products: Understanding the mechanisms of action, recent findings, and applications. *Critical Reviews in Food Science and Nutrition*, *60*(2), 310–321. https://doi.org/10.1080/10408398.2018.1525601

Hamcerencu, M., Desbrieres, J., Popa, M., & Riess, G. (2009). Stimuli-sensitive xanthan derivatives/N-isopropylacrylamide hydrogels: influence of cross-linking agent on interpenetrating polymer network properties. *Biomacromolecules*, *10*(7), 1911–1922.

Heyman, B., De Vos, W. H., Van der Meeren, P., & Dewettinck, K. (2014). Gums tuning the rheological properties of modified maize starch pastes: Differences between guar and xanthan. *Food Hydrocolloids*, *39*(2014), 85–94. https://doi.org/10.1016/j.foodhyd.2013.12.024

Jiang, Y., Li, F., Li, D., Sun-Waterhouse, D., & Huang, Q. (2019). Zein/Pectin Nanoparticle-Stabilized Sesame Oil Pickering Emulsions: Sustainable Bioactive Carriers and Healthy Alternatives to Sesame Paste. *Food and Bioprocess Technology*, *12*(12), 1982–1992.

Karthikeyan, K., Guhathakarta, S., Rajaram, R., & Korrapati, P. S. (2012). Electrospun zein/eudragit nanofibers based dual drug delivery system for the simultaneous delivery of aceclofenac and pantoprazole. *International Journal of Pharmaceutics*, *438*(1–2), 117–122.

Kulkarni, C. V. (2017). Ultrasonic processing of butter oil (ghee) into oil-in-water emulsions. *Journal of Food Processing and Preservation*, *41*(5), 1–7. https://doi.org/10.1111/jfpp.13170

Li, J., Xu, X., Chen, Z., Wang, T., Lu, Z., Hu, W., & Wang, L. (2018). Zein/gum Arabic nanoparticle-stabilized Pickering emulsion with thymol as an antibacterial delivery system. *Carbohydrate Polymers*, *200*, 416–426.

Li, Z., Ramay, H. R., Hauch, K. D., Xiao, D., & Zhang, M. (2005). Chitosan–alginate hybrid scaffolds for bone tissue engineering. *Biomaterials*, *26*(18), 3919–3928.

Liang, Q., Ren, X., Zhang, X., Hou, T., Chalamaiah, M., Ma, H., & Xu, B. (2018). Effect of ultrasound on the preparation of resveratrol-loaded zein particles. *Journal of Food Engineering*, *221*, 88–94. https://doi.org/10.1016/j.jfoodeng.2017.10.002

Liu, S., Elmer, C., Low, N. H., & Nickerson, M. T. (2010). Effect of pH on the

functional behaviour of pea protein isolate–gum Arabic complexes. *Food Research International*, *43*(2), 489–495.

Liu, X., Sun, Q., Wang, H., Zhang, L., & Wang, J.-Y. (2005). Microspheres of corn protein, zein, for an ivermectin drug delivery system. *Biomaterials*, *26*(1), 109–115.

Luo, Y., Teng, Z., & Wang, Q. (2012). Development of zein nanoparticles coated with carboxymethyl chitosan for encapsulation and controlled release of vitamin D3. *Journal of Agricultural and Food Chemistry*, *60*(3), 836–843.

Luo, Y., & Wang, Q. (2014). Zein-based micro-and nano-particles for drug and nutrient delivery: A review. *Journal of Applied Polymer Science*, *131*(16).

Mahdi Jafari, S., He, Y., & Bhandari, B. (2006). Nano-emulsion production by sonication and microfluidization—a comparison. *International Journal of Food Properties*, *9*(3), 475–485.

Moneret-Vautrin, D. A., Kanny, G., & Beaudouin, E. (1998). L'allergie alimentaire au maïs existe-t-elle? *Allergie et Immunologie (Paris)*, *30*(7).

Mukherjee, I., Sarkar, D., & Moulik, S. P. (2010). Interaction of gums (Guar, Carboxymethylhydroxypropyl Guar, Diutan, and Xanthan) with surfactants (DTAB, CTAB, and TX-100) in aqueous medium. *Langmuir*, *26*(23), 17906–17912. https://doi.org/10.1021/la102717v

Santos, J., Alcaide-González, M. A., Trujillo-Cayado, L. A., Carrillo, F., & Alfaro-Rodríguez, M. C. (2020). Development of food-grade Pickering emulsions stabilized by a biological macromolecule (xanthan gum) and zein. *International Journal of Biological Macromolecules*, *153*, 747–754. https://doi.org/10.1016/j.ijbiomac.2020.03.078

Santos, Jenifer, Calero, N., Guerrero, A., & Muñoz, J. (2015). Relationship of rheological and microstructural properties with physical stability of potato protein-based emulsions stabilized by guar gum. *Food Hydrocolloids*, *44*, 109–114.

Santos, Jenifer, Jiménez, M., Calero, N., Undabeytia, T., & Muñoz, J. (2019). A comparison of microfluidization and sonication to obtain lemongrass submicron emulsions. Effect of diutan gum concentration as stabilizer. *Lwt*, *114*(February), 108424. https://doi.org/10.1016/j.lwt.2019.108424

Shen, Y., & Li, Y. (2021). Acylation modification and/or guar gum conjugation enhanced functional properties of pea protein isolate. *Food Hydrocolloids*, *117*, 106686.

Sonebi, M., & McKendry, D. (2008). Effect of mix proportions on rheological and hardened properties of composite cement pastes. *The Open*

Construction and Building Technology Journal, *2*(1).

Wang, L.-J., Yin, S.-W., Wu, L.-Y., Qi, J.-R., Guo, J., & Yang, X.-Q. (2016). Fabrication and characterization of Pickering emulsions and oil gels stabilized by highly charged zein/chitosan complex particles (ZCCPs). *Food Chemistry*, *213*, 462–469.

Weissmueller, N. T., Lu, H. D., Hurley, A., & Prud'homme, R. K. (2016). Nanocarriers from GRAS zein proteins to encapsulate hydrophobic actives. *Biomacromolecules*, *17*(11), 3828–3837.

Xia, X., Wei, H., Hu, L., & Peng, J. (2021). Hydratability and improved fermentability in vitro of guar gum by combination of xanthan gum. *Carbohydrate Polymers*, *258*, 117625.

Xu, L., Qiu, Z., Gong, H., Liu, C., Li, Y., & Dong, M. (2018). Effect of diutan microbial polysaccharide on the stability and rheological properties of O/W nanoemulsions formed with a blend of Span20-Tween20. *Journal of Dispersion Science and Technology*, *39*(11), 1644–1654. https://doi.org/10.1080/01932691.2018.1461636

Xu, L., Qiu, Z., Gong, H., Zhu, C., Sang, Q., Li, Y., & Dong, M. (2019). Synergy of microbial polysaccharides and branched-preformed particle gel on thickening and enhanced oil recovery. *Chemical Engineering Science*, *208*, 115138.

Chapter 4.

Impact of microfluidization on the emulsifying properties of zein-based emulsions. Influence of diutan gum concentration.

Abstract

Microfluidization is a preparation method that can be used to obtain emulsions with submicron droplet sizes. The first objective of this study was evaluate the influence of homogenization pressure and cycles on droplet sizes using response surface methodology. Secondly, the influence of diutan gum concentration incorporated to the optimised emulsion on rheological properties, microstructure and physical stability were investigated. Taking into account response surface analysis, the emulsion processed at 20000 psi after 4 cycles seems to show the smallest Sauter diameter values. Hence, this emulsion was the starting point to incorporate diutan gum. Interestingly, the formation of a 3D-network in the emulsion, observed by FESEM, was provoked by diutan gum. The emulsion formulated with 0.4 wt% of diutan gum presented rheological gel properties and enhanced physical stability. This work wants to highlight the importance of select the optimised processing variables using in microfluidization technique and extend the knowledge of using diutan gum in combination with zein.

Keywords: microfluidization, zein, diutan gum, rheology.

4.1. Introduction

Pickering emulsions, which can be defined as dispersed systems stabilised by colloidal particles, present some advantages comparing to emulsions stabilised by surfactants. For example, Pickering emulsions stabilisers are able to reduce coalescence, aggregation of droplets and Ostwald ripening (Albert et al., 2019; Berton-Carabin & Schroën, 2015). Natural Pickering stabilisers have no problems concerning biodegradability and compatibility in food and pharmaceuticals products (Patel & Velikov, 2011), in contrast to inorganic or synthetic Pickering stabilisers (Chevalier & Bolzinger, 2013). Because of that, food-grade colloidal particles have been used more and more as Pickering stabilisers such as cellulose derivatives, modified starch, plant proteins or

cereal proteins. A cereal protein, zein, is considered a promising biopolymer of the 21st century (Luo & Wang, 2014). Zein is the main storage protein of corn and is rich in prolamin. Their colloidal particles are very interesting due to the potential applications in food industry. Nevertheless, prolamins present high hydrophobicity, which can be a problem to form Pickering emulsions. Previously, different authors have researched about how adjust the zein aggregation and its structure modifying the pH of the solvent where zein is dissolved (Zhang, Luo, & Wang, 2011). Microfluidization could also be an interesting method to modify the protein structure and its emulsifying properties (Ozturk & Mert, 2019; Ye & Harte, 2014). On the other hand, some studies report that the interaction between prolamins and natural biopolymers reduce the hydrophobicity and can form stable Pickering emulsions. For example, it has been proved that gum arabic, pectins, and xanthan gum can improve the hydrophilicity of zein and their conjugates can act as effective emulsifiers (Jiang et al., 2020; Ma et al., 2021; J. Santos, Alcaide-González, Trujillo-Cayado, Carrillo, & Alfaro-Rodríguez, 2020). However, there is no information available about the formation of diutan gum-zein complex.

Diutan gum, secreted by *Sphingomonas sp*., is a combination of β-D-glucose, β-D-glucuronic acid and α-L-rhamnose units forming a biodegradable and biocompatible natural biopolymer. This little-known polysaccharide has proved its stabilization role reducing creaming in lemongrass nanoemulsions (Jenifer Santos, Jiménez, Calero, Undabeytia, & Muñoz, 2019). In addition, it is possible to modulate the viscoelasticity and viscosity of diutan gum solutions as a function its concentration in order to enhance the physical stability of emulsions developed (Carmen García, Trujillo, Carmona, Muñoz, & Carmen Alfaro, 2019). However, there is no information available about this polysaccharide used in combination with a protein.

Many types of methods can be used to prepare food emulsions: ultrasonication, rotor-stator, high-pressure homogenisers and microfluidizers. The latter that in based on passing a pre-emulsion through microchannels on the interaction chamber at very high shear, can obtain droplets in the submicron range (Mahdi Jafari, He, & Bhandari, 2006). Concerning interaction chambers, there are two different types: type Y and type Z. Type Y chamber possesses microchannels of 75 µm while Z-type of 200 µm. This provokes that the use of Y chamber can reach up to $8 \cdot 10^6$ s^{-1} of shear, whereas Z-type can reach up to $2 \cdot 10^6$ s^{-1}. Furthermore, it has been proved that the use of chambers Y+Z in series increased the capacity of the devise to obtain not only smaller droplets but also narrower droplet size distributions (Muñoz, Alfaro, Trujillo-Cayado, Santos, & Martín-Piñero, 2019; Trujillo-Cayado, Santos, Ramírez, Alfaro, & Muñoz, 2018).

The main goal of this study is to compare the formation of food emulsions formulated with zein via microfluidization. An extensive research about the microfluidization method on the formation zein-based emulsions was carried out. The effect of microfluidized processing parameters such as homogenization pressure and number of cycles on droplet size distributions were analysed by response surface methodology. Finally, the formation of diutan-zein complex and the influence of its concentration on rheological properties and physical stability of these food emulsions were evaluated. This study wants to bring to light the importance of adjust the microfluidization technique for specific emulsions like zein-based emulsions and extend the knowledge of using diutan gum in combination with a protein.

4.2. Materials and methods

4.2.1. Materials

Zein protein and rosemary essential oil, used as natural food preservative, were provided by Sigma Aldrich. Sunflower oil containing 40 wt.% of oleic acid was bought in the local supermarket. The gum solutions were prepared using KELTROL® diutan gum, donated by CP Kelco (Atlanta, USA), with deionized water.

4.2.2. Microfluidization of food emulsions formulated with zein protein

The formulation of the emulsions developed was: 2.1 wt.% of zein, 40 wt.% of sunflower oil and 0.25 wt.% of rosemary essential oil (natural food preservative) (Gavahian, Chu, Lorenzo, Mousavi Khaneghah, & Barba, 2020). This formulation was previously optimised by Santos at al., 2020 (J Santos, Alcaide-González, Trujillo-Cayado, Carrillo, & Alfaro-Rodríguez, 2020). In the first part of this research, the influence of homogenization pressure and cycles through microfluidizer on droplet size distributions were studied. The continuous phase contains zein protein and deionized water. The pH was adjusted to 11.5 using a NaOH solution. Then, a coarse emulsion (batches of 250 g) was prepared, at room temperature, using a Silverson L5 M for 60 s at 8000 rpm. Finally, finer emulsions were homogenized using a Microfluidizer M110P (Microfluidics company) at different processing parameters (see Table 1). Microfluidizer was used with a configuration of Y+Z and a refrigeration of 20^{o}C.

The emulsion with optimized values of processing was used as a starting point for the addition of the biopolymer (diutan gum, DG) to form a protein-polysaccharide complex. A primary gum solution containing 1.6 wt% of DG was prepared using an IKa-Visc MR-D1 homogenizer for 8 hours at 500 rpm at 20^{o}C. Then, this solution was kept at 7^{o}C for at least 48 hours for the completely hydration of the polysaccharide. The final emulsions were prepared mixing the gum solution and the optimal emulsion using the Ikavisc MR-D1 at 500 rpm

for 10 minutes. Final emulsions contain different DG concentrations (0.1, 0.2, 0.3 and 0.4 wt.%).

Table 4.1. Processing variable conditions used for the present study

Independent variable	Value	Level
Number of cycles (C)	1	-1
	2	-0,5
	3	0
	4	0,5
	5	1
Homogenization pressure (P)	5000	-1
	10000	-0,5
	15000	0
	20000	0,5
	25000	1

4.2.*3 Experimental design and data analysis*

An experimental design and response surface methodology were used for describe and for the analysis the relationship between the dependent variables (mean droplet diameter and span) and independent variables (number of cycles and homogenization pressure). The experimental design consisted of five levels and two factors, generating 5^2 = 25 experiments (see Table 1). The experiments were carried out in duplicates, and the design contained three additional center points (corresponding to 3 cycles at 15000 psi), therefore yielding 28 samples. All the data were analyzed with a one-way analysis of variance (ANOVA) at a 95% confidence level. For model construction, terms with $p > 0.05$ were removed and the analysis was recalculated without these terms. All experimental design and data analyses were performed using Echip software (Experimentation by Design, Wilmington, DE, United States of America).

4.2.4. Droplet size analysis

Droplet size distributions of emulsions developed were characterized by using a Malvern Mastersizer 2000 (laser diffraction technology). In order to characterize these distributions, Sauter diameter and span value were calculated as follows:

$$D_{3.2} = \sum_{i=1}^{N} \frac{n_i d_i^3}{n_i d_i^3} \text{ (EQ. 4.1)}$$

$$span = \frac{d_{90} - d_{10}}{d_{50}} (EQ. 4.2)$$

where d_i is the droplet diameter, N is the total number of droplets and n_i is the number of droplets having a diameter d_i, and d_{90}, d_{50}, d_{10} are the diameters at 90%, 50% and 10% cumulative volume.

4.2.5. Rheological characterization

Rheological tests were carried out using a controlled-stress rheometer MARS II equipped with a serrated plate-plate (60 mm diameter; 1 mm gap) in order to avoid slip effects. Stress sweeps at 1 Hz were performed in order to obtain the Linear Viscoelastic Range (LVR) of the different samples. Frequency sweeps were carried out from 20 to 0.05 rad/s at a stress in the LVR at 20°C. In addition, flow curves were conducted using a multistep protocol of 3 minutes per point (20 points) at 20°C.

4.2.6. Field Emission Scanning Electron Microscopy (FESEM)

The optimized emulsion containing 0.4 wt% DG was observed by FESEM technique. This sample was fixed using glutaraldehyde (4 wt.%, cacodylate 0.1M) and osmium tetroxide (1 wt.%, cacodylate 0.1M). Subsequently, it was dehydrated with ethanol and acetone. Then, the sample was dried using a critical point dryer (CPD; Leica EM CPD 300). The conditions of the dehydration and the drying used were reported by Santos et al 2020 (J. Santos et al., 2020).

4.2.7. Physical stability

In order to evaluate the physical stability of emulsions developed, Multiple Light Scattering technique was conducted. Measurements of backscattering (BS) were carried out at different times of aging to identify and characterize the destabilization processes that could take part in emulsions. In addition, Turbiscan Stability Index (TSI) was calculated to clearly compare the kinetics of destabilization process (Equation 3).

$$TSI = \sum_j \left| scan_{ref}\left(h_j\right) - scan_i\left(h_j\right) \right| \text{(EQ. 4.3)}$$

where $scan_{ref}$ and $scan_i$ are the initial backscattering value and the backscattering-value at a specific time, respectively and h_j is a specific height in the measuring cell.

4.3. Results

4.3.1 Influence of processing parameters in Microfluidizer on droplet sizes

Figures 4.1A, B, C, D and E show the droplet size distributions for emulsions processed by microfluidization at 5000, 10000, 15000, 20000 and 25000 psi, respectively, as a function of number of cycles. A reduction of droplet size can be observed from coarse emulsion to emulsion processed at microfluidizer, regardless the homogenization pressure used. Then, more cycles, smaller droplet sizes. However, it seems that an increase of cycles (cycles > 2) at 5000 psi, 10000 psi and 15000 psi provokes an increase of width of the peak, even the appearance of a second peak. The microfluidization at 20000 and 25000 psi of the coarse emulsion lead to a bimodal droplet size distribution at any number of cycles. The presence of a second peak at bigger droplet size than the main one is related to the recoalescence effect, due to an over-processing emulsification. In order to get a deeper insight into these results, figure 4.2A and 4.2B are shown.

(A)

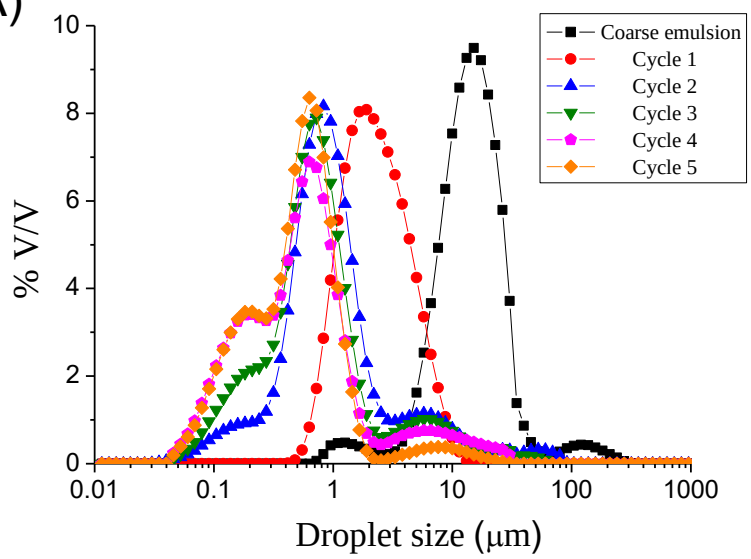
Coarse emulsion
Cycle 1
Cycle 2
Cycle 3
Cycle 4
Cycle 5
% V/V
Droplet size (μm)
0
2
4
6
8
10
0.01
0.1
1
10
100
1000

(B)

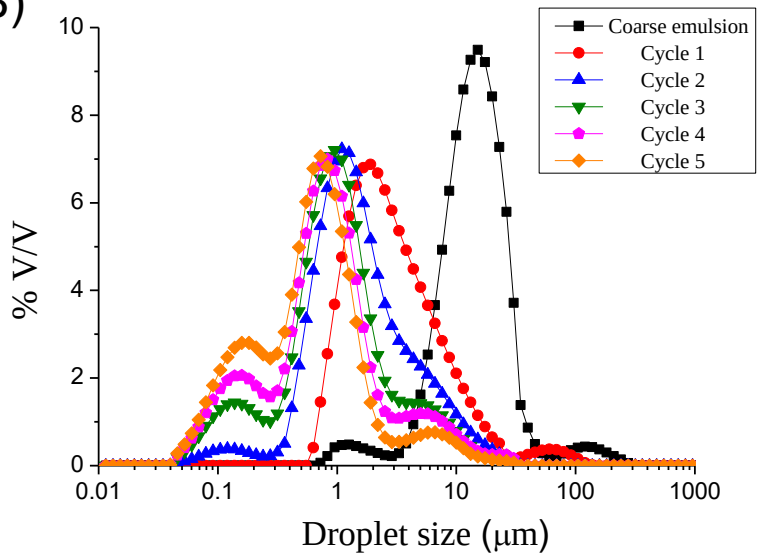
Coarse emulsion
Cycle 1
Cycle 2
Cycle 3
Cycle 4
Cycle 5
% V/V
Droplet size (μm)
0
2
4
6
8
10
0.01
0.1
1
10
100
1000

(C)

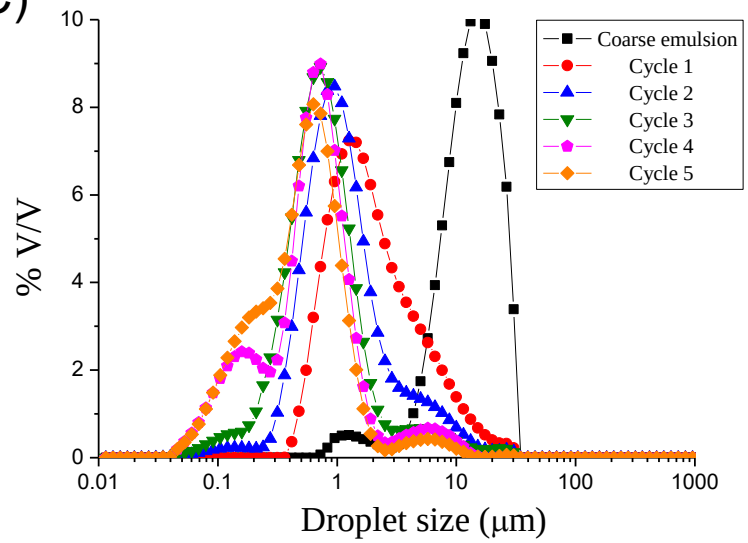
Coarse emulsion
Cycle 1
Cycle 2
Cycle 3
Cycle 4
Cycle 5
% V/V
Droplet size (μm)
0
2
4
6
8
10
0.01
0.1
1
10
100
1000

(D)

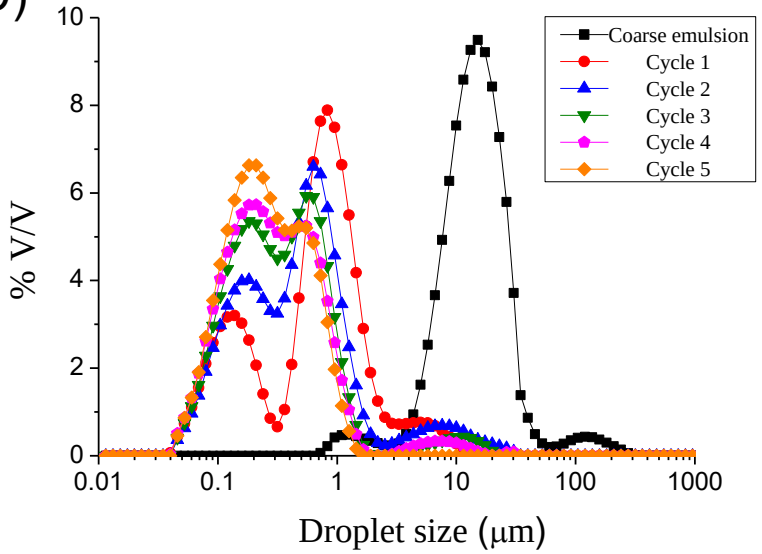
Coarse emulsion
Cycle 1
Cycle 2
Cycle 3
Cycle 4
Cycle 5
% V/V
Droplet size (μm)
0
2
4
6
8
10
0.01
0.1
1
10
100
1000

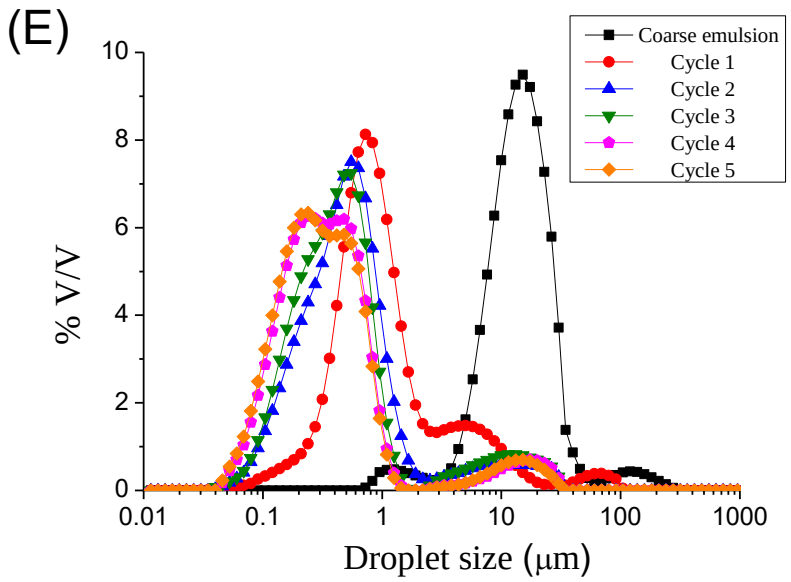

Figure 4.1. Droplet size distributions for emulsions processed by microfluidization at (A) 5000 psi, (B) 10000 psi, (C) 15000 psi and (D) 25000 psi as a function of number of cycles.

Figure 4.2A illustrates the influence of number of cycles in Sauter mean diameter ($D_{3,2}$) as a function of homogenization pressure. Generally, a reduction of $D_{3,2}$ is observed with the number of cycles, regardless of the homogenization pressure. Interestingly, this figure brings to light the occurrence of submicron Sauter diameters at homogenization pressures higher than 15000 psi. It is well-known the relation between submicron droplets diameter and longer physical stabilities (Jafari, Assadpoor, He, & Bhandari, 2008; Llinares, Santos, Trujillo-Cayado, Ramírez, & Muñoz, 2018). In addition, $D_{3,2}$ obtained at 20000 psi are smaller than those obtained at 25000 psi, regardless of the pressure used. This fact could be due to the abovementioned over-processing.

On the other hand, span values with number of cycles as a function of homogenization pressure are shown in figure 2B. The most remarkable result

in this figure is the increase of span values with number of cycles at 25000 psi. This fact is not observed at other pressures. This unusual trend in span can be explained by the recoalescence effect due to over-processing.

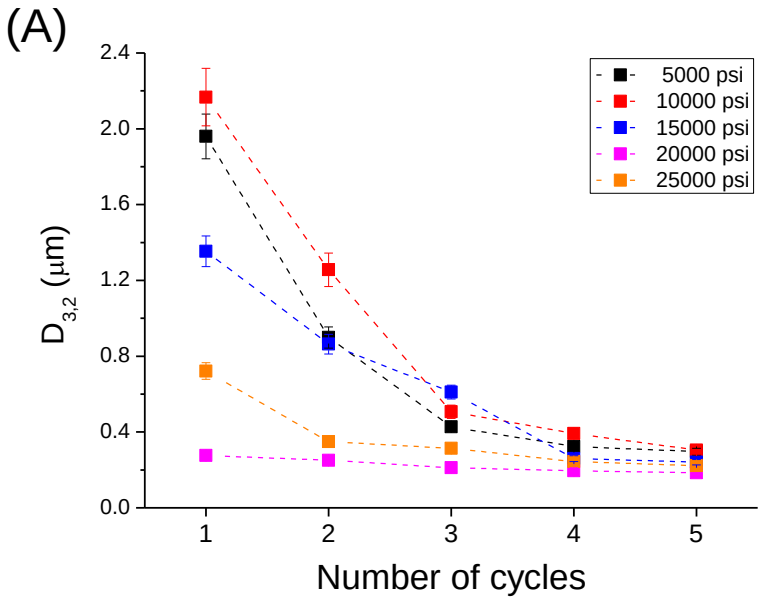

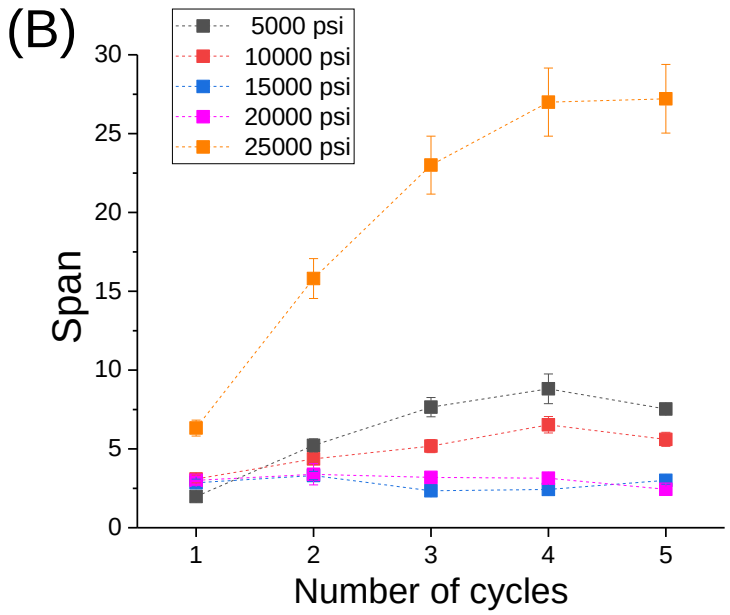

Figure 4.2. (A) Sauter mean diameter and (B) span values for emulsions developed by microfluidization as a function of number of cycles and homogenization pressure.

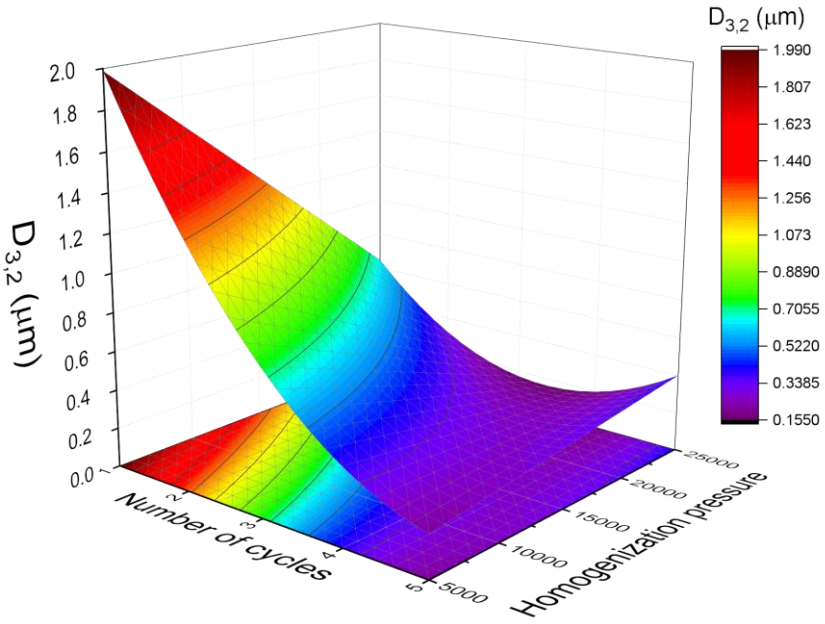

Figure 4.3. Response surface 3D plot of Sauter mean diameter ($D_{3,2}$) as a function of the number of cycles and homogenization pressure

The response surface methodology was used to model the experiments statistically and optimize the parameters for emulsions development. Figure 3 indicates the relationship between Sauter mean diameter ($D_{3,2}$), with homogenization pressure and number of cycles. Sauter mean diameter fitted a quadratic function of number of cycles (C) and homogenization pressure (P):

$$D_{3,2} = 0.459 - 0.504 \cdot C - 0.289 \cdot P + 0.354 \cdot C^2 + 0.382 \cdot C \cdot P \quad \text{(EQ. 4.4)}$$

The coefficient of determination (R^2) value of 0.88 indicated a good correlation between the experimental results and predicted responses. In addition, no significant lack of fit (Fcrit > Flof, with p = 0.05) was obtained, indicating that the model employed was adequate. In this sense, the model predicted that $D_{3,2}$ was sensitive to both studied variables, number of cycles and

homogenization pressure. In the present study, the increase of number of cycles from 1 to 4 cycles and homogenization pressure from 5000 to 20000 psi resulted in the decrease of droplet sizes. However, when the homogenization pressure was increased from 20000 to 25000 psi, there was an increase droplet mean diameter. In addition, there is no significant differences between 4 and 5 cycles at 20000 psi. Hence, the optimum processing variables were limited to 4 cycles and 20000 psi. Taking into account all these results analysis, the emulsion processed at 20000 psi after 4 cycles seems to show the smallest $D_{3,2}$ values. For this reason, these conditions were fixed for the following tests.

4.3.2. Influence of diutan gum concentration in rheological properties, physical stability and microstructure.

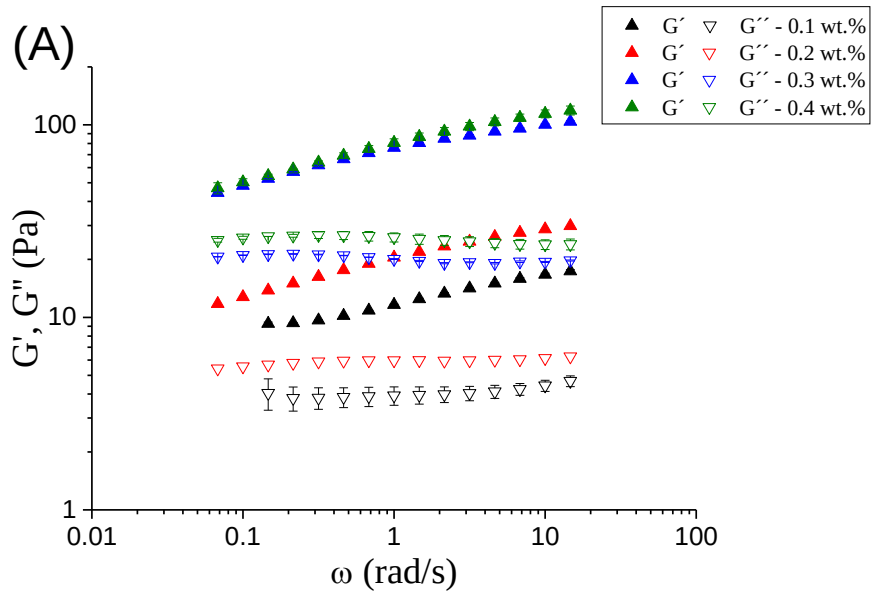

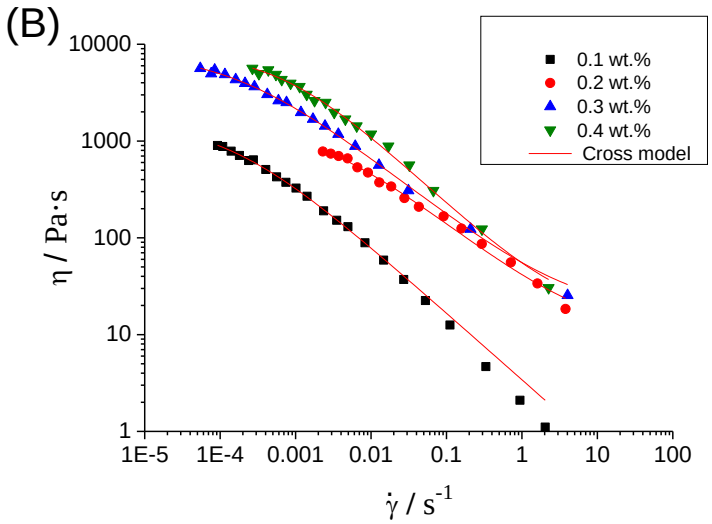

Figure 4.4. (A) Mechanical spectra and (B) flow curves for emulsions formulated with zein as a function of diutan gum concentration.

In order to enhance the physical stability of the optimised emulsion, a study of the influence of diutan gum concentration has been carried out. Interestingly, G' (elastic modulus) is higher than G'' (viscous modulus) in all the frequency range studied at any diutan gum concentration. However, the differences of G' and G'' values are not large. These facts bring to light the existence of a weak gel-like behaviour. The results obtained by Garcia et al, 2019 (Carmen García et al., 2019) showed a cross-over point in the mechanical spectra for the aqueous solutions of diutan gum. Hence, the appearance of zein and droplets have provoked the occurrence of a stronger network. Furthermore, there is an increase in G' and G'' with diutan gum concentration, as expected. Figure 4B presents the flow behaviour for zein-based emulsions as a function of diutan gum concentration. All systems show a decrease of apparent viscosity with shear rate, which is a clear evidence of shear-thinning behaviour. In addition, they are fitted to the well-known Cross model observed in equation 4 (R^2> 0.98). Fitting parameters can be observed in table 4.2.

$$\eta = \frac{\eta_0 - \eta_\infty}{1 + (k\dot{\gamma})^{1-n}} \qquad \text{(EQ. 4.5)}$$

Where, η is the viscosity, $\dot{\gamma}$is the shear rate, $\eta_0$is the viscosity at very low shear rates, η_∞ is the viscosity at very high shear rates, k is the inverse of critical shear rate, and n is the flow index

There is an increase of zero-shear viscosity with diutan gum concentration, as expected. However, there is a big jump in this parameter from 0.2 to 0.3 wt.% and a tendency to level off from 0.3 to 0.4 wt.%. This could be related to a depletion flocculation process. A depletion effect can provoke an attractive force between the oil droplets and form aggregates. This may increase the viscosity from 0.2 wt.% to 0.3 wt.%. Furthermore, flow index values did not present significant differences, showing similar shear-thinning degrees.

Table 4.2. Fitting parameter values for the Cross model. The values were obtained by a non-linear regression analysis.

Standard deviation of the mean (2 replicates) for η_o , η_∞ < 8%

Standard deviation of the mean (2 replicates)for k< 10%

Standard deviation of the mean (2 replicates) for n < 10%

Diutan gum concentration (wt.%)	η_o (Pa·s)	η_∞ (Pa·s)	k (s)	n
0.1	1598	0.0001	7382	0.31
0.2	1620	10	453	0.37
0.3	8286	14	5395	0.38
0.4	8321	15	1346	0.27

In figure 4.5, the microstructure created by droplets, zein and diutan gum is observed for emulsion containing 0.4 wt.% diutan gum. The size of the droplets is very wide, as expected taking into account laser diffraction results. In addition, the emulsion form flocs, but these flocs are immobilized withing the network of diutan macromolecules.

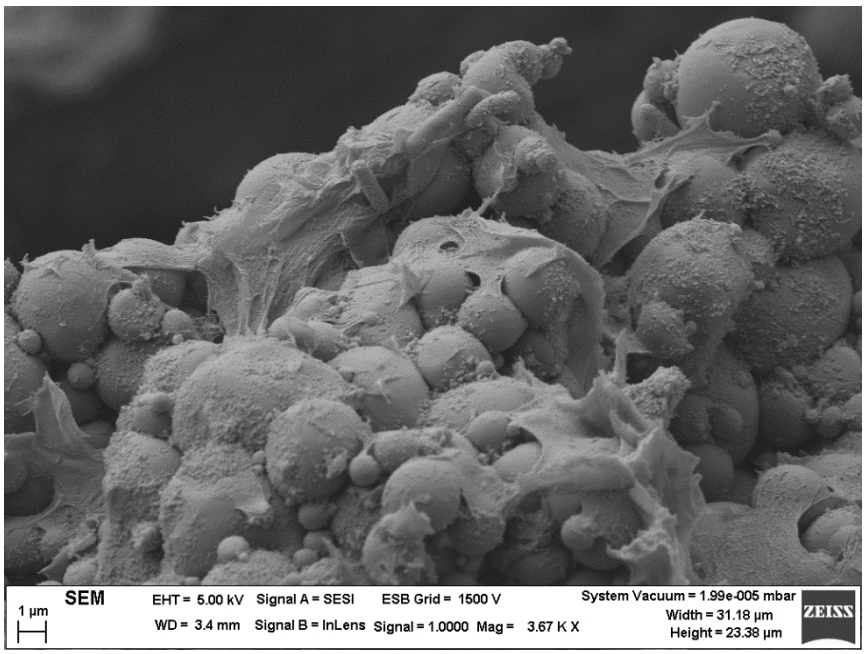

Figure 4.5. Representative Cryo-SEM micrographs for the emulsion formulated with 0.4 wt.% of diutan gum

Backscattering (BS) measurements were carried out in order to study the destabilization mechanism of these emulsions. Figure 4.6A, B, C and D illustrates the BS values with the height of the measuring cell as a function of aging time for emulsions with 0.1 wt.%, 0.2 wt.%, 0.3 wt.% and 0.4 wt.% of diutan gum, respectively. A decrease in BS in the low zone of the measuring cell is shown in figure 4.6A. This fact is related to a clarification process in this zone, i.e. droplets in the low zone migrate to the upper zone leading to a creaming process. The possible solution to this destabilization process is the increase of the continuous phase viscosity. Therefore, emulsions with higher content of biopolymer should be more stable. Backscattering values for 0.2 wt.% emulsion are shown in figure 4.6B. There is a clear drop in BS in the upper zone of the measuring cell, that is related to a destabilization process called oiling-off. By contrast, 0.3 wt.% and 0.4 wt.% diutan gum emulsion do not show wide variations in BS values with aging time. In order to get a deeper insight into these results, figure 4.7 is shown. This figure presents the

Turbiscan Stability Index (TSI) values for the emulsions studied with aging time. An increase in this value is directly related to a decrease of physical stability. Hence, 0.1 wt.% DG-emulsion shows a marked increase in TSI in the first week after preparation. This is less and less accused with diutan gum concentration. The smallest variation of this parameter was obtained by the emulsion formulated with 0.4 wt.% of biopolymer. This result suggests that the strongest network (highest viscosity) is able to reduce the creaming process observed in the emulsion containing 0.1 wt.% of diutan gum.

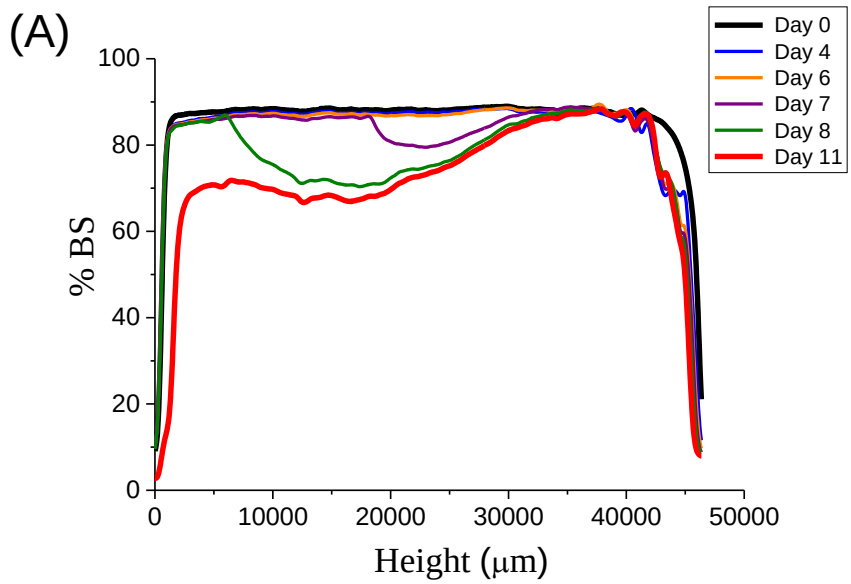

(B)

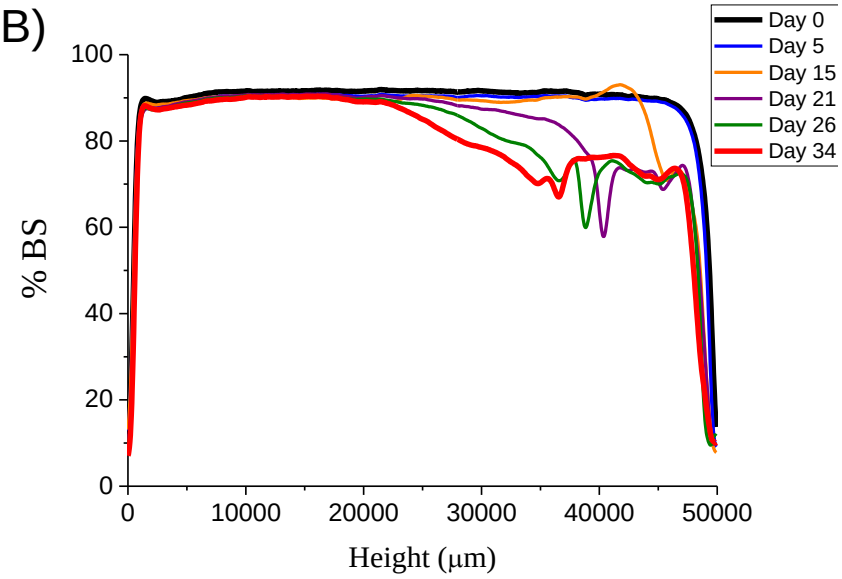
Day 0
Day 5
Day 15
Day 21
Day 26
Day 34
% BS
100
80
60
40
20
0
0
10000
20000
30000
40000
50000
Height (μm)

(C)

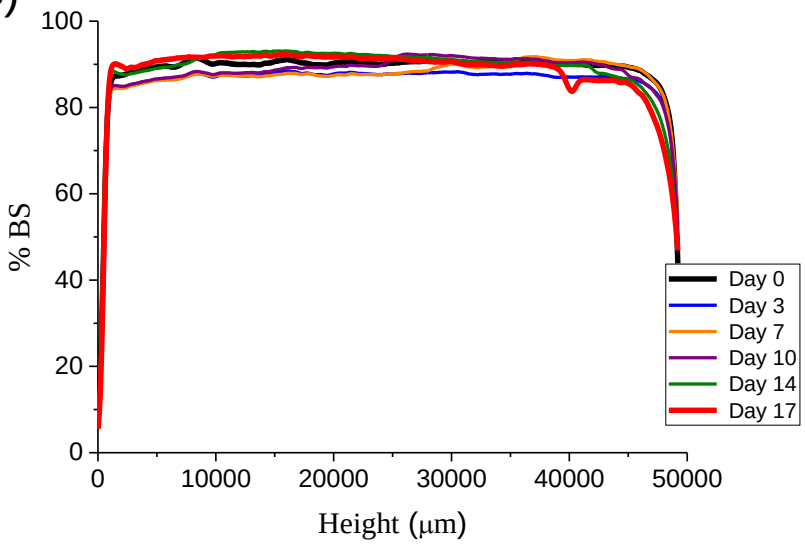
Day 0
Day 3
Day 7
Day 10
Day 14
Day 17
% BS
100
80
60
40
20
0
0
10000
20000
30000
40000
50000
Height (μm)

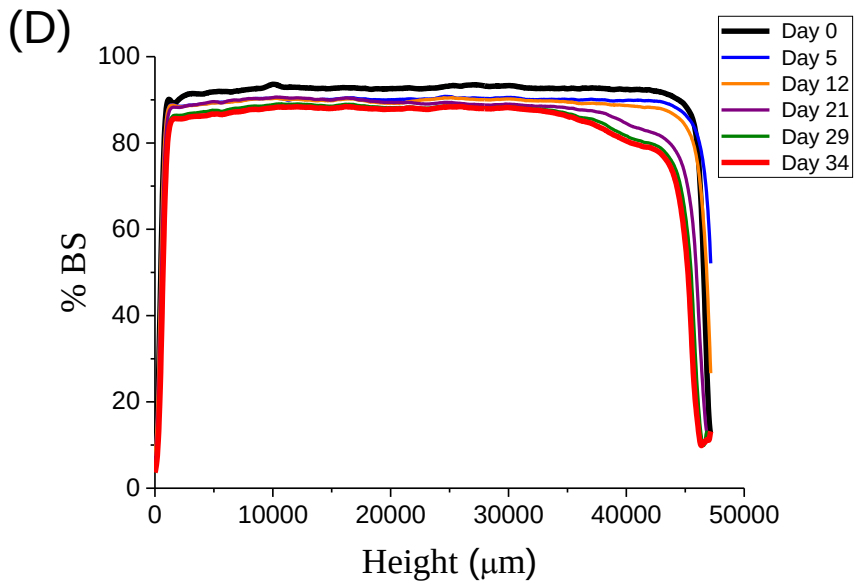

Figure 4.6. Backscattering measurements with the height of the measuring cell as a function of aging time for emulsion containing (A) 0.4 wt.%, (B) 0.2 wt.%, (C) 0.3 wt.% and (D) 0.4 wt.% of Diutan Gum.

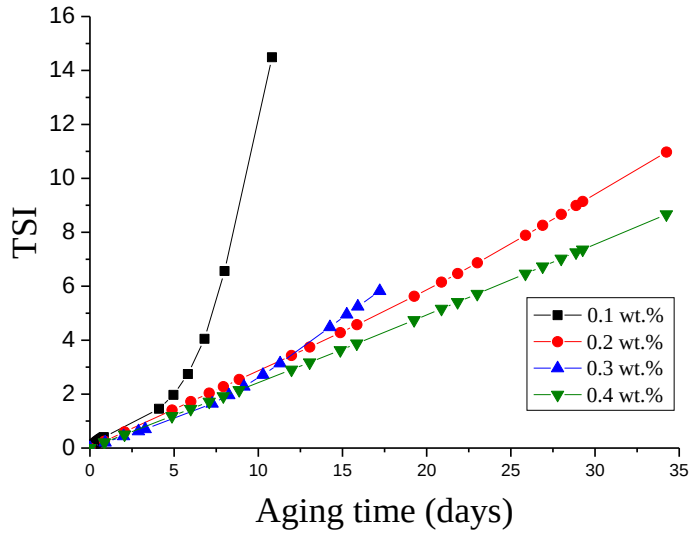

Figure 4.7. Influence of aging time on Turbiscan Stability Index as a function of diutan gum concentration for emulsions developed.

Conclusions

Optimization of microfluidization parameters in order to minimise the Sauter diameter and the span value of emulsions containing zein and sunflower oil was carried out. It has been proved that microfluidization provokes multimodal distributions regardless homogenization pressure after two cycles. Surface Response Methodology has been a powerful tool to obtain a clear result about the optimised emulsion (20000 psi and 4 cycles).

Once the microfluidization process was optimised, diutan gum was evaluated to enhance the physical stability of emulsions formulated with zein. It has been proved that the combination of zein and diutan gum formed a stronger network that the diutan gum solutions. In addition, the increase of diutan gum concentration showed higher values of viscoelastic moduli. In addition, this network formed is observed by FESEM technique. This microstructure is the reason why the enhanced physical stability of zein-diutan gum complex containing more than 0.1 wt% DG. This study has revealed the impact of microfluidization on emulsions formulated with proteins and has developed systems with potential applications to encapsulate active ingredients.

References

Albert, C., Beladjine, M., Tsapis, N., Fattal, E., Agnely, F., & Huang, N. (2019). Pickering emulsions: Preparation processes, key parameters governing their properties and potential for pharmaceutical applications. *Journal of Controlled Release*, *309*, 302–332.

Berton-Carabin, C. C., & Schroën, K. (2015). Pickering emulsions for food applications: background, trends, and challenges. *Annual Review of Food Science and Technology*, *6*, 263–297.

Carmen García, M., Trujillo, L. A., Carmona, J. A., Muñoz, J., & Carmen Alfaro, M. (2019). Flow, dynamic viscoelastic and creep properties of a biological polymer produced by Sphingomonas sp. as affected by concentration. *International Journal of Biological Macromolecules*, *125*, 1242–1247. https://doi.org/10.1016/j.ijbiomac.2018.09.100

Chevalier, Y., & Bolzinger, M.-A. (2013). Emulsions stabilized with solid

nanoparticles: Pickering emulsions. *Colloids and Surfaces A: Physicochemical and Engineering Aspects*, *439*, 23–34.

Gavahian, M., Chu, Y. H., Lorenzo, J. M., Mousavi Khaneghah, A., & Barba, F. J. (2020). Essential oils as natural preservatives for bakery products: Understanding the mechanisms of action, recent findings, and applications. *Critical Reviews in Food Science and Nutrition*, *60*(2), 310–321. https://doi.org/10.1080/10408398.2018.1525601

Jafari, S. M., Assadpoor, E., He, Y., & Bhandari, B. (2008). Re-coalescence of emulsion droplets during high-energy emulsification. *Food Hydrocolloids*, *22*(7), 1191–1202.

Jiang, Y., Zhu, Y., Li, F., Du, J., Huang, Q., Sun-Waterhouse, D., & Li, D. (2020). Antioxidative pectin from hawthorn wine pomace stabilizes and protects Pickering emulsions via forming zein-pectin gel-like shell structure. *International Journal of Biological Macromolecules*, *151*, 193–203.

Llinares, R., Santos, J., Trujillo-Cayado, L. A., Ramírez, P., & Muñoz, J. (2018). Enhancing rosemary oil-in-water microfluidized nanoemulsion properties through formulation optimization by response surface methodology. *LWT*, *97*, 370–375.

Luo, Y., & Wang, Q. (2014). Zein-based micro-and nano-particles for drug and nutrient delivery: A review. *Journal of Applied Polymer Science*, *131*(16).

Ma, C., Jiang, W., Chen, G., Wang, Q., McClements, D. J., Liu, X., … Ngai, T. (2021). Sonochemical effects on formation and emulsifying properties of zein-gum Arabic complexes. *Food Hydrocolloids*, *114*, 106557.

Mahdi Jafari, S., He, Y., & Bhandari, B. (2006). Nano-emulsion production by sonication and microfluidization—a comparison. *International Journal of Food Properties*, *9*(3), 475–485.

Muñoz, J., Alfaro, M. C., Trujillo-Cayado, L. A., Santos, J., & Martín-Piñero, M. J. (2019). Production of food bioactive-loaded nanostructures by microfluidization. In *Nanoencapsulation of Food Ingredients by Specialized Equipment* (pp. 341–390). Elsevier.

Ozturk, O. K., & Mert, B. (2019). Characterization and evaluation of emulsifying properties of high pressure microfluidized and pH shifted corn gluten meal. *Innovative Food Science & Emerging Technologies*, *52*, 179–188.

Patel, A. R., & Velikov, K. P. (2011). Colloidal delivery systems in foods: A general comparison with oral drug delivery. *LWT-Food Science and*

Technology, *44*(9), 1958–1964.

Santos, J., Alcaide-González, M. A., Trujillo-Cayado, L. A., Carrillo, F., & Alfaro-Rodríguez, M. C. (2020). Development of food-grade Pickering emulsions stabilized by a biological macromolecule (xanthan gum) and zein. *International Journal of Biological Macromolecules*, *153*, 747–754. https://doi.org/10.1016/j.ijbiomac.2020.03.078

Santos, J, Alcaide-González, M. A., Trujillo-Cayado, L. A., Carrillo, F., & Alfaro-Rodríguez, M. C. (2020). Development of food-grade Pickering emulsions stabilized by a biological macromolecule (xanthan gum) and zein. *International Journal of Biological Macromolecules*.

Santos, Jenifer, Jiménez, M., Calero, N., Undabeytia, T., & Muñoz, J. (2019). A comparison of microfluidization and sonication to obtain lemongrass submicron emulsions. Effect of diutan gum concentration as stabilizer. *Lwt*, *114*(February), 108424. https://doi.org/10.1016/j.lwt.2019.108424

Trujillo-Cayado, L. A., Santos, J., Ramírez, P., Alfaro, M. C., & Muñoz, J. (2018). Strategy for the development and characterization of environmental friendly emulsions by microfluidization technique. *Journal of Cleaner Production*, *178*, 723–730. https://doi.org/10.1016/j.jclepro.2018.01.028

Ye, R., & Harte, F. (2014). High pressure homogenization to improve the stability of casein–hydroxypropyl cellulose aqueous systems. *Food Hydrocolloids*, *35*, 670–677.

Zhang, B., Luo, Y., & Wang, Q. (2011). Effect of acid and base treatments on structural, rheological, and antioxidant properties of α-zein. *Food Chemistry*, *124*(1), 210–220.

Conclusiones

1. La zeína protege la interfase aceite-agua ya que las emulsiones formuladas solo con esta proteína no muestran recoalescencia, incluso a altas velocidades de homogeneización. Además, se ha comprobado que la zeína se coloca en la interfase mediante microscopía confocal. Los resultados han mostrado que la formulación óptima es 2.15% p/p de zeína y 40.9 % p/p de aceite de girasol. Sin embargo, la viscosidad parece ser un factor clave en estas emulsiones ya que necesitan de un espesante para ser estables frente al cremado. El uso de la goma Xantana de alto rendimiento provocó un notable incremento de la viscosidad Newtoniana y de las propiedades viscoelásticas de las emulsiones. Además, mejoró notablemente la estabilidad física de éstas gracias a la formación de un complejo proteína-polisacárido. Este complejo forma capas que recubren las gotas protegiendo al aceite de una posible oxidación y de procesos físicos de desestabilización.
2. Se han optimizado los parámetros de procesado en ultrasonidos para minimizar el tamaño de gota de las emulsiones que están formuladas solo con zeína. Se ha probado que un incremento de la energía suministrada provoca una disminución de dicho tamaño de gota, con una tendencia a estabilizarse a altas energías. Por lo tanto, no se presenta recoalescencia tampoco en estas emulsiones. Se probaron dos gomas para aumentar la estabilidad física de las emulsiones preparadas en ultrasonidos: la goma guar y la goma diutan. Por un lado, el uso de goma guar no consiguió formar un gel ni formar una red tridimensional por lo que estas emulsiones no fueron estables con el tiempo. Por otro lado, el uso de goma diutan en estas emulsiones con zeína sí mejoró notablemente la estabilidad física formando una red tridimensional (observada por FESEM) y una estructura tipo gel. Este trabajo extiende el conocimiento de los complejos zeína-polisacárido, mostrando la importancia de la correcta elección de la goma.
3. Finalmente, se optimizaron los parámetros de procesado de la microfluidización para las emulsiones formuladas con zeína. Se comprobó que el uso del Microfluidizer provoca distribuciones de tamaño de gota multimodales independientemente de la presión utilizada después de dos pasadas. La metodología de las superficies de respuesta muestra que la emulsión optimizada es la que se consigue después de cuatro ciclos a 20000 psi. Se vuelve a demostrar el gran papel de la goma diutan para estabilizar este tipo de emulsiones, esta vez procesada vía microfluidización. Solo con un 0.2% p/p de goma

diutan se obtienen resultados de alta estabilidad para emulsiones preparadas con microfluidizer.